RESTORE

Renewable Energy based seasonal Storage Technology in Order to Raise Economic and environmental sustainability of DHC

D1.5: Report on the assessment of environmental sustainability (V2)

This project has received funding from the European Union's Horizon 2020 research and innovation programme under grant agreement No 101036766.

PROJECT INFORMATION SHEET	
Project Acronym	RESTORE
Project Full Title	Renewable Energy based seasonal Storage Technology in Order to Raise Environmental sustainability of DHC
Grant Agreement	101036766
Call Identifier	H2020-LC-GD-2020-1
Topic	Innovative land-based and offshore renewable energy technologies and their integration into the energy system
Project Duration	48 months (October 2021 – September 2025)
Project Website	www.restore-dhc.eu
Disclaimer	The sole responsibility for the content of this document lies with the authors. It does not necessarily reflect the opinion of the funding authorities. The funding authorities are not responsible for any use that may be made of the information contained herein.

DELIVERABLE INFORMATION SHEET	
Number	Deliverable D1.5
Full Title	Report on the assessment of environmental sustainability (V2)
Related WP	WP1
Related Task	Task 1.6
Lead Beneficiary	UBB
Author(s)	Letitia Petrescu, Stefan Cristian Galusnyak, Alessandra-Diana Selejan-Ciubancan, Calin-Cristian Cormos
Contributor(s)	CENER, SIMTECH, TUW, POLIMI
Reviewer(s)	Francisco Cabello (CENER)
Dissemination level	Public
Due Date	M48, 2025
Submission Date	September 30th, 2025
Status	Final

QUALITY CONTROL ASSESSMENT SHEET			
ISSUE	DATE	COMMENT	AUTHOR
V0.1	24.09.2024	Draft	Letitia Petrescu (UBB) Stefan Cristian Galusnyak (UBB) Alessandra-Diana Selejan-Ciubancan (UBB) Calin-Cristian Cormos (UBB)
V0.2	29/09/2025	Review	Francisco Cabello (CENER)
V0.3	30/09/2025	Reviewed version	Letitia Petrescu (UBB) Stefan Cristian Galusnyak (UBB) Alessandra-Diana Selejan-Ciubancan (UBB) Calin-Cristian Cormos (UBB)
V1.0	30/09/2025	Submission to the EC	Francisco Cabello (CENER)

Summary

The current deliverable addresses the environmental assessment of six virtual use cases through the application of the Life Cycle Assessment (LCA) methodology. The main objective is to evaluate the integration of the RESTORE solution and renewable energy sources (RESs) within various plants connected to district heating and cooling (DHC) networks. The Use Case models combined with the RESTORE virtual tool, and developed on the IPSE Go platform, are based on data provided by the Use Case partners. additional details on the development of these models are available in Deliverables D5.4, D5.5, D5.6, D5.7, D5.8, and D5.9.

The LCA calculations are based on the mass and energy balance data obtained from both modelling activities and relevant scientific literature. The system boundaries considered in the LCA include: i) Upstream processes, such as raw material supply chains (e.g., organic fluids, Therminol V66, oil, copper sulphate), equipment manufacturing, and energy generation; ii) operational processes, including charging and discharging cycles; iii) Downstream processes, such as recycling and reuse of materials (e.g., organic fluids (Cyclopentane, NOVEC 649), Therminol V66, oil, copper sulphate), wastewater treatment (WWT), and final waste management.

Conventional LCA methodology has been employed to comprehensively address each of the four LCA steps: 1) definition of the goal and objectives of the intended study; 2) Life Cycle Inventory (LCI) – building the input and output inventory; 3) Life Cycle Impact Assessment (LCIA) – impact evaluation step; and 4) Interpretation – analysing the results while providing recommendations to further enhance the overall performance of the system. The ReCiPe 2016 impact assessment method has been employed to perform the impact analysis during the LCIA stage by following the Hierarchist (H) cultural perspective. LCA for Experts software (formerly known as GaBi software) version 10.8 has been used throughout this investigation.

The results of the environmental analysis indicate that, during the charging phase, electricity is the dominant contributor to environmental impacts. It accounts for the highest share in both Global Warming Potential (GWP) and Fossil Depletion Potential (FDP), underlining the importance of increasing the use of RESs while reducing dependence on fossil-based resources. In the discharging phase, five out of six virtual use cases achieve negative emissions in GWP and FDP, primarily due to the electricity produced during this stage. The exception is Use Case VI, which shows positive emissions, largely explained by the significant contributions from the production of copper sulphate and organic fluid used. With respect to plant construction, the analysis reveals that its overall impact is considerably lower compared to the operational phases.

Further details on the main impact drivers across key environmental categories, along with recommendations to reduce the environmental footprint, are provided in the present deliverable.

Table of Contents

1. Introduction

The ongoing reliance on fossil fuels is making the adverse effects of climate change ever more visible, with altered weather patterns, rising seas, and more frequent occurrences of severe floods, droughts, and heatwaves now clearly emerging [1]. As population and urbanization expand, energy needs will continue to rise, underscoring the need for decision-makers to adopt cleaner, yet more sustainable energy options to protect the environment and curb climate change impact [2]. The European Union (EU), a global leader in combating climate change, has committed through key frameworks such as the Kyoto Protocol, Europa 2020, and the Paris Agreement to substantial greenhouse gas (GHG) reductions, ultimately aiming for a 55% decrease from 1990 levels by 2030, and full climate neutrality by 2050 [3]. Without considerable worldwide initiatives to diminish CO_2 emissions, the Intergovernmental Panel on Climate Change (IPCC) forecasts an increase in global surface temperature of 1.5°C to 4°C during the course of the next century [4].

Currently, more than three-quarters of the EU's GHG emissions originate from energy production and use (energy sector CO_2 emissions globally rose to a record 37 Gt in 2022), thus emphasizing the urgency of action [5]. Therefore, energy system transformation is essential to achieving climate objectives [6]. Among the available options, researchers have focused on measures such as improving energy efficiency, adopting Carbon Capture, Utilization, and Storage (CCUS) technologies, and/or increasing the share of renewable energy sources (RES) to reduce environmental burden [7]. Such actions are consistent with the Paris Agreement, which aims to keep the rise in global temperatures below 2°C compared with pre-industrial levels [8].

In addition to the GHG emissions associated with thermal and power generation, substantial amounts of CO_2 are also released by the industrial sector. According to the International Energy Agency (IEA), this sector accounted for approximately 37% of global energy consumption in 2022. The sustained growth of energy-intensive industrial processes (e.g., iron and steel, cement, pulp and paper, etc.) has been a key driver of the increase in power consumption over the past decade [9]. While the majority of GHG emissions are directly linked to on-site fossil fuel combustion for power generation, additional CO_2 emissions arise either as by-products of primary production processes or as a result of unavoidable chemical transformations (e.g., mineral decomposition, metallurgical reactions) [10]. As reported, over the past five years, the CO_2 emission intensity of the iron and steel sector has remained relatively stable, ranging from 1.43 to approximately 1.41 t CO_2 per t of steel. To meet the targets set by the Net-Zero Emissions (NZE) by 2050 Scenario, this intensity must be reduced to 0.7 t CO2 per t of steel. In the cement sector, the primary challenge lies in reducing GHG emissions while meeting global demand [9]. Similar to the iron and steel sector, the direct CO_2 emission intensity of cement production has remained largely stable over the past five years, at 0.58 t CO_2 per t of cement. Achieving the NZE by 2050 Scenario requires an annual reduction in CO_2 intensity of approximately 4% until 2030. This necessitates improving energy and material efficiency, adopting RES, substituting clinker with alternative materials, and developing near-zero-emission manufacturing processes [9].

However, reducing emissions in the energy sector can be advanced by capturing and reusing heat that is currently wasted [11]. Industrial waste heat recovery, in particular, offers substantial

potential, as such losses account for over 50% of global industrial energy use [12]. Luberti et al. estimated that power plants and industrial facilities in the EU generate roughly 2,400 TWh of waste heat annually, at temperatures below 100°C [13]. Moser and Lassacher proved that integrating this excess heat into district heating and cooling (DHC) networks represents one of the most efficient ways to utilize it, providing thermal efficiency for buildings and urban infrastructure while cutting GHG releases [14]. Following a recent study, Mathiesen et al. assessed the potential surplus heat from different sources, including industrial processes, wastewater treatment (WWT), etc., throughout the 27 EU countries and the United Kingdom. Their findings suggest a combined potential of approximately 1,408 TWh per year [15].

The RESTORE project, short for Renewable Energy-based Seasonal Storage Technology in Order to Raise Economic and Environmental Sustainability, seeks to design a system capable of integrating a broad range of RES into DHC systems. This concept combines two key innovative technologies – Thermochemical energy storage (TCES) and the Organic Rankine Cycle (ORC)/Heat Pump (HP) – to enhance efficiency and sustainability. The efficiency and benefits of the RESTORE prototype have been experimentally proven, and the overall concept has been virtually implemented and optimized for six DHC Use Cases, which are based upon real operational data provided by the network operators. These virtual assessments explore potential configurations for integrating RESTORE technology and locally available RES into various DHC-connected facilities. The six Use Cases represent a range of real DHC networks across EU, covering both large- and small-scale systems located in various EU countries: 1) mixed residential – industrial network with biomass and solar thermal collectors in Denmark; 2) integration of multiple heat sources into the DHC of a cement plant in Austria; 3) deployment of RESTORE alongside different heat sources in a paper mill's DHC system in Slovakia; 4) integration of various heat sources into the DHC of a steel industry in Italy; 5) a geothermal-based DHC network in Germany; and 6) a small-scale DHC network serving a university campus in Italy. The following sections present a concise description of each of the aforementioned Use Cases.

1.1. Baseline Plant: Brønderslev CHP Hybrid Plant

The Brønderslev Combined Heat and Power (CHP) hybrid facility, situated in Northern Jutland, Denmark, serves as an exemplary model of an innovative district energy system. It is among the first facilities globally to integrate Concentrated Solar Power (CSP) with biomass combustion within a single integrated system, simultaneously producing electricity and thermal power, while enhancing performance through waste heat recovery. Initiated by the local utility provider, Brønderslev Forsyning, the project forms part of Denmark's broader strategy to phase out fossil fuels, decrease reliance on natural gas, and maintain cost-effective heating for residents in light of the gradual discontinuation of subsidies for gas-fuelled CHP operations. At present, the system supplies roughly 90% of Brønderslev's annual DHC requirements.

The hybrid plant comprises a parabolic trough collector (PTC) field with a thermal capacity of 16.6 MW_{th}, two biomass-fired boilers each rated at 10 MW_{th}, and an ORC turbine with an electrical output of 3.90 MW_{th}. All units are interconnected via a common thermal oil loop, employing Therminol V66 as the heat transfer fluid. It is important to highlight that the biomass boilers and the ORC unit fall outside the scope of the planned integration. Additional

information is available in Deliverable “D5.4 – Implementation and validation of RESTORE Use Case I: Residential / Industrial DH with Biomass and Solar Collectors”.

1.2. Baseline Plant: Gmunden Cement Plant

The cement facility examined through this case study is situated in Gmunden, Austria. It operates as part of the Rohrdorfer Group, which is a well-established enterprise in the cement and construction materials sector in Central Europe. The plant is dedicated to producing clinker, an intermediate in the manufacture of Portland cement. Clinker is obtained by sintering limestone together with other raw materials at elevated temperatures, serving as the key constituent in cement production.

Having a daily production capacity of about 1,900 tons of clinker, the Gmunden plant holds a significant position both in regional and international cement supply chains. Owing to the thermal efficiency of cement production, the facility is also linked to a DHC network. This connection allows surplus thermal energy generated during the clinker firing process to be transferred to the local heating system, thereby increasing efficiency and contributing to cleaner, more sustainable energy use in the surrounding area.

The performance of the DHC system relies heavily on the consistent and stable production of surplus thermal energy during clinker manufacturing. Because the potential for heat recovery is directly tied to the kiln’s operating schedule and efficiency, fluctuations in clinker output, planned shutdowns, or maintenance work can markedly affect the heat available for DHC. Consequently, thermal energy storage becomes an essential measure to decouple heat generation from immediate consumption. Integrating the RESTORE solution enables the plant to capture surplus heat during periods of high clinker production and supply it when production is reduced or temporarily suspended. Supplementary information about the technical part of the Gmunden facility and its integration with the RESTORE concept is available in Deliverable “D5.5 – Implementation and validation of RESTORE Use Case II: Integration of different heat sources in DH of Cement Industry”.

1.3. Baseline Plant: Ružomberok Paper Mill Plant

MONDI SCP in Ružomberok is one of the company’s largest facilities and represents the biggest integrated pulp and paper mill in Slovakia. It has an annual production capacity of 560,000 tons of uncoated fine paper, 66,000 tons of packaging paper, and 100,000 tons of market pulp. Following its recent investment in a new recovery boiler, the mill has achieved full energy self-sufficiency, with over 95% of its energy derived from renewables. The wood used in production is sourced from certified, sustainably managed forests, and the mill continuously works to minimize its environmental footprint. A portion of the thermal energy generated at the plant is supplied to the DHC network in the form of 5-bar steam. This steam passes through a heat exchanger station, where energy is transferred to water. Further, the heated water is circulated through the distribution network into the city, supplying local heat exchangers before returning to the steam/water heat exchanger station to be reheated.

The virtual implementation of the RESTORE solution within the MONDI SCP Pulp and Paper facility is intended to enhance renewable energy adoption and improve the recovery and use of surplus industrial heat from the plant, facilitating effective seasonal thermal energy storage.

Additional information is available in Deliverable “D5.6 – Implementation and validation of RESTORE Use Case III: Integration of different heat sources in DH of Paper Mills Industry”.

1.4. Baseline Plant: Alfa Acciai Steel Production

Alfa Acciai ranks among the largest Electric Arc Furnace (EAF) steel producers in Italy. The Brescia facility comprises two EAF units and three rolling mills. The current waste heat recovery strategy involves a large HP designed to capture waste heat from the furnaces’ pipe-to-pipe cooling circuit. The available heat, having a temperature range of 30 – 40°C, can be upgraded by the HP to approximately 90°C, thus making it suitable for district heating. This waste heat originates from the flue gases released during steel production, particularly from high-temperature processes, such for example combustion and metal-melting stages. Within the framework of the RESTORE project, an in-depth thermal analysis was carried out on the cooling water circuit of Alfa Acciai’s EAF1 furnace, with particular emphasis on evaluating the recovery potential from the return lines linked to the dust extraction system. By facilitating the recovery of thermal streams that would otherwise be dissipated into the environment, the RESTORE solution enhances the overall energy efficiency of industrial processes while supporting decarbonization efforts through reduced dependence on fossil fuels and the mitigation of thermal pollution. Supplementary information regarding the integration of the RESTORE concept within the steel sector is available in Deliverable “D5.7 – Implementation and validation of RESTORE Use Case IV: Integration of different heat sources in DH of Steel working industry”.

1.5. Baseline plant: Holzkirchen Facility

The geothermal power facility situated in Holzkirchen, Bavaria, Germany, employs an ORC system supplied by Turboden project partner, specifically made to convert geothermal energy into both electricity and heat. The plant has an installed electrical output of 3.6 MW and sources geothermal fluid from a depth of roughly 4,800 m, where the temperature reaches approximately 140°C. The ORC installation operates in a closed-loop configuration, utilizing an organic working fluid that is vaporized through geothermal heat, expanded within a turbine to produce electricity, and subsequently condensed before being recirculated. This system demonstrates remarkable operational adaptability as it is capable of functioning between 10% and 110% of its nominal capacity, while maintaining an average availability rate above 98%. Within the framework of the RESTORE project, the goal is to enhance the utilization of the available geothermal resource to maintain a steadier thermal energy extraction over the entire year. This strategy seeks to optimize the output of the geothermal well while more closely matching the heat supply with the end user’s demand profile. Additional data in regards to the RESTORE Geothermal Use Case is available in Deliverable “D5.8 – Implementation and validation of RESTORE Use Case V: District heating with Geothermal Technology”.

1.6. Baseline plant: POLIMI Campus Energy Network

In 2015, Politecnico di Milano commissioned PoliGrid, which is an advanced microgrid system developed to optimize the generation, consumption and distribution of energy within the Leonardo campus. The network interconnects more than 25 buildings via a medium-voltage grid, with electricity supplied primarily through on-site generation from a cogeneration unit and

photovoltaic (PV) panels. It is worth noting that the PV panels are installed on building rooftops. When the campus demand surpasses the internal generation capacity, the additional electricity is sourced from the external distribution grid.

The central element of PoliGrid is a 2 MW electric cogeneration facility producing both electricity and thermal power at an overall efficiency of over 82%, distributed via a 2-km DH circuit. In warmer months, the system operates in trigeneration mode using residual heat to power an absorption chiller with a cooling capacity of 1.4 MW for selected buildings. Supplemental thermal energy is provided by natural gas boilers during peak demand. The energy demand of the Leonardo campus varies considerably over the year, influenced by seasonal changes and the academic schedule. Annually, the campus consumes around 14 GWh of electricity and 11 GWh of thermal energy, corresponding to an overall natural gas usage of approximately 3.3 million cubic meters. The goal of this Use Case is to incorporate these technologies within the RESTORE framework and evaluate storage performance under varying operational scenarios and control strategies. Additional information about the technical aspects and simulation results is available in Deliverable “D5.9 – Implementation and validation of RESTORE Use Case VI: Small-scale DHC network of Politecnico di Milano campus”.

2. Methodology

To evaluate the environmental footprint of processes and products, impact assessments have become increasingly important analytical tools. Within this context, Life Cycle Assessment (LCA) offers a comprehensive framework for identifying and mitigating adverse environmental effects. It systematically quantifies energy and material consumption, as well as waste emissions, while assessing potential ecological impacts. Moreover, LCA highlights opportunities for improvement across all stages of a product's life cycle, from raw material extraction to end-of-life treatment [16].

LCA was developed as a method to determine the most sustainable option among different alternatives by quantifying the environmental impact of each system, making it a valuable tool to support informed decision-making. In practice, it is often applied to assess and compare technological solutions, while also revealing critical impact trade-offs and identifying key hotspots where improvements can yield the greatest environmental benefits. The European Commission (EC), in its pursuit of advancing sustainable consumption and production, has recognized LCA as the most reliable and comprehensive tool currently available for evaluating the environmental footprint of products [17]. This endorsement has significantly promoted its widespread application across multiple sectors, where it is now used both to quantify environmental impacts and to guide strategies for long-term sustainability. By examining a product or system in relation to its specific function, LCA evaluates its influence on both the environment and human health, while considering every stage of the life cycle. Today, the methodology is widely applied in fields such as the sustainable manufacturing of biomaterials and green chemicals, the development of Environmental Product Declarations (EPD), and product design. Furthermore, LCA complements technological progress by offering valuable insights that help prioritize areas for improvement [18].

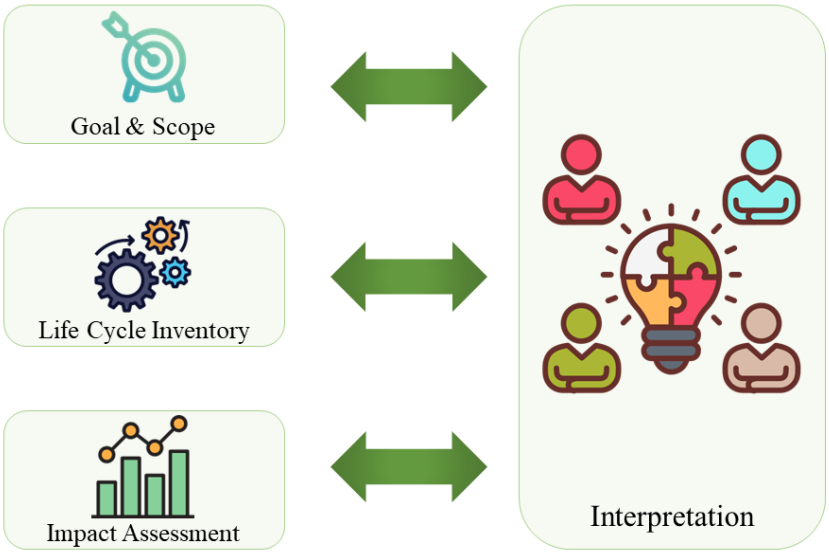

Figure 1. LCA methodology framework

As illustrated in Figure 1, the LCA framework is defined by the International Organization for Standardization (ISO) in four distinct stages through ISO 14040:2006 (i.e., principles and

framework) and ISO 14044:2006 (i.e., requirements and guidelines): Goal and scope definition, Life cycle inventory (LCI), Life cycle impact assessment (LCIA), and Interpretation [19].

The user may enhance the LCA's final results through an iterative process by gathering more precise data or modifying the objectives and/or parameters of the study.

2.1. Goal and scope definition

The effectiveness of any LCA in fulfilling its intended objectives is largely determined by the clarity and precision with which its goal is formulated at the outset of the study. Defining the purpose of an LCA should encompass the specific applications under consideration, the justification for undertaking the study, the audience to whom the outcomes are addressed, and whether the resulting conclusions will serve as a foundation for comparative assertions [20].

The RESTORE solution, founded on the synergy of two breakthrough technologies, presents an innovative pathway toward decarbonizing the DHC sector. This study aims to assess the environmental impacts associated with the RESTORE concept, which has been implemented and optimized using process modelling tools across six DHC Use Cases by using datasets provided by the respective Use Case operators. The RESTORE solution facilitates the integration of various RES with practical seasonal/daily storage, promoting complete sustainability and markedly strengthening their environmental performance. The IPSE GO platform (https://simtechnology.com), an advanced web-based simulation tool, provides public access to the Use Case models. Each Use Case can be directly explored and simulated online, allowing anyone interested to examine how the technology works within a specific sector or certain technical parameters.

Comprehensive descriptions of each Use Case, together with the main outcomes regarding the integration of the RESTORE concept, are presented in deliverables D5.4, D5.5, D5.6, D5.7, D.5.8 and D5.9.

The current investigation focuses on the RESTORE project, funded under grant agreement No. 101036766 by the European Union's Horizon 2020 research and innovation initiative. The intended audience targets stakeholders of DHC networks, who can utilize the IPSE GO platform to develop their own models while analyzing the technical outcomes. In addition, the study is accessible to both technical and non-technical members of the general public, with its findings offering valuable guidance for decision-making regarding heating and cooling systems.

Once the study's objectives are clearly defined, the next step is to establish its scope. This involves specifying the main function of the product or system under investigation, defining the functional unit (FU), and setting the system boundaries – including temporal, geographical, and life cycle stages. This phase also entails choosing the impact assessment method along with relevant impact categories, addressing methodological aspects such as allocation procedures, as well as any underlying assumptions and potential limitations [20].

2.1.1. Function of the system and functional unit

Defining the system's function is a critical step, as it provides the foundation for determining the FU and establishing system boundaries. The RESTORE system's function is the generation and storage of the thermal energy, with the objective of enhancing the availability

and reliability of energy distribution in supply networks. The FU quantifies the performance of this function and establishes a standard reference for associated input and output flows. Reference flows indicate the amount of goods or services required to deliver the FU. In this analysis, 1 kWh of thermal energy has been selected as the FU, thus, all environmental impact categories are expressed accordingly.

2.1.2. **System boundaries**

A system boundary represents the interface between the set of unit processes under consideration and the external environment, thereby defining which processes are integrated into the analysis and which are excluded. Following ISO 14040:2006 [21], system boundaries should account for relevant life cycle stages, individual unit processes, and associated material and energy flows, including [20]:

- Sourcing and extraction of the raw materials;
- Material and energy inputs and outputs throughout the primary production/processing chain;
- Transportation and distribution of the materials;
- Generation and supply of fuels, electricity, and thermal energy;
- Use and maintenance of products;
- Treatment, disposal, or management of process residues and end-of-life products;
- Recovery and circular management of used products (including reuse, recycling, and energy recovery);
- Production of auxiliary or supporting materials;
- Manufacturing, maintenance, and end-of-life handling of equipment and infrastructure;
- Supplementary activities such as facility lighting, space heating, and other operational energy uses.

There are four primary ways to determine the system boundaries, as shown in Table 1, depending on the LCA's objectives.

Table 1: Boundary system defining options

Boundary types	Description
Cradle-to-grave	Encompasses the full supply chain for materials and energy, including raw material extraction, production, transportation, usage, and final product treatment stages.
Cradle-to-gate	Includes all stages of the production process, from raw material extraction to the plant gate, and is used to evaluate the environmental impact of a product’s manufacture.
Gate-to-gate	Covers only the production-phase operations and is employed to assess the environmental impacts of a specific production step or process.
Gate-to-grave	Encompasses all post-production activities, including use and end-of-life treatment stages, and is used to evaluate a product’s environmental impacts after it leaves the plant.

The current investigation stands as a cradle-to-gate LCA study as it covers every stage of production, starting from the raw materials' supply chain (Novec 649, Therminol V66, cyclopentane, oil, Copper Sulphate) and manufacturing of plant equipment (where data is available), up to the final product (heat and energy generation). Figure 2 better illustrates the sub-processes considered within the boundaries of the system: a) upstream processes: supply chains for Novec 649, mineral oil, Copper Sulphate (pentahydrate) and manufacturing of plant equipment; b) main processes: charging (production of Monohydrated Copper Sulphate) and discharging (production of Pentahydrate Copper Sulphate) of the long-term storage; and c) downstream processes: ORC fluid degradation and disposal of the other process materials.

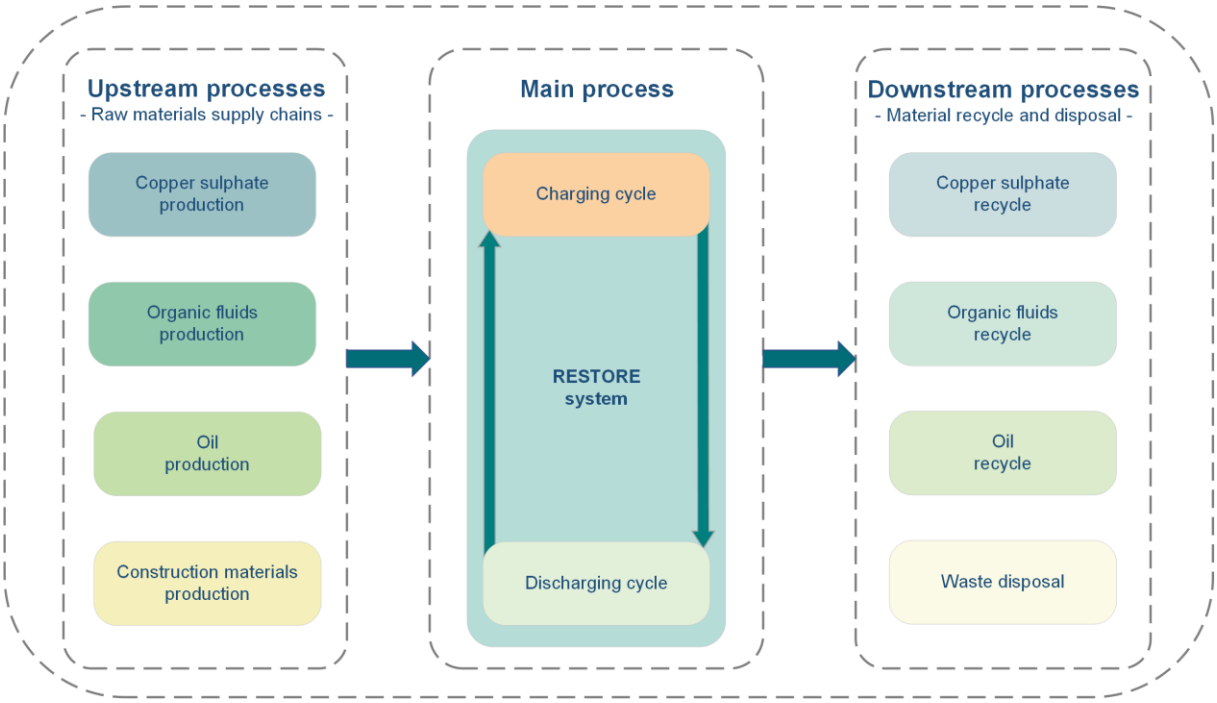

Figure 2: System boundaries for the investigated Use Cases

It is essential to define both spatial and temporal boundaries, as environmental conditions, resource availability, and technological developments can vary across regions and over time [22]. The system parameters under investigation, defined both spatially and temporally, assume distinct configurations corresponding to each Use Case scenario: the plant located in Denmark, Austria, Italy (i.e., two Use Case models are assumed as being located in Italy), Slovakia, and Germany, each with a 25-year operational lifespan.

2.1.3. **Impact categories and impact assessment method**

As previously stated, ISO 14044:2006 offers guidelines and suggestions for the proper selection of impact categories. An impact category represents a group of environmental issues (i.e., greenhouse effect, ozone formation, human toxicity, etc.) to which the results of the LCI study may be related. On the other hand, an impact category indicator is a measurable representation of an impact category. A life cycle impact assessment (LCIA) method is derived from a set/collection of impact categories. A large number of such methods are already included in LCA software and may be used under different names, such as for example ReCiPe, CML, TRACI, Eco-indicator, or ILCD [22].

The Life Cycle Initiative developed a framework linking inventory results to environmental impact. Inventory data with similar effects are grouped into midpoint categories, and each flow is multiplied by a characterization factor to quantify its contribution. Midpoint categories are then associated with damage categories, representing impacts on areas of protection, or endpoint indicators (i.e., human health, ecosystem quality, resource availability). Thus, impact categories can be classified as problem-oriented (midpoint) or damage-oriented (endpoint) [23]. Midpoint impact indicators are positioned early in the cause-and-effect chain, offering more precise results with lower uncertainty, whereas endpoint categories are located at the end of the chain, making them easier to interpret but associated with higher parameter uncertainty [24].

For this investigation, the environmental analysis was performed using the ReCiPe 2016 impact assessment method, which calculates both midpoint and endpoint categories through a cause-and-effect chain. Developed in 2008 through collaboration between RIVM, CML at Leiden University, Pré Sustainability, Radboud University, and CE Delft, ReCiPe reduces uncertainty in translating LCI results to impact categories by applying three cultural perspectives that differ in time horizon:

- Individualist (I) – short-term view, assuming technology will mitigate future problems;
- Hierarchist (H) – balanced short- and long-term perspective based on scientific consensus;
- Egalitarian (E) – conservative long-term approach, considering uncertain impacts with limited evidence.

A detailed description of the environmental impact categories considered in the ReCiPe 2016 assessment method is further provided [24].

Table 2. Overview and description of environmental category indicators of ReCiPe 2016 impact assessment method [13]

Impact indicator	**Characterization**	**Main contributors**
Global Warming Potential (GWP)	Anthropogenic emissions leading to an increase in surface temperature. Unit: kg of CO_2 equivalents to air	CO_2, CH_4, N_2O, NO_2, CFCs, HCFCs, HFCs
Terrestrial Acidification Potential (TAP)	Increased proton levels in the natural soils due to the impact of acidifying contaminants. Unit: kg of SO_2 equivalents to air	SO_X, NO_X, HCl, HF, HNO_3, H_2SO_4, H_2S
Freshwater Eutrophication Potential (FEP)	Excessive quantities of nutrients detected in the internal water ecosystem. Unit: kg of P equivalents to freshwater	Nitrogen and phosphorus chemicals
Ozone Depletion Potential (ODP)	Anthropogenic emissions that are causing the stratospheric ozone layer to thin. Unit: kg of CFC-11 equivalents to air	CFCs, HCFCs, halons
Particulate Matter Formation Potential (PMFP)	The ingestion of contaminants in the form of particulate matter ($PM_{2.5}$) by individuals. Unit: kg of $PM_{2.5}$ equivalents to air	NH_3, NO_X, SO_2
Fossil Depletion Potential (FDP)	Excess energy used for the extraction of one MJ, kg or m^3 of fossil fuel. Unit: kg of oil equivalents (with a lower heating value of 42 MJ)	Extraction of fossil resources
Mineral Depletion Potential (MDP)	Ore grade decrease. Unit: kg of Cu equivalents	Extraction of mineral resources
Photochemical Oxidant Formation Potential ecosystem ($POFP_{ecosystem}$)	Increase in ozone concentration at the troposphere level. Unit: kg of NO_x equivalents to air	Particulate matter, NMVOCs, NO_x

Table 2. continued

Photochemical Oxidant Formation Potential human health ($POFP_{human\text{-}health}$)	Tropospheric ozone population intake increase. Unit: kg of NO_x equivalents to air	Particulate matter, NMVOCs, NO_x
Human Toxicity Potential cancer (HTP_{cancer})	Risk increases of cancer disease incidence Unit: kg of 1,4 DCB equivalents to air	Chemical substances toxic to human health
Human Toxicity Potential non-cancer ($HTP_{non\text{-}cancer}$)	Risk increases of non-cancer disease incidence Unit: kg of 1,4 DCB equivalents to air	Chemical substances toxic to human health
Water Depletion Potential (WDP)	Increase in water consumed. Unit: m^3 of water consumed	Use of freshwater
Freshwater Ecotoxicity Potential (FETP)	Relates to the possible harm of toxic compounds to the aquatic environment. Unit: kg of 1,4 DCB equivalents to freshwater	Toxic chemicals with a reported lethal concentration to rodents and fish (e.g., Pb, Hg, Cd, halogenated organic compounds, pesticides or sewage sludge)
Marine Ecotoxicity Potential (METP)	Impact on the marine environment due to the increasing amounts of metals in the ocean. Unit: kg of 1,4 DCB equivalents to marine water	
Terrestrial Ecotoxicity Potential (TETP)	Accounts for the potential impact of toxic substances on terrestrial ecosystems. Unit: kg of 1,4 DCB equivalents to industrial soil	

2.1.4. **Assumptions used in the study**

Numerous judgments are required during the LCA, particularly when real data is unavailable, necessitating assumptions by the LCA practitioner. These assumptions can significantly influence the study's results. Therefore, sensitivity analyses are recommended to evaluate their impact on system performance. The following sections outline the assumptions made in this study for each boundary condition (e.g., upstream, main, and downstream processes).

In addition to general LCA assumptions outlined in the subsequent sections, specific considerations related to the plant construction phase have been incorporated for each Use Case. Nevertheless, owing to the low Technology Readiness Level (TRL) of the investigated technology and the resulting challenges in obtaining comprehensive and reliable datasets for the construction stage, the present analysis is restricted to the inclusion of primary equipment (i.e., storage tanks, reactors, etc.). A more extensive and detailed evaluation of the construction phase, specifically concerning the RESTORE prototype solution, is provided in Deliverable D1.5: Report on the assessment of Environmental Sustainability (V1).

2.1.4.1. Assumptions for Novec 649

The assumptions used for the reference case scenario are presented in Table 3, along with the ones considered for the production of 1.01 kg of Novec 649. This quantity of Novec 649 was chosen in order to meet the study's FU, which is the generation of 30 kWh of thermal power.

It is considered that Novec 649 is purchased from a factory located in the USA and delivered to the plant when needed. The production route of this organic fluid is considered to start with basic materials such as methane, chlorine, oxygen and hydrogen fluoride and it can be observed in the chemical reactions' succession listed below:

$$CH_4 + Cl_2 \rightleftarrows CH_3Cl + HCl \quad (1)$$

$$CH_3Cl + Cl_2 \rightleftarrows CH_2Cl_2 + HCl \quad (2)$$

$$CH_2Cl_2 + Cl_2 \rightleftarrows CHCl_3 + HCl \quad (3)$$

$$CHCl_3 + 2HF \rightleftarrows CHClF_2 + 2HCl \quad (4)$$

$$2CHClF_2 \rightleftarrows F_2C = CF_2 + 2HCl \quad (5)$$

$$3F_2C = CF_2 \rightleftarrows 2CF_3CF = CF_2 \quad (6)$$

$$2CF_3CF = CF_2 + O_2 \rightleftarrows 2F_3C - CF(O)CF_2 \quad (7)$$

$$F_3C - CF(O)CF_2 + CF_3CF = CF_2 \rightleftarrows \mathbf{CF_3 - CF_2 - C(O) - CF(CF_3)_2} \quad (8)$$

Table 3: Assumptions considered in the Novec 649 supply chain

Assumption	Value of the LCA model		Source
	Unit	Reference case	
Methane	kg	0.308	UBB
Chlorine	kg	4.09	UBB
Hydrofluoric acid	kg	0.77	UBB
Oxygen	kg	0.051	UBB

Main assumptions considered for the Novec 649 supply chain:

- Methane is coming from natural gas used in the USA;
- Chlorine is obtained by Sodium chloride solution electrolysis in the USA;
- Hydrofluoric acid is obtained through the conversion of dried fluorspar with sulphuric acid, in the USA;
- Oxygen comes from the cryogenic separation of air, in the USA.

2.1.4.2. Assumptions for Cyclopentane

For this study, the manufacture of 1 kg of cyclopentane was approximated to require 6.67 kWh of electricity (including upstream processes in the energy balance) and one kg of crude oil. These values serve as representative inputs for life cycle modelling, since no detailed, publicly available inventory data for cyclopentane production was found in the scientific literature. Cyclopentane is derived as part of the C5 fraction during petroleum refining, and both crude oil requirements and electricity consumption vary depending on crude type, refinery configuration, and process technology. To address this variability, the present assumptions should be interpreted as average estimates that enable a consistent and comparable assessment across Use Cases.

For the purpose of this study, cyclopentane is assumed to be produced in Speyer, Germany, and subsequently transported to individual plants by rail. The specific diesel consumption for rail transport is estimated at 0.474 kg per ton of freight. The main assumptions underlying the cyclopentane supply chain are as follows:

- Crude oil for cyclopentane production is assumed to be sourced from various locations (e.g., North Sea, Italy, etc.) depending on the specific Use Case;
- Electricity requirements for the production process are considered to be supplied by the country-specific grid mix;
- Distribution of cyclopentane to the plants is carried out by a diesel-powered extra-large freight train, with a gross weight of 2000 tons and a payload capacity of 1452 tons.

2.1.4.3. Assumptions for Copper Sulphate

The assumptions used for the reference case scenario are presented in Table 4, along with the ones considered for the production of 0.285 kg of $CuSO_4 \cdot H_2O$. Similarly, to the amount of Novec 649, the quantity of copper sulphate was chosen to satisfy the functional unit of 30 kWh of thermal power.

The $CuSO_4 \cdot H_2O$ is purchased from another factory located in Germany and delivered to the plant when needed. In this facility, the copper sulphate is made from copper and sulphuric acid.

The copper is produced through both pyrometallurgy and hydrometallurgy, and the mining for it takes place via conventional techniques such as drilling and blasting. The ore is crushed and ground in the hydrometallurgical process, then flotation is used to concentrate the material. After the final product is melted, electrolysis yields 99.99% copper. Ore is processed via leaching, solvent extraction, and electrowinning in the hydrometallurgical process. The needed electricity comes from the grid mix, accounting for both renewable and non-renewable power plants.

Sulphuric acid is produced by oxidizing sulphur to sulphur dioxide, further to sulphur trioxide and then dissolving the latter in water. When sulphur is first burned with dry air, sulphur dioxide is formed predominantly. Then comes the crucial step, its oxidation to sulphur trioxide. This is accomplished by the contact method using various catalysts in several reactors. To produce highly concentrated sulphuric acid, sulphur trioxide is then dissolved in concentrated sulphuric acid using several columns. Since sulphur dioxide is a by-product of many industrial processes, it is often the starting material without undergoing the initial oxidation step.

Table 4: Assumptions considered in the $CuSO_4 \cdot H_2O$ supply chain

Assumption	Value of the LCA model		Source
	Unit	Reference case	
Copper	kg	0.133	UBB
Sulphuric acid	kg	0.175	UBB

Main assumptions considered for the $CuSO_4 \cdot H_2O$ supply chain:

- Copper is coming from European ore;
- Sulphuric acid is obtained by multiple oxidations, starting from sulphur, in Germany;
- Oxygen, required in the oxidation process, comes from the cryogenic separation of air, in Germany.

2.1.4.4. Assumptions for Oil

For the reference case scenario, 4.55 kg of oil (90% rapeseed oil and 10% mineral oil) are needed to be produced. Since mineral oil is in a small quantity and its production is very complex, implying petrochemical processes, only the production of rapeseed oil will be further discussed. The oil will be purchased when needed from a factory situated in Austria.

There are two different procedures for the production of rapeseed oil (canola seed oil): 1. small-scale (local) production; 2. large-scale (central). From an economic point of view, the large-scale (central) production is advantageous due to its higher daily output of 3000 t/d compared to 10 t/d for the small-scale production, it shows better and a more uniform oil quality than the other option, and for these reasons only it will be taken into consideration for the current study.

Approximately 1000 t to 4000 t of canola seeds can be processed in various ways each day in a large-scale industrial facility. In addition to only crushing the seeds or removing the oil fruit

on their own, the two methods can be combined. To extract the leftover oil, a solvent is applied to the pressing cake that remains after the seeds are pressed. With this combination method—which is currently the greatest technology available—roughly 99% of the rapeseed oil content is extracted. The several sub-processes that make up the central large-scale production of plant oil are listed below [25].

1. *Tidying up*: Even though the canola seeds are preconditioned, there is still a need for a second cleaning process because the quality is different. Wastes and contaminants. Impurities and wastes are separated in this step.

2. *Crushing*: Using flat and impregnating rollers, the seed shells and storage tissue are crushed to increase the surface area of the kernels and reduce oil leakage.

3. *Conditioning*: The water content and temperature of the crushed seeds are regulated during the conditioning phase, which comes after the crushing step. These are important variables for the later processing stages. Is the water content too high, meaning that not enough of the extraction solvent can seep through? If there is insufficient water present, the seeds will get crushed. Following the conditioning stage, the pulverised seeds are heated between 80-90°C.

4. *Prepressing*: An auger press is used to mechanically prepress the canola seeds. Following pressing, the canola seeds retain between 15-25% of their initial oil content. This technique yields pressing cake and crude oil that has been tainted with tiny seed fragments. As a result, the oil production process is split into two distinct processing lines going forward. The crude oil's conditioning

5. *Filter*: A filtering process is required since the crude oil is tainted with tiny seed fragments. The pressing cake is combined with the reminder of the filter process and then extracted.

6. *Drying*: The crude oil's water content must be lowered to prepare it for further processing. Rapeseed pressing cake processing

7. *Flaking*: The pressing cake's surface needs to be increased before extraction. The tiny bits are flattened into approximately 0.3 mm thick flakes on specialised flaking rollers. The solvent diffuses more widely due to the surface expansion, which significantly raises the oil output.

8. *Extraction*: This process can be done intermittently or continuously. The continuous process is state-of-the-art for large-scale oil extraction. The flakes are moved in open containers within a closed space. In order to dissolve the oil from the flakes, a solvent (n-Hexane, 50-60°C) is flowing through them simultaneously. The miscella, or hexane-rapeseed oil mix, is pumped into the following chamber, where it is once more enhanced with oil, against the direction in which the flakes are transported. Until the miscella exits the process enriched with oil, this process is repeated multiple times. Nearly oil-free extraction groats exit the process next to the miscella.

9. *Miscella distillation*: The miscella is cleaned by centrifuging or filtering it before distillation. The Hexane, which has a lower boiling point than the extraction oil, is then stripped using a multi-stage distillation process. Less than 100 parts per million of solvent are present in the distilled crude oil. The distilled oil is sent to raffination together with the oil fraction from pressing. Hexane that has evaporated is turned back into liquid and used once more in the extraction process. A total estimated hexane loss per seed is one kilogram. Approximately

0.375 kg are burned, 0.375 kg are released into the atmosphere as emissions, and 0.25 kg are left in the rapeseed oil and extraction groats.

10. *Purifying, drying, and cooling*: Using a specific Desolventizer-Toasters, the residual solvent must be removed from the extraction groats to use them as feed material going forward. The groats are then boiled to remove any lingering toxic materials, dried, chilled, and, in certain situations, milled and/or pelleted. In the extraction procedure, the separated hexane is used once more.

2.1.5 Limitations of the study

Clearly stating study limitations is essential, as it is often impractical to include all anticipated data or adjust the goal and scope for new datasets. Any gaps, such as reliance on older data or missing LCI information for certain impact categories, should be noted in the goal and scope or interpretation sections. Explicitly reporting these limitations ensures reliable conclusions, supports informed decision-making, and prevents misleading LCA results.

The following elements are excluded from the system boundaries in the present LCA evaluation:

- Decommissioning of the plant;
- Repair and maintenance activities;
- Construction of infrastructure (e.g., roads, railways, etc.) and transportation equipment (e.g., trucks, trains, ships);
- Installation of unloading facilities;
- Human labour tasks;
- Low-frequency, high-impact, unpredictable events (e.g., fugitive, accidental releases).

2.2 Life cycle inventory

Based on unit processes – considered the smallest components in a life cycle inventory (LCI) for which input and output data can be quantified – the LCI of a product or process characterizes the flow of materials (e.g., resources and emissions) between the system delineated by the boundary limits and the external environment [26]. The core elements of an LCA are unit processes, often conceptualized as “black boxes” that convert a set of inputs into a corresponding set of outputs. Inputs may include products (consisting of parts, materials, and services), waste destined for processing, and natural resources such as fossil fuels, minerals, and biological materials. Outputs can take various forms as well, including residuals released into the environment (pollutants in air, water, and soil), waste requiring treatment, and products (comprising parts, materials, and services). Data for these flows are typically compiled and presented in a table format.

2.1.1. Importance of data sources and data quality

According to ISO 14044:2006, all data may comprise a mix of measured, calculated, and/or estimated values and must satisfy quality criteria, including temporal, geographical, and technological coverage; precision, completeness, representativeness, consistency, and repeatability; as well as source reliability and uncertainty [27]. Data quality is a critical aspect of the LCI. To ensure that these quality requirements are fulfilled, data validation should be

performed during the data collection phase. Approaches such as mass and energy balance checks or comparative analyses of emission factors can be employed to achieve this validation [20].

LCI data can be classified into two categories: primary data, obtained through direct means such as online and offline data collection, surveys, in-person measurements, and interviews; and secondary data, derived from sources including databases, scientific literature, research papers, statistics, estimation, and modelling activities. In the present investigation, both primary and secondary data were utilized, as the analysis is based upon the simulations provided by other project partners using the IPSE Go platform. Nevertheless, all simulations reflect real data retrieved from the Use Case providers.

2.1.2. **LCI for various subsystems**

The most significant datasets, taken into account in each Use Case explored, are presented in Annex 1.

2.2. Life cycle impact assessment

The Life Cycle Impact Assessment (LCIA) phase aims to link the system's elementary flows to their potential environmental consequences. Given that the LCI step involves numerous input and output flows, such as resource use and emissions, the LCIA stage translates these reference flows into defined environmental impact categories.

For widely accepted and straightforward effect indicators, all inventory results are initially allocated to pre-selected impact categories that are available in various LCA software platforms (e.g., SimaPRO, LCA for Experts, OpenLCA, etc.), for which characterization factors have already been defined.

LCA for Experts was chosen as the software tool for conducting the present study. Formerly known as GaBi and originally developed by the German company PE International, LCA for Experts provides all the necessary components to model products and systems from a life cycle perspective. The software also includes access to comprehensive environmental databases that cover a broad range of user requirements, including material production, fuel and energy generation and consumption, product transportation, and waste management [25].

LCA for Experts is a modular software platform with a parametrized architecture. It supports LCA studies in compliance with ISO 14040:2006 and ISO 14044:2006, as well as applications in Life Cycle Engineering (LCE), Life Cycle Costing (LCC), EPD, product and process optimization, Design for Environment (DfE), and economic or social sustainability assessments.

3. LCA – Interpretation stage

The primary objective of the interpretation phase is to derive conclusions, acknowledge study limitations, and formulate recommendations based on the issues identified in the LCI and LCIA outcomes, while remaining consistent with the defined goals and constraints of the research. The presentation of the assessment results should ensure that the intended audience can readily comprehend them. In this deliverable, six Use Cases were analyzed.

3.1. Use Case 1 – Brønderslev CHP Hybrid Plant – Results and discussions

Table 5 presents the LCA results for the Use Case 1 scenario, taking into account the study's limitations and assumptions.

Table 5. LCA results for Use Case 1

KPI	Units	Charging	Discharging	Plant construction
GWP	kg CO_2 eq./kWh	1.54	$-4.40 \cdot 10^{-1}$	$1.41 \cdot 10^{-4}$
FDP	kg oil eq./kWh	$4.58 \cdot 10^{-1}$	$-1.34 \cdot 10^{-1}$	$3.60 \cdot 10^{-5}$
FETP	kg 1.4-DB eq./kWh	$8.89 \cdot 10^{-5}$	$-2.09 \cdot 10^{-5}$	$3.08 \cdot 10^{-6}$
FEP	kg P eq./kWh	$2.82 \cdot 10^{-4}$	$4.38 \cdot 10^{-5}$	$1.94 \cdot 10^{-10}$
HTP_{cancer}	kg 1.4-DB eq./kWh	$4.48 \cdot 10^{-4}$	$-1.07 \cdot 10^{-4}$	$1.64 \cdot 10^{-4}$
$HTP_{non\text{-}cancer}$	kg 1.4-DB eq./kWh	$4.97 \cdot 10^{-1}$	$4.99 \cdot 10^{-2}$	$1.31 \cdot 10^{-3}$
MDP	kg Cu eq./kWh	$3.18 \cdot 10^{-3}$	$-4.97 \cdot 10^{-4}$	$4.03 \cdot 10^{-6}$
$POFP_{ecosystem}$	kg NO_x eq./kWh	12.36	-2.72	$2.68 \cdot 10^{-7}$
ODP	kg CFC eq./kWh	$1.01 \cdot 10^{-6}$	$-2.22 \cdot 10^{-8}$	$3.39 \cdot 10^{-11}$
TAP	kg SO_2 eq./kWh	$2.44 \cdot 10^{-3}$	$1.86 \cdot 10^{-5}$	$7.92 \cdot 10^{-7}$
TETP	kg 1.4-DB eq./kWh	$1.76 \cdot 10^{-1}$	$-5.11 \cdot 10^{-2}$	$1.48 \cdot 10^{-2}$

Information, comments, and discussions regarding the main sub-processes influencing the most important impact indicators are included in the section that follows.

3.1.1. Global Warming Potential (GWP)

Figure 3 illustrates the GWP associated with the charging phase in Use Case 1. To enhance clarity, the share of the contributions is displayed through two complementary visualisations. Figure 3a highlights the sub-systems with the highest impact, namely the electricity consumption, thus the electric import from the grid mix (1.52 kg CO_2 eq./kWh), as well as the Therminol V66 production process, which accounts for only $1.93 \cdot 10^{-2}$ kg CO_2 eq./kWh. Collectively, these sub-processes dominate the charging-phase GWP, with their relative magnitudes identifying them as the primary contributors to the overall score at this stage.

a.

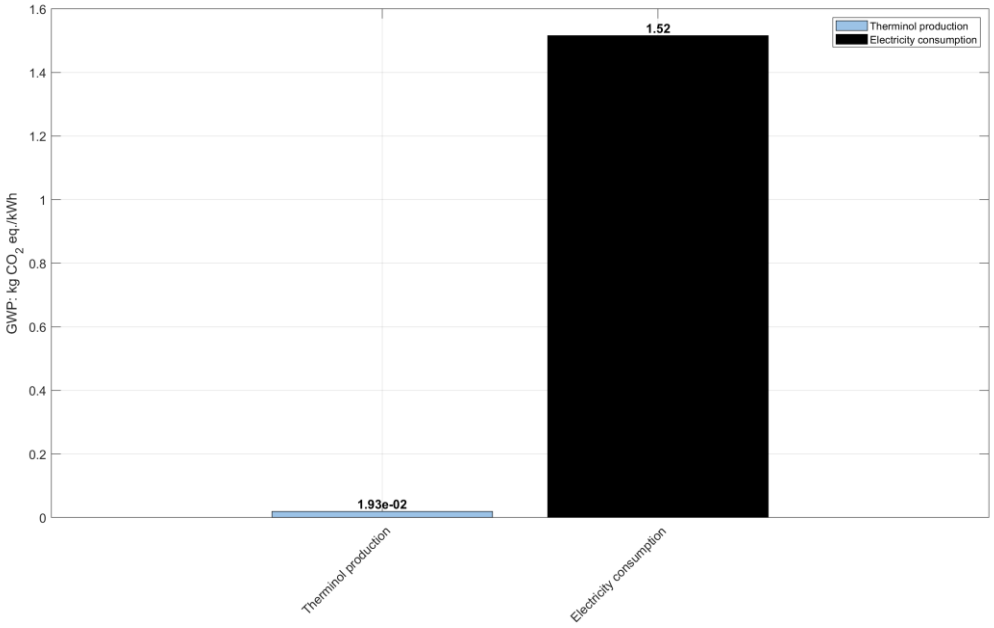

b.

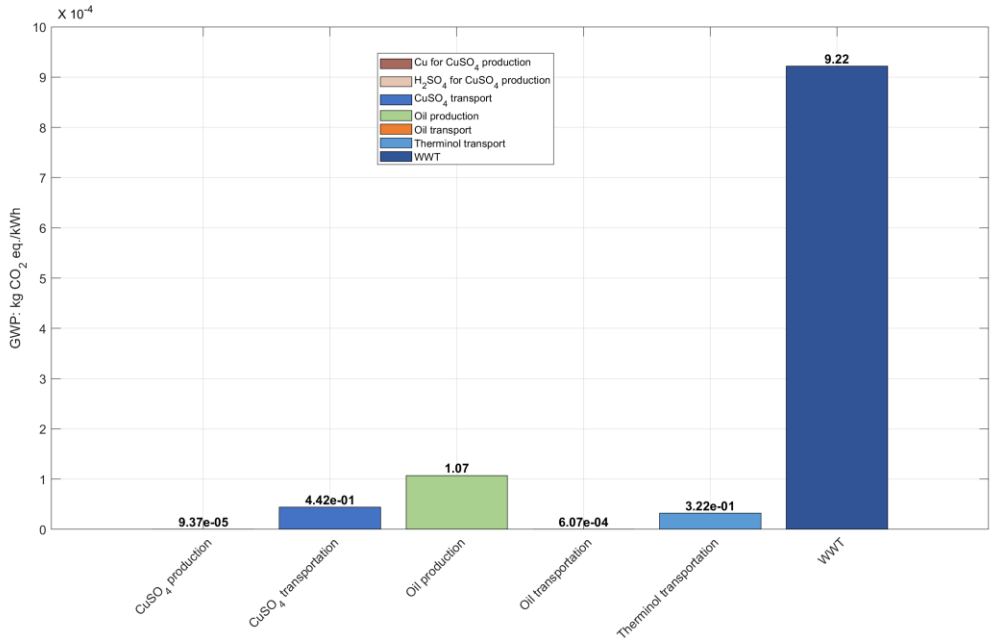

Figure 3. *GWP of Use Case 1 – The charging phase: a) major contributors and b) minor contributors*

Additionally, Figure 3b highlights the sub-systems with significantly smaller contributions, including municipal WWT ($9.22 \cdot 10^{-4}$ kg CO_2 eq./kWh), oil production and transportation ($1.07 \cdot 10^{-4}$ kg CO_2 eq./kWh and $6.07 \cdot 10^{-8}$ kg CO_2 eq./kWh, respectively), CuSO4 and Therminol V66 transportation ($4.42 \cdot 10^{-5}$ kg CO_2 eq./kWh and $3.22 \cdot 10^{-5}$ kg CO_2 eq./kWh, respectively). Although their absolute values are relatively low, they remain important in assessing the full environmental profile of the charging phase. Their inclusion underscores the fact that numerous minor contributors collectively represent a non-negligible share of the total GWP burden. Taken together, Figure 3a and Figure 3b provide a more comprehensive perspective:

while few sub-systems dominate the overall indicator, several others make modest yet meaningful contributions that must be considered when identifying optimisation opportunities.

Figure 4 illustrates the GWP associated with the discharging phase in Use Case 1. Similar to the charging phase, the results are divided into two complementary visualizations to distinguish the dominant contributors from the minor ones.

a.

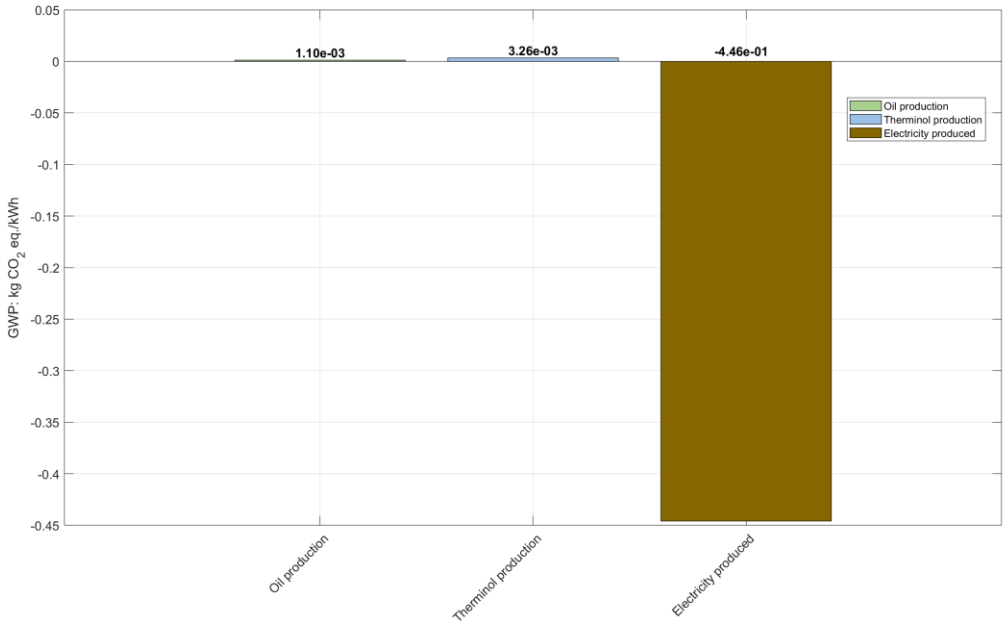

b.

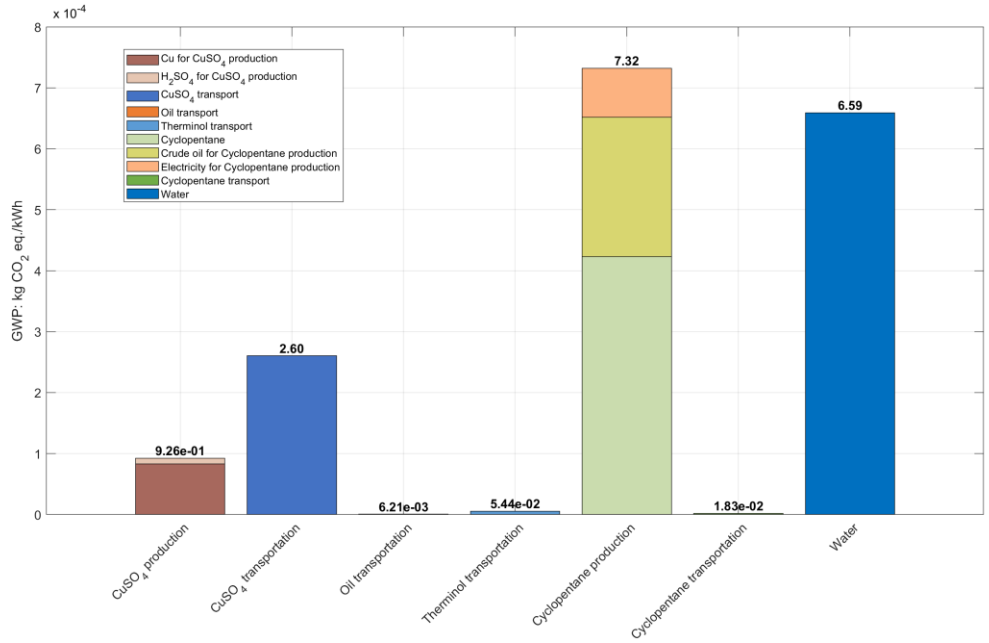

Figure 4. *GWP of Use Case 1 – The discharging phase: a) major contributors and b) minor contributors*

Figure 4a highlights the sub-systems with the highest contributions to the GWP during the discharging phase. As may be observed, the electricity generated in this stage exhibits the largest influence over the discharging step, around $-4.46 \cdot 10^{-1}$ kg CO_2 eq./kWh, thus dominating and clearly shaping the discharging profile. Nevertheless, there are relatively small positive

contributions exhibited by the oil and Therminol V66 production, respectively, leading to a final GWP for the discharging phase of $-4.40 \cdot 10^{-1}$ kg CO_2 eq./kWh.

By contrast, Figure 4b emphasizes minor contributors, such as the production and transportation of cyclopentane ($7.32 \cdot 10^{-4}$ kg CO_2 eq./kWh and $1.83 \cdot 10^{-6}$ kg CO_2 eq./kWh, respectively), water consumption ($6.59 \cdot 10^{-4}$ kg CO_2 eq./kWh), $CuSO_4$ production and transportation ($9.26 \cdot 10^{-5}$ kg CO_2 eq./kWh and $2.60 \cdot 10^{-4}$ kg CO_2 eq./kWh, respectively), as well as oil and Therminol V66 transportation-related processes. Although their absolute impacts are comparatively smaller, their inclusion completes the overall discharging profile.

Together, Figure 4a and Figure 4b illustrate the dual nature of the discharging phase: while electricity generation dominates the GWP, smaller contributors also exhibit an influence over the whole outcome. This comprehensive perspective is crucial for identifying mitigation strategies that both target major hotspots and leverage the benefits of processes with offsetting impacts.

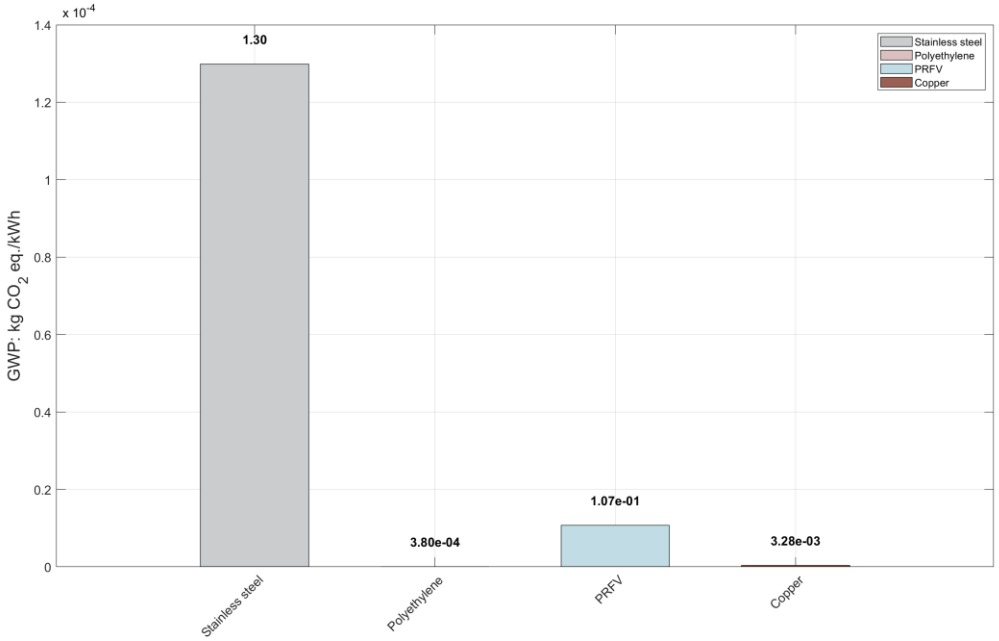

Figure 5. *GWP of Use Case 1 – The plant construction*

Figure 5 shows how the plant construction of Use Case 1 influences the GWP. From this subsystem total GWP of $1.41 \cdot 10^{-4}$ kg CO_2 eq./kWh, the use of stainless steel has the highest influence ($1.30 \cdot 10^{-4}$ kg CO_2 eq./kWh), while the other construction material (i.e., polyethylene, Polyester Reinforced Fiber-glass (PRFV) and copper) register minor contributions.

3.1.2. **Fossil Depletion Potential (FDP)**

The aggregated indicator (see Table 5) reports a total FDP value of $4.58 \cdot 10^{-1}$ kg oil eq./kWh for the charging phase of Use Case 1. This value is predominantly driven by the electricity required for dehydrating the thermal energy storage compound, which alone accounts for nearly $4.58 \cdot 10^{-1}$ kg oil eq./kWh (see Figure 6), thus representing the primary hotspot of this phase. Smaller contributions also arise from $CuSO_4$ and oil production along with the WWT processes.

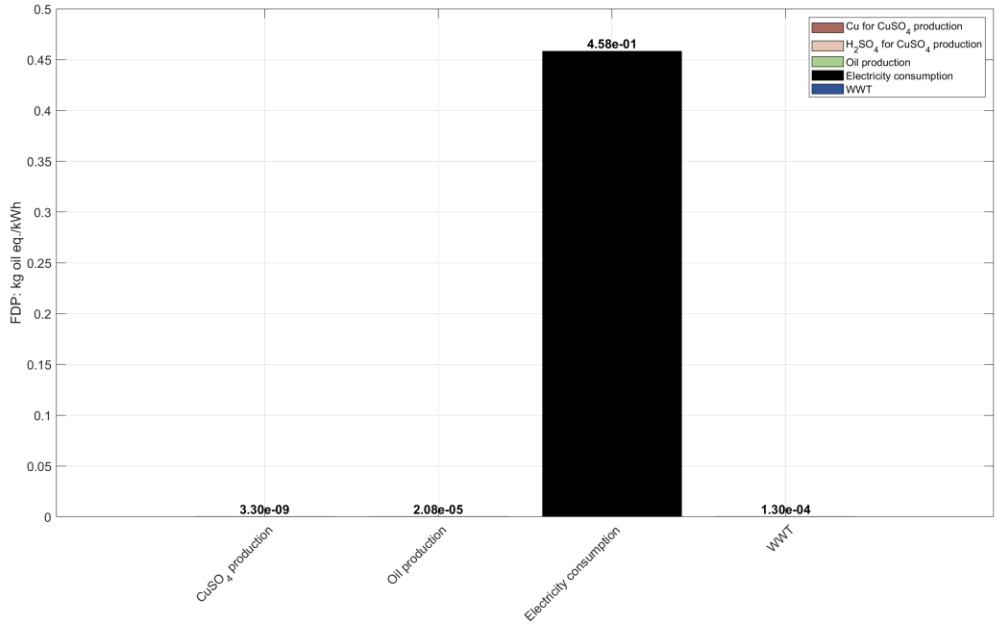

Figure 6. *FDP of Use Case 1 – The charging phase*

Figure 7 depicts the contributions of various sub-systems to the FDP during the discharging phase of the RESTORE system in Use Case 1. Notably, the electricity generated exhibits a negative contribution of ($-1.35 \cdot 10^{-1}$ kg oil eq./kWh), indicating that the discharging phase offsets fossil resource consumption by displacing conventional electricity production. In other words, the system effectively compensates for fossil resource use elsewhere in the energy network.

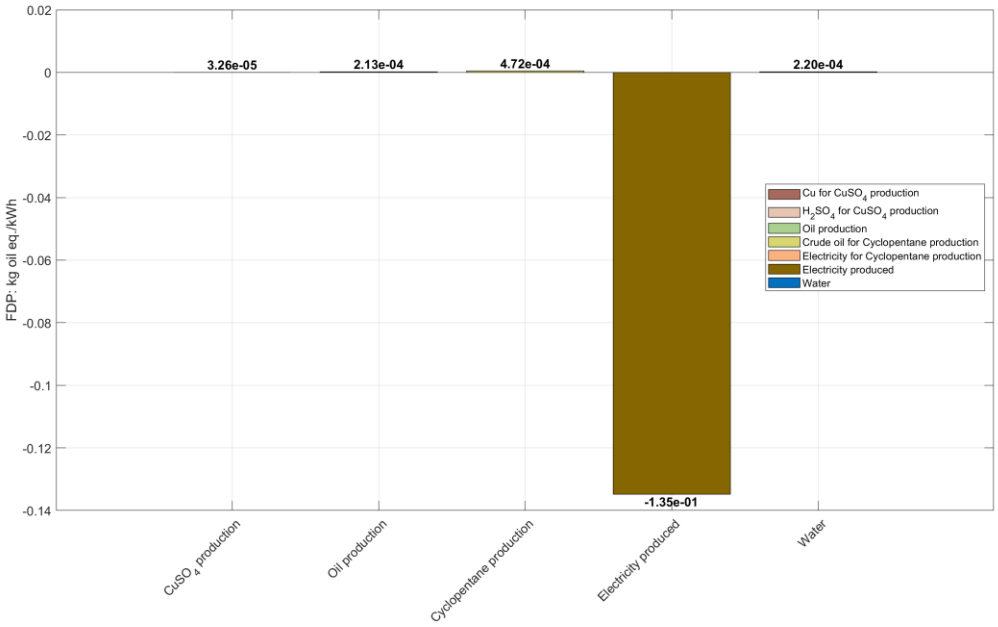

Figure 7. *FDP of Use Case 1 – The discharging phase*

In contrast, the production of $CuSO_4$ ($3.26 \cdot 10^{-5}$ kg oil eq./kWh), oil ($2.13 \cdot 10^{-4}$ kg oil eq./kWh), and cyclopentane ($4.72 \cdot 10^{-4}$ kg oil eq./kWh) along with water consumption ($2.20 \cdot 10^{-4}$ kg oil eq./kWh) exhibit certain influence though to a much lesser extent.

Overall, although the discharging phase is marked by considerable fossil resource consumption primarily due to cyclopentane production, the negative contribution from electricity generation offers a significant compensatory effect. This balancing dynamic explains the aggregated FDP value of $-1.34 \cdot 10^{-1}$ kg oil eq./kWh reported for the discharging phase in Table 5.

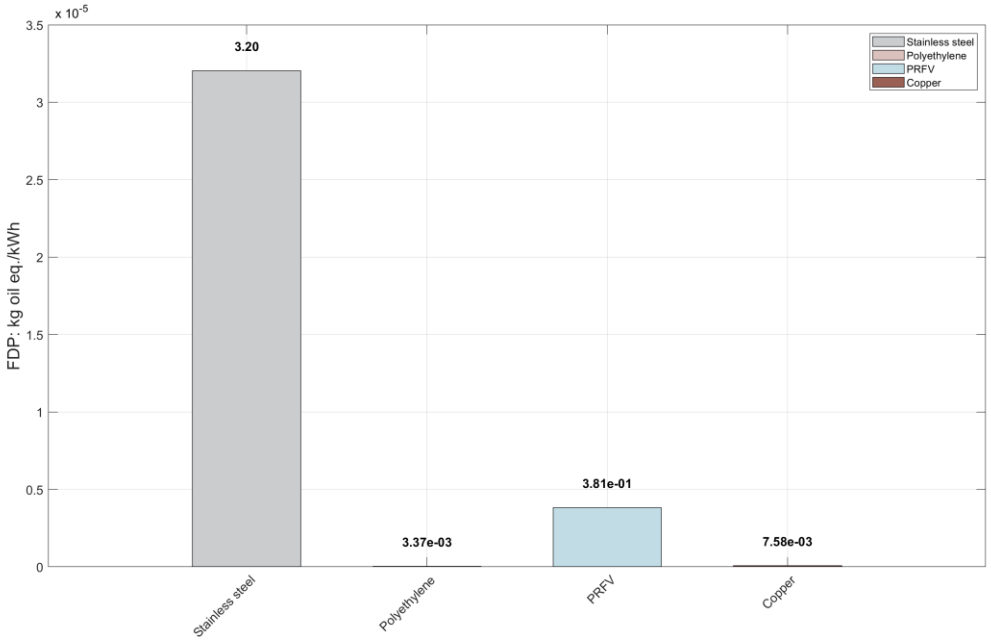

Figure 8. *FDP of Use Case 1 – The plant construction*

The plant construction has a minor contribution to FDP, as seen in Figure 8. In this KPI, the stainless-steel subsystem has the highest contribution, of the total of $3.60 \cdot 10^{-5}$ kg oil eq./kWh, it accounts for $3.20 \cdot 10^{-5}$ kg oil eq./kWh.

3.1.3. **Freshwater Ecotoxicity Potential (FETP)**

Freshwater ecotoxicity potential quantifies the potential effects of toxic substances on aquatic ecosystems. The charging phase results in $8.89 \cdot 10^{-5}$ kg 1.4-DB eq./kWh, whereas the discharging stage generates $-2.09 \cdot 10^{-5}$ 1.4-DB eq./kWh, representing nearly a fivefold increase. Impacts during charging are primarily driven by the electricity import from the grid ($7.90 \cdot 10^{-5}$ 1.4-DB eq./kWh) and wastewater emissions ($9.90 \cdot 10^{-6}$ 1.4-DB eq./kWh), while discharging is dominated by the water inlet ($1.57 \cdot 10^{-6}$ 1.4-DB eq./kWh). The plant construction has a very small contribution of $3.08 \cdot 10^{-6}$ kg 1.4-DB eq./kWh for this KPI. These findings indicate that although both phases contribute to aquatic toxicity, material-related processes during discharging substantially amplify the environmental burden compared to energy-related emissions in charging.

3.1.4. **Freshwater Eutrophication Potential (FEP)**

Freshwater eutrophication potential reflects nutrient emissions that can stimulate excessive algal growth in aquatic systems. In this use case, the charging phase results in $2.82 \cdot 10^{-4}$ kg P eq./kWh, while the discharging step scores $4.38 \cdot 10^{-5}$ kg P eq./kWh. Therminol V66 production is the primary contributor during charging ($2.73 \cdot 10^{-4}$ kg P eq./kWh), whereas discharging shows smaller yet notable contributions from Therminol V66 production as well $4.62 \cdot 10^{-5}$ kg P eq./kWh). The plant construction has a negligible contribution of $1.94 \cdot 10^{-10}$ kg P eq./kWh for this KPI. These results indicate that charging has a relatively higher eutrophication potential, largely due to heat transfer fluid production, making it the more critical phase for eutrophication impacts in Use Case 1.

3.1.5. **Human Toxicity Potential cancer (HTP_{cancer})**

In this impact category, HTP_{cancer}, the charging phase produces $4.48 \cdot 10^{-4}$ kg 1.4-DB eq./kWh, whereas discharging results in $-1.07 \cdot 10^{-4}$ kg 1.4-DB eq./kWh. During charging, the electricity generation and WWT are the primary contributors. In contrast, discharging is dominated by $CuSO_4$ and cyclopentane production ($1.04 \cdot 10^{-6}$ kg 1.4-DB eq./kWh and $1.21 \cdot 10^{-6}$ kg 1.4-DB eq./kWh, respectively). The plant construction has a very small contribution of $1.64 \cdot 10^{-4}$ kg 1.4-DB eq./kWh in this KPI. These findings suggest that material-related processes during discharging pose substantially greater carcinogenic risks than energy-related emissions in the charging phase.

3.1.6. **Human Toxicity Potential non-cancer ($HTP_{non\text{-}cancer}$)**

Non-carcinogenic human toxicity represents potential health risks from long-term exposure to toxic substances. In this case, the charging phase totals $4.97 \cdot 10^{-1}$ kg 1.4-DB eq./kWh, while the impact score during the discharging step decreases to $4.99 \cdot 10^{-2}$ kg 1.4-DB eq./kWh. Therminol V66 production is the main contributor during charging ($4.17 \cdot 10^{-1}$ kg 1.4-DB eq./kWh), whereas discharging impacts are shared between Therminol V66 and oil production ($7.06 \cdot 10^{-2}$ kg 1.4-DB eq./kWh and $1.46 \cdot 10^{-3}$ kg 1.4-DB eq./kWh, respectively). The plant construction has a contribution of $1.31 \cdot 10^{-3}$ kg 1.4-DB eq./kWh for this KPI.

3.1.7. **Metal Depletion Potential (MDP)**

Metal depletion quantifies the consumption of finite metal resources. The charging step accounts for $3.18 \cdot 10^{-3}$ kg Cu eq./kWh, whereas the score during discharging reaches $-4.97 \cdot 10^{-4}$ kg Cu eq./kWh. Charging impacts are dominated by electricity consumption ($3.17 \cdot 10^{-3}$ kg Cu eq./kWh), while discharging shows substantial contributions from water usage ($3.42 \cdot 10^{-4}$ kg Cu eq./kWh) and generated power ($-9.33 \cdot 10^{-4}$ kg Cu eq./kWh). The plant construction has an almost negligible contribution of $4.03 \cdot 10^{-6}$ kg Cu eq./kWh for this KPI. These results indicate that charging imposes higher metal depletion than the discharging step, making it the most resource-intensive stage with respect to metal use.

3.1.8. **Photochemical Ozone Formation Potential ecosystem ($POFP_{ecosystem}$)**

The photochemical ozone formation potential ($POFP_{ecosystem}$) evaluates the contribution of emitted precursors (e.g., NO_x, VOCs) to the formation of ground-level ozone, expressed in kg

NO_x equivalents per FU. This indicator reflects impacts on ecosystems, including vegetation and crop productivity, as high ozone concentrations can induce oxidative stress and reduce photosynthesis. In this study, $POFP_{ecosystem}$ provides insights into the contribution of the RESTORE system to ground-level ozone (commonly referred to as summer smog), expressed in kg NO_x eq./kWh. According to the results reported in Table 5, $POFP_{ecosystem}$ values of 12.30 kg NO_x eq./kWh are registered in the charging phase, while negative impacts of -2.72 kg NO_x eq./kWh are seen during discharging. These results indicate that while the charging stage contributes substantially to ozone precursor emissions, the discharging phase exerts a net mitigating effect due to electricity generation during the operation of the system.

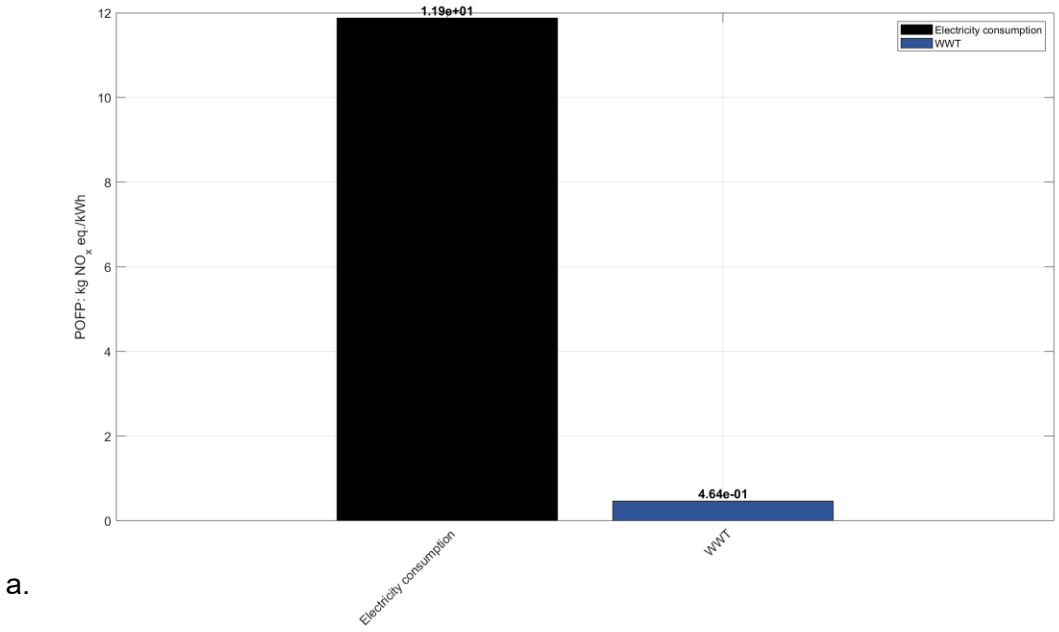

a.

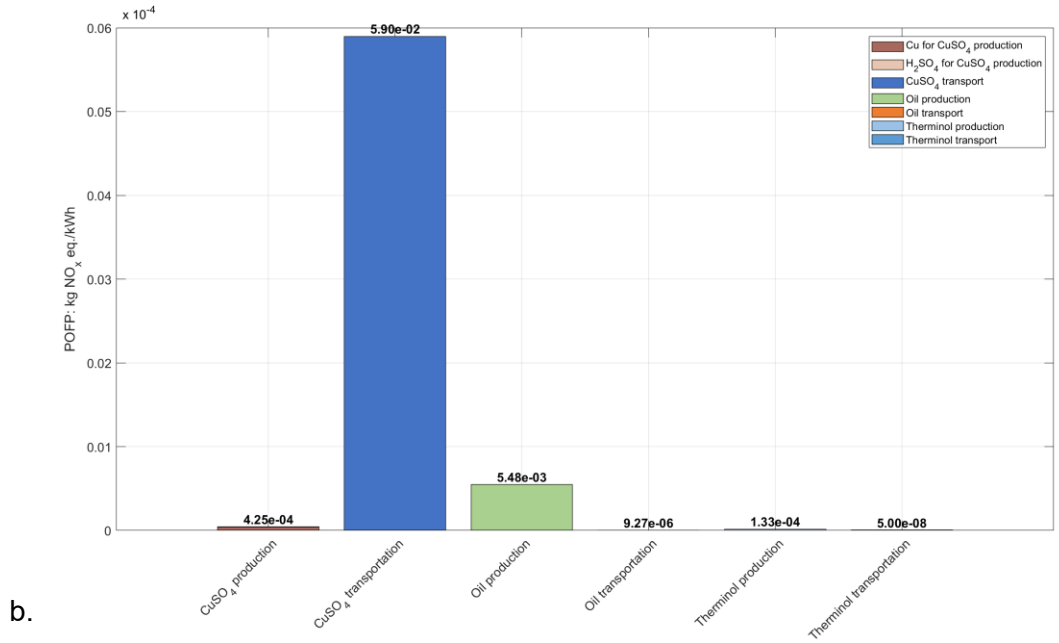

b.

Figure 9. *$POFP_{ecosystem}$ of Use Case 1 – The charging phase: a) major contributors and b) minor contributors*

Figure 9a and Figure 9b provides a detailed breakdown of contributors for the charging phase. As illustrated in Figure 9a, the two dominant contributors are electricity consumption ($1.19 \cdot 10^{1}$ kg NO_x eq./kWh) and WWT ($4.64 \cdot 10^{-1}$ kg NO_x eq./kWh), together accounting for the vast majority of the total $POFP_{ecosystem}$ impact during this stage. Notably, electricity import from the grid mix represents the vast majority of the overall impact for the charging phase.The minor contributors are illustrated in Figure 9b and include sub-systems such as chemical production and transportation processes, each contributing only marginal amounts (ranging from 10^{-6} up to 10^{-12} kg NO_x eq./kWh). While their impact on the overall $POFP_{ecosystem}$ is negligible compared to the dominant effects of electricity consumption and WWT, they complete the comprehensive profile of upstream and downstream processes associated with the charging phase.

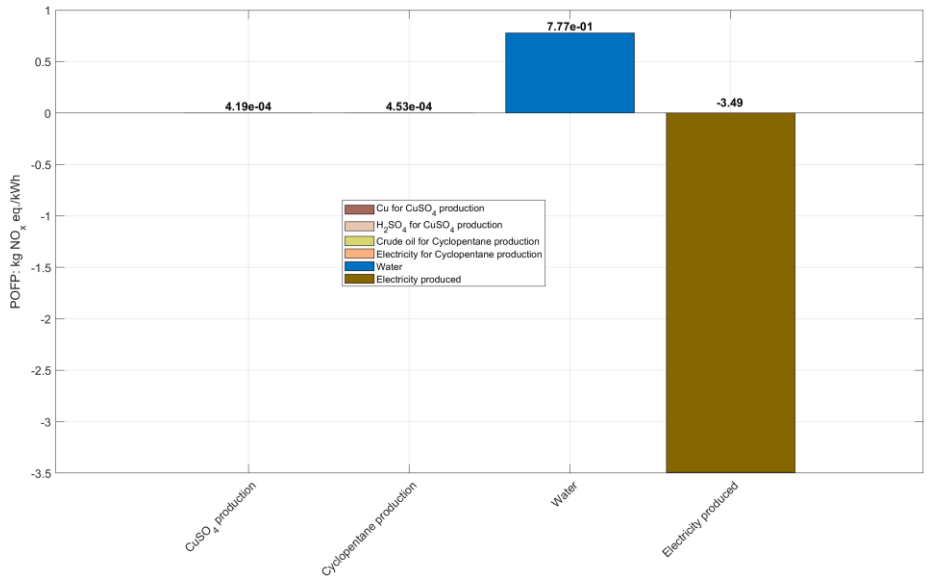

a.

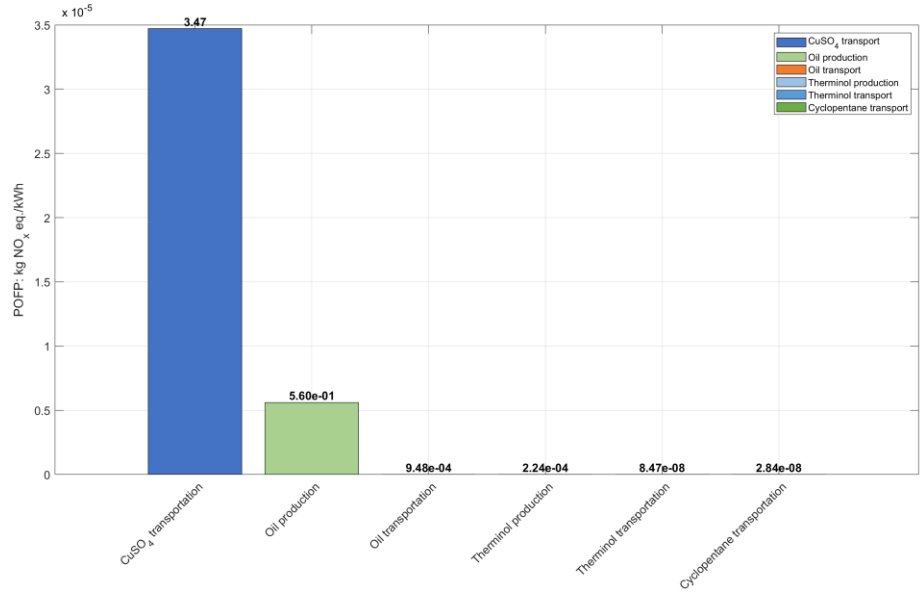

b.

Figure 10. *$POFP_{ecosystem}$ of Use Case 1 – The discharging phase: a) major contributors and b) minor contributors*

In contrast, the discharging phase exhibits a net negative $POFP_{ecosystem}$ of -2.72 kg NO_x eq./kWh, reflecting an avoided burden effect. This result stems from the electricity generation during discharging, which offsets emissions that would otherwise occur from conventional grid-based electricity production.

As shown in Figure 10a, the main contributors during this phase include residual chemical use and minor production processes; however, their effects are overshadowed by the substantial negative contribution from electricity generation.

Figure 10b further illustrates the negligible contributors, whose impacts are minimal and do not affect the overall negative outcome.

The comparative results reveal a pronounced asymmetry between the charging and discharging stages. The charging phase represents the critical hotspot for $POFP_{ecosystem}$, driven mostly by electricity use and WWT, which together account for approximately 12.36 kg NO_x eq./kWh, and thus explain the positive result reported in Table 5. In contrast, the discharging phase provides a modest mitigating effect, reducing ozone precursor emissions by about 2.72 kg NO_x eq./kWh; however, this reduction is insufficient to offset the substantial burden of the charging phase.

From a life-cycle perspective, these findings suggest that mitigation strategies for the $POFP_{ecosystem}$ should primarily target the charging stage, focusing on reducing electricity consumption and exploring alternative treatment pathways to limit the significant contribution of WWT.

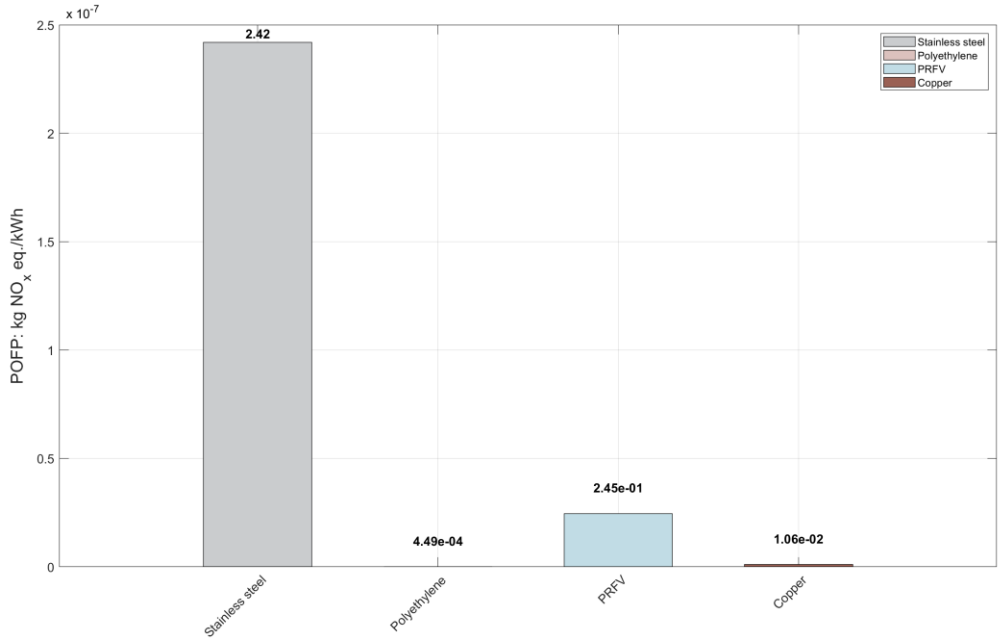

Figure 11. *$POFP_{ecosystem}$ of Use Case 1 – The plant construction*

The plant construction has a minor contribution to the $POFP_{ecosystem}$, as seen in Figure 11. In the case of this KPI, the stainless-steel subsystem has the biggest contribution, exhibiting $2.42 \cdot 10^{-7}$ kg NO_x eq./kWh of the total of $2.68 \cdot 10^{-7}$ kg NO_x eq./kWh.

3.1.9. **Stratospheric Ozone Depletion Potential (ODP)**

As shown in Figure 12, the charging phase exhibits a very low ODP impact score ($1.01 \cdot 10^{-6}$ kg CFC-11 eq./kWh). The profile is highly dominated by electricity consumption and Therminol V66 transportation, each accounting for nearly half of the total impact score ($5.18 \cdot 10^{-7}$ kg CFC-11 eq./kWh and $4.92 \cdot 10^{-7}$ kg CFC-11 eq./kWh, respectively). All other processes, including $CuSO_4$ production and transportation, oil production and transportation, as well as WWT, exhibit significantly lower impact.

Taken together, these results indicate that upstream processes – particularly the transport step in the Therminol V66 supply chain – and the electricity import from the current grid mix are the only factors with significant influence on charging-phase ODP. Accordingly, the most effective mitigation strategies would imply (i) further decarbonizing the charging electricity supply, especially targeting residual use of refrigerants/halocarbons in electricity generation and grid services and (ii) shifting Therminol V66 logistics toward lower-ODP transport chains (e.g., fuels/vehicles and routes with lower halogenated refrigerant leakage footprints in their upstream).

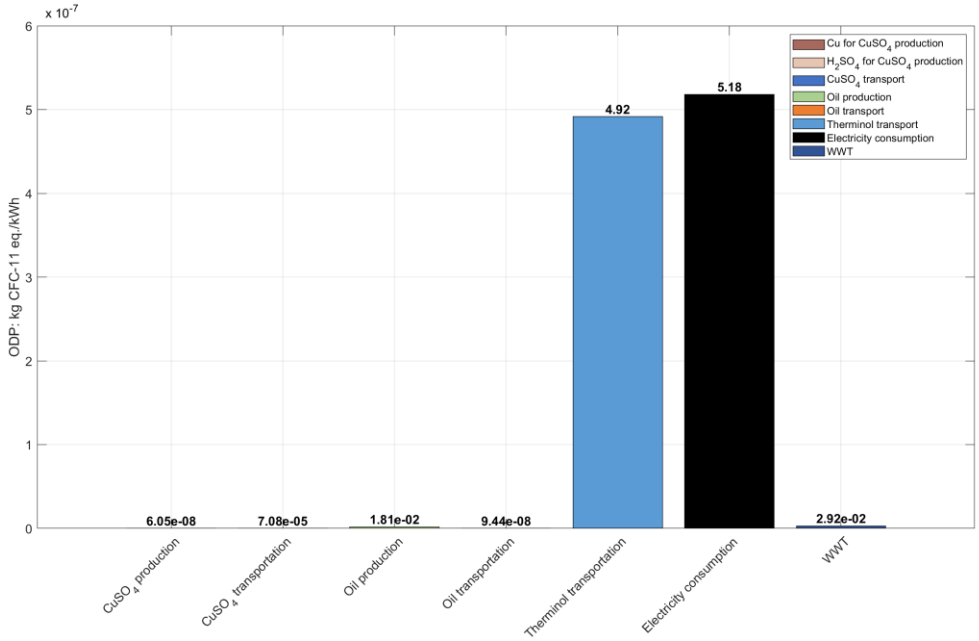

Figure 12. *ODP of Use Case 1 – The charging phase*

In contrast, the ODP impact score during the discharging phase shows a negative impact score ($-2.22 \cdot 10^{-8}$ kg CFC-11 eq./kWh), which is due to the electricity generated at this stage (see Figure 13). Positive contributions arise from several processes, such as the Therminol V66 transport up to the plant ($8.32 \cdot 10^{-8}$ kg CFC-11 eq./kWh), cyclopentane transport ($2.79 \cdot 10^{-8}$ kg CFC-11 eq./kWh), oil production ($1.85 \cdot 10^{-8}$ kg CFC-11 eq./kWh), and water use ($4.71 \cdot 10^{-10}$ kg CFC-11 eq./kWh), among others. The electricity generated exhibits a negative contribution of $-1.52 \cdot 10^{-7}$ kg CFC-11 eq./kWh, reflecting system-specific offsets.

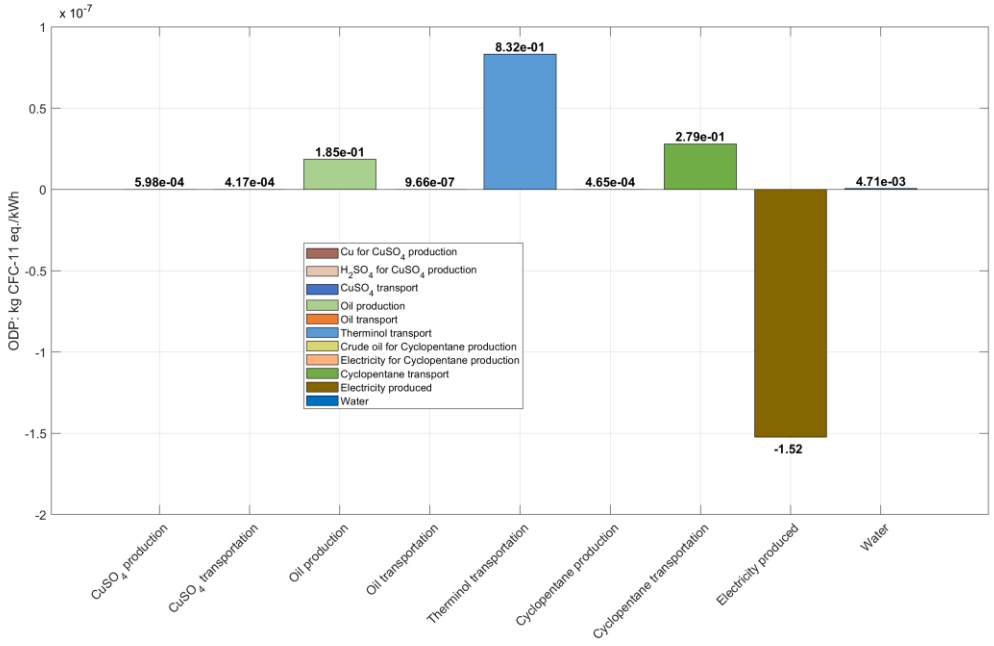

Figure 13. *ODP of Use Case 1 – The discharging phase*

This pattern clearly emphasizes Therminol V66 and cyclopentane transportation as the primary drivers of ODP during the discharging step, yet highlights the offset added through power generation. Consequently, mitigation efforts should focus on the Therminol V66 and cyclopentane supply chains, including ensuring that process refrigerants, blowing agents, and other halogenated substances used upstream are minimized, properly managed, and leak-free; seeking alternative process routes or suppliers with lower ODP profiles; and critically reviewing background datasets to ensure conservative treatment of halocarbon releases.

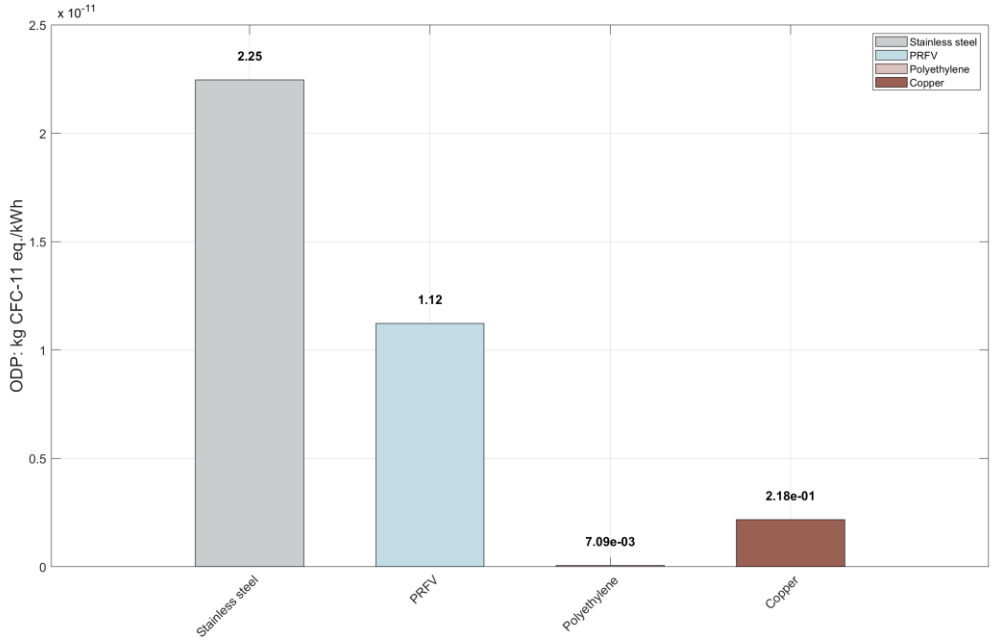

Figure 14. *ODP of Use Case 1 – The plant construction*

The plant construction has a minor contribution to ODP, as seen in Figure 14. In this instance, the stainless-steel subsystem has the largest contribution, contributing by $2.25 \cdot 10^{-11}$ kg CFC eq./kWh of the total of $3.39 \cdot 10^{-11}$ kg CFC eq./kWh.

3.1.10. **Terrestrial Acidification Potential (TAP)**

Terrestrial acidification reflects emissions that increase soil and water acidity. In this Use Case, the charging totals $2.44 \cdot 10^{-3}$ kg SO_2 eq./kWh, while the impact related to the discharging step reaches $1.86 \cdot 10^{-5}$ kg SO_2 eq./kWh. Charging impacts are mainly driven by Therminol V66 production and electricity consumption, while discharging is dominated by Therminol V66 production, but also by water usage. The plant construction has a negligible contribution of $7.92 \cdot 10^{-7}$ kg SO_2 eq./kWh for this KPI. These results indicate that discharging imposes significantly lower terrestrial acidification potential impacts compared to the charging step.

3.1.11. **Terrestrial Ecotoxicity Potential (TETP)**

Terrestrial ecotoxicity measures the adverse effects of chemical emissions on terrestrial ecosystems. In this Use Case, the charging phase amounts to $1.76 \cdot 10^{-1}$ kg 1.4-DB eq./kWh, whereas discharging reaches a negative impact score of $-5.11 \cdot 10^{-2}$ kg 1.4-DB eq./kWh. Charging impacts are largely driven by electricity use, while discharging is dominated by water consumption and $CuSO_4$ production ($1.02 \cdot 10^{-4}$ kg 1.4-DB eq./kWh and $2.97 \cdot 10^{-4}$ kg 1.4-DB eq./kWh, respectively). As observed, discharging results in negative emissions and this is mainly due to the power generation within this step. The plant construction has a contribution of $1.48 \cdot 10^{-2}$ kg 1.4-DB eq./kWh in this KPI.

3.1.12. **Use Case 1 – Main conclusions**

The main conclusions for the Use Case 1 are the following:

- The charging phase exhibits a high overall GWP value, primarily driven by the electricity imports from the grid, whereas the discharging phase results in a net negative GWP due to electricity generation.
- The FDP associated with the charging phase is largely governed by electricity demand, in particular the energy required for dehydrating the thermochemical compound. By contrast, the discharging phase provides a fossil resource credit through the displacement of grid-based electricity.
- $POFP_{ecosystem}$ is substantial during the charging phase, mainly due to grid electricity consumption and municipal WWT, while the discharging phase shows a reduction through avoided grid emissions.
- Overall, the sourcing of operational electricity is the dominant factor influencing climate and fossil resource outcomes, whereas the contributions of chemicals and construction materials remain relatively minor.

3.2. Use Case 2 – Gmunden Cement Plant – Results and discussions

Table 6 presents the LCA results for the Use Case 2 scenario, considering the limitations and assumptions applied in this study.

Table 6. LCA results for Use Case 2

KPI	Units	Charging	Discharging	Plant construction
GWP	kg CO_2 eq./kWh	$6.20 \cdot 10^{-1}$	$-4.35 \cdot 10^{-1}$	$6.38 \cdot 10^{-3}$
FDP	kg oil eq./kWh	$1.87 \cdot 10^{-1}$	$-1.34 \cdot 10^{-1}$	$5.12 \cdot 10^{-3}$
FETP	kg 1.4-DB eq./kWh	$4.24 \cdot 10^{-5}$	$-2.03 \cdot 10^{-5}$	$2.08 \cdot 10^{-4}$
FEP	kg P eq./kWh	$1.35 \cdot 10^{-5}$	$1.13 \cdot 10^{-4}$	$8.25 \cdot 10^{-9}$
HTP_{cancer}	kg 1.4-DB eq./kWh	$2.12 \cdot 10^{-4}$	$-1.06 \cdot 10^{-4}$	$1.17 \cdot 10^{-3}$
$HTP_{non\text{-}cancer}$	kg 1.4-DB eq./kWh	$4.86 \cdot 10^{-2}$	$1.61 \cdot 10^{-1}$	$8.88 \cdot 10^{-2}$
MDP	kg Cu eq./kWh	$1.33 \cdot 10^{-3}$	$-2.06 \cdot 10^{-4}$	$4.04 \cdot 10^{-5}$
$POFP_{ecosystem}$	kg NO_x eq./kWh	5.30	-2.75	$8.19 \cdot 10^{-6}$
ODP	kg CFC eq./kWh	$2.50 \cdot 10^{-7}$	$1.75 \cdot 10^{-7}$	$1.24 \cdot 10^{-9}$
TAP	kg SO_2 eq./kWh	$5.79 \cdot 10^{-4}$	$4.23 \cdot 10^{-4}$	$9.77 \cdot 10^{-6}$
TETP	kg 1.4-DB eq./kWh	$7.21 \cdot 10^{-2}$	$-5.13 \cdot 10^{-2}$	$9.90 \cdot 10^{-1}$

The following sections provides information, commentary, and discussions on the main sub-processes that drive the most relevant impact indicators for this Use Case scenario.

3.2.1. Global Warming Potential (GWP)

As shown in Figure 15a, the charging phase results in a total GWP of $6.20 \cdot 10^{-1}$ kg CO_2 eq./kWh. The dominant hotspot is the electricity consumption, which accounts for the vast majority of emissions due to the fact that it is primarily based on fossil-fuel resources, thus reflecting the carbon intensity of the regional electricity supply. By contrast, the minor contributors shown in Figure 15b, including $CuSO_4$ and Therminol V66 transportation processes, as well as the municipal wastewater treatment, together account for a significantly lower impact. Overall, this distribution highlights that the climate change impacts of the charging phase are driven primarily by electricity consumption, emphasizing the importance of sourcing low-carbon electricity supply.

a.

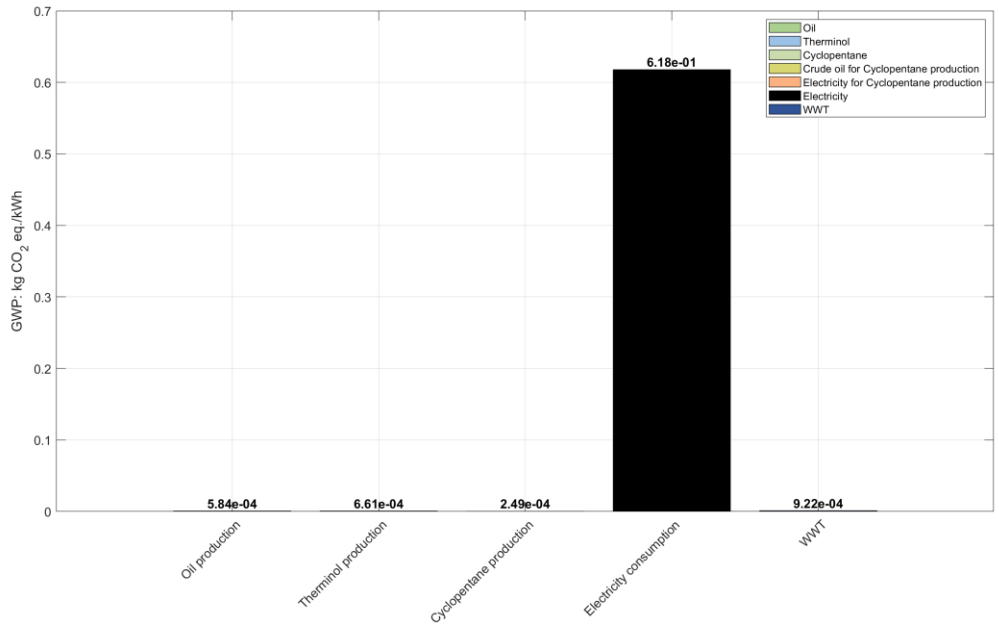

b.

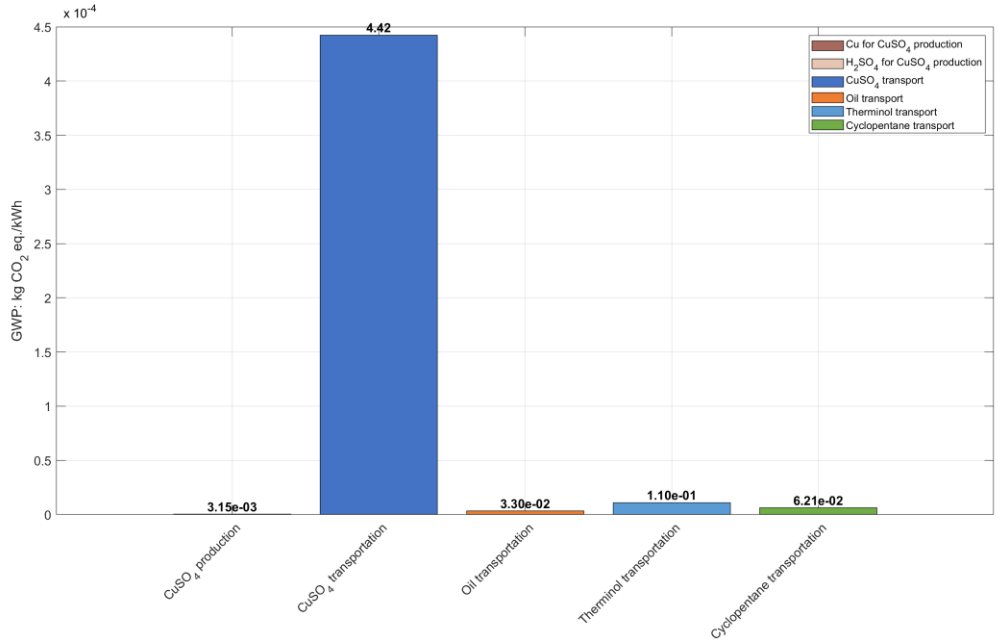

Figure 15. *GWP of Use Case 2 – The charging phase: a) major contributors and b) minor contributors*

In the discharging phase, the GWP reaches negative values of $-4.35 \cdot 10^{-1}$ kg CO_2 eq./kWh. This is mainly due to the electricity generation which contributes by $-4.51 \cdot 10^{-1}$, as shown in Figure 16a. Positive contributions arise from other processes, including $CuSO_4$ production and transportation, Therminol V66 production and transport, as well as oil production (see Figure 16a and 16b). The negative GWP impacts during discharging highlights the decisive role of electricity generation in shaping the life cycle climate impacts of the system.

a.

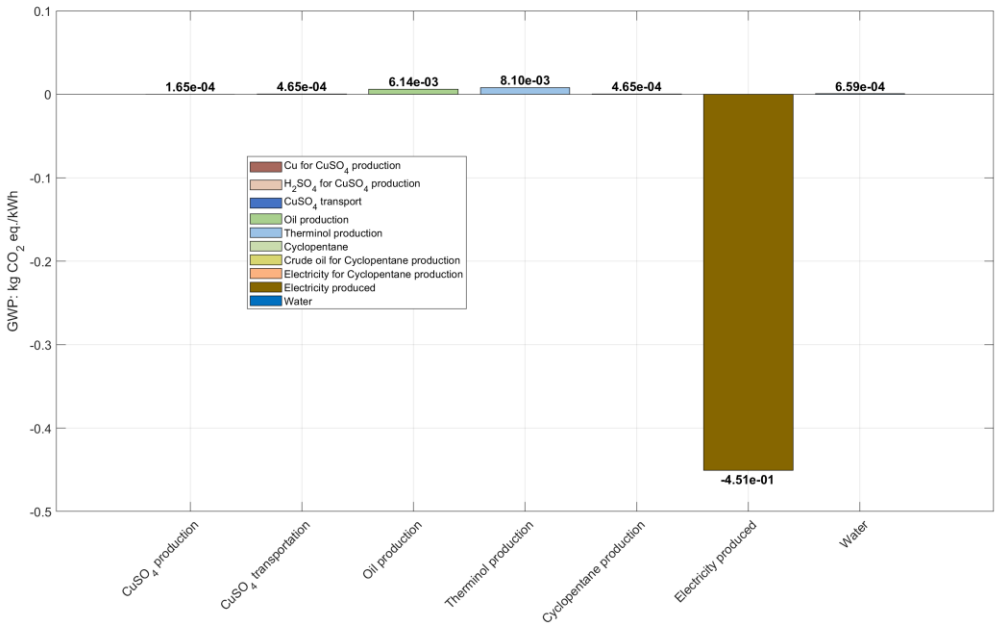

b.

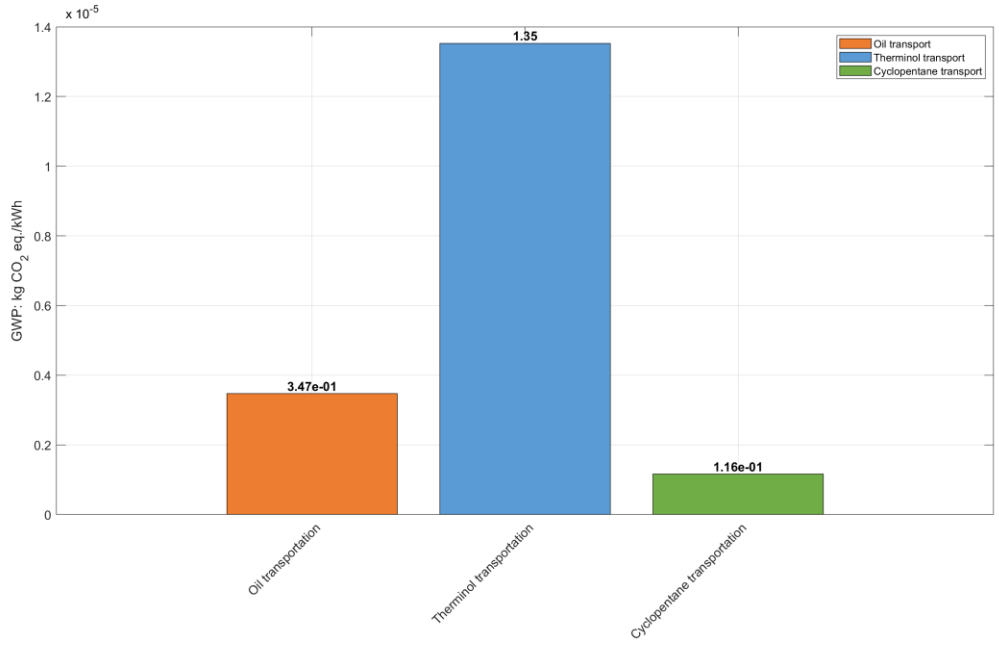

Figure 16. *GWP of Use Case 2 – The discharging phase: a) major contributors and b) minor contributors*

As illustrated in Figure 17, the GWP associated with plant construction is considerably lower than that of the operational phases. The construction-related GWP amounts to $6.38 \cdot 10^{-3}$ kg CO_2 eq./kWh, a major contribution coming from the storage tanks, which are made out of polyethylene. Contributions from fiberglass (PRFV) and copper are comparatively negligible. Overall, the results indicate that plant construction has only a minor effect on life cycle GWP, with operational emissions dominating the climate impact profile. It should also be noted that the construction data considered did not cover the full range of required materials, which may result in an underestimation of this stage's absolute contribution.

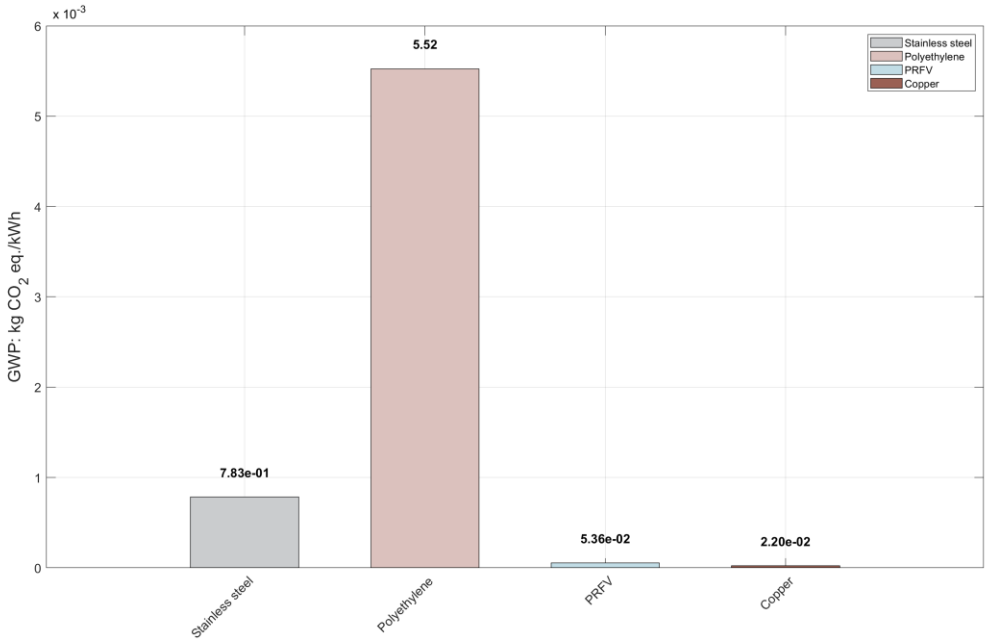

Figure 17. *GWP of Use Case 2 – The plant construction*

3.2.2. **Fossil Depletion Potential (FDP)**

During the charging phase, the total FDP amounts to $1.87 \cdot 10^{-1}$ kg oil eq./kWh. Electricity import from the grid mix exhibits the largest influence, thus underlining the role of energy demand as a key driver of fossil resource depletion (Figure 18). Smaller contributions stem from $CuSO_4$ production ($1.11 \cdot 10^{-8}$ kg oil eq./kWh), oil production ($1.13 \cdot 10^{-4}$ kg oil eq./kWh), municipal WWT ($1.30 \cdot 10^{-4}$ kg oil eq./kWh), as well as cyclopentane production ($1.60 \cdot 10^{-4}$ kg oil eq./kWh), while transportation impacts are negligible. Overall, fossil resource depletion in charging is primarily linked to the electricity use, suggesting that mitigation strategies should prioritize the integration of low-carbon electricity sources and the adoption of alternative manufacturing routes.

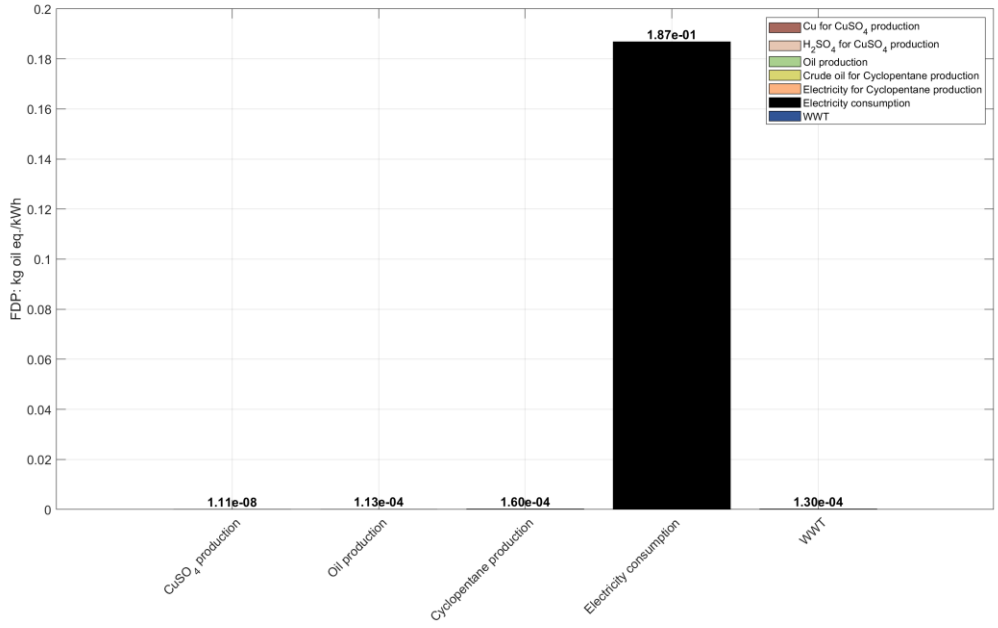

Figure 18. *FDP of Use Case 2 – The charging phase*

In the discharging phase, FDP totals -1.34·10^{-1} kg oil eq./kWh, with electricity generation dominating the profile (Figure 19). Minor positive contributions come from $CuSO_4$, oil, and cyclopentane production, as well as water consumption. Overall, the pattern closely reflects that observed for GWP, underscoring that fossil resource depletion is largely dictated by energy-intensive chemical production and energy sourcing. This highlights the importance of reducing reliance on fossil-based feedstocks and integrating cleaner energy pathways.

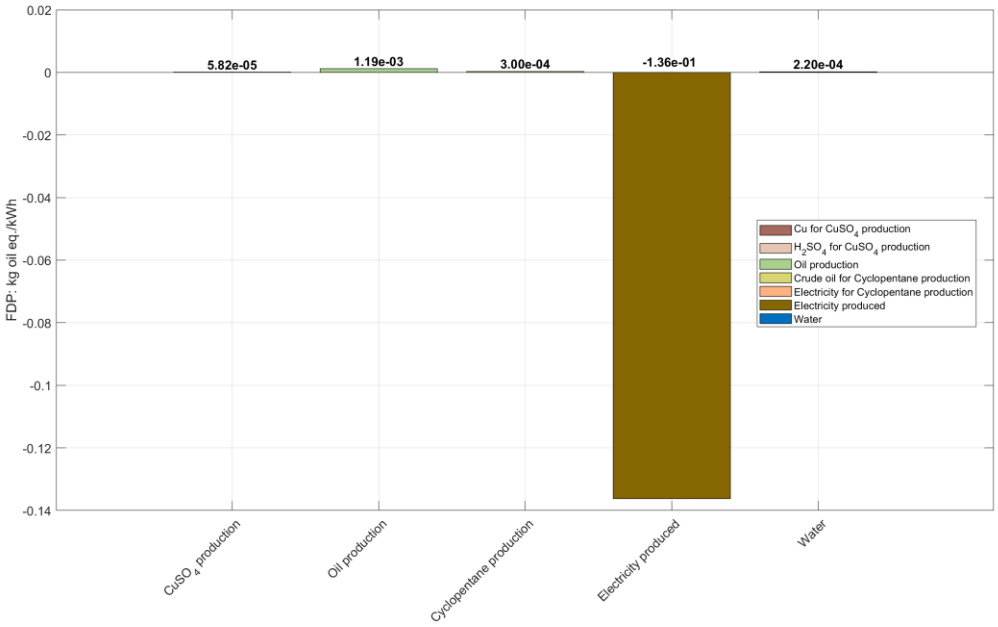

Figure 19. *FDP of Use Case 2 – The discharging phase*

For plant construction, FDP remains relatively minor compared to operational phases. As seen in Figure 20, it contributes with a total of 5.12·10^{-3} kg oil eq./kWh. The main contributors are polyethylene and stainless steel, while copper and fiberglass, PRFV, exhibit only negligible

contributions. Overall, construction-related fossil depletion is small relative to charging and discharging phases, indicating that while material selection can slightly influence embodied fossil use, the dominant drivers of FDP remain the power and chemical requirements during operation.

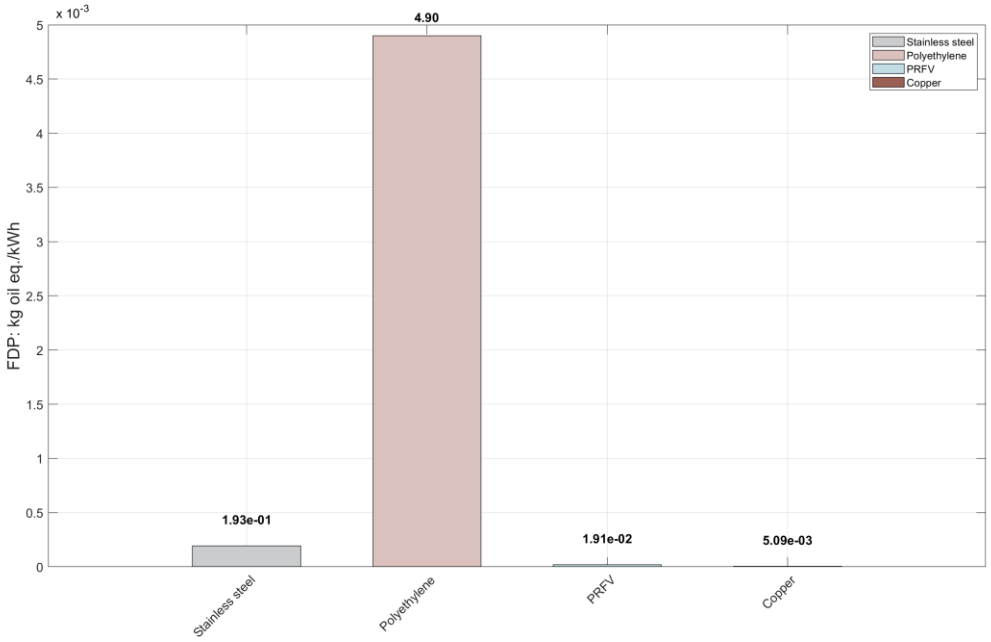

Figure 20. *FDP of Use Case 2 – The plant construction*

3.2.3. **Freshwater Ecotoxicity Potential (FETP)**

For the FETP impact category, the charging phase contributes $4.24 \cdot 10^{-5}$ kg 1.4-DB eq./kWh, mainly driven by electricity import from the grid and WWT. The impact for the discharging phase reaches a negative impact score of $-2.03 \cdot 10^{-5}$ kg 1.4-DB eq./kWh, and it may be explained by the electricity produced during this stage. Plant construction impact reaches a total value of $2.08 \cdot 10^{-4}$ kg 1.4-DB eq./kWh, primarily due to the use of polyethylene tanks for thermochemical storage material.

3.2.4. **Freshwater Eutrophication Potential (FEP)**

Charging phase results in $1.35 \cdot 10^{-5}$ kg P eq./kWh, whereas the impact in the discharging step reaches a total impact of $1.13 \cdot 10^{-4}$ kg P eq./kWh, largely due to contributions from Therminol V66 production and electricity consumption. Plant construction impact is negligible in comparison, with a total impact of $8.25 \cdot 10^{-9}$ kg P eq./kWh, indicating that material selection during construction is virtually irrelevant for this category. Overall, phosphorus-related impacts are clearly dominated by the operational phases, particularly discharging.

3.2.5. **Human Toxicity Potential cancer (HTP_{cancer})**

In the charging phase, the impact reaches $2.12 \cdot 10^{-4}$ kg 1.4-DB eq./kWh, decreasing up to $-1.06 \cdot 10^{-4}$ kg 1.4-DB eq./kWh during discharging. Electricity consumption is the main contributor during the charging phase, while the negative scores during discharging may be explained by the electricity generation through this step. Plant construction impact reaches a

total value of $1.17 \cdot 10^{-3}$ kg 1.4-DB eq./kWh, primarily due to the use of polyethylene tanks for thermochemical storage material.

3.2.6. **Human Toxicity Potential non-cancer ($HTP_{non\text{-}cancer}$)**

In the charging step, the $HTP_{non\text{-}cancer}$ impact registers a total of $4.86 \cdot 10^{-2}$ kg 1.4-DB eq./kWh, while the impact increases in the discharging step up to $1.61 \cdot 10^{-1}$ kg 1.4-DB eq./kWh. The main contributors are Therminol V66 production and electricity consumption, for the charging phase, while for the discharging phase, electricity generation offsets part of the high contribution of Therminol V66 production. Plant construction impact scores a total of $8.88 \cdot 10^{-2}$ kg 1.4-DB eq./kWh, primarily due to the use of polyethylene tanks for thermochemical storage material.

3.2.7. **Metal Depletion Potential (MDP)**

In the MDP impact category, the charging phase contributes by $1.33 \cdot 10^{-3}$ kg Cu eq./kWh, whereas the discharging step reaches negative impacts of $-2.06 \cdot 10^{-4}$ kg Cu eq./kWh. In comparison, plant construction impact is negligible, with a total of 4.04·10-5 kg Cu eq./kWh, thus indicating that material selection during construction is virtually irrelevant for this category. Overall, metal depletion impacts are clearly dominated by the charging step.

3.2.8. **Photochemical Ozone Formation Potential ecosystem ($POFP_{ecosystem}$)**

During the charging phase, the $POFP_{ecosystem}$ reaches 5.30 kg NOx eq./kWh. Electricity consumptions, thus electricity import from the grid mix, followed by the wastewater treatment, WWT, rank as the primary and secondary contributors (Figure 21a). Minor contributions arise from cyclopentane production and other production and transport processes, as detailed in Figure 21b. These results indicate that electricity use, water treatment, and chemical production and transport are all significant sources of ozone precursors. The high $POFP_{ecosystem}$ suggests the potential for ground-level ozone formation to affect local ecosystems and vegetation in the vicinity of production and electricity generation sites.

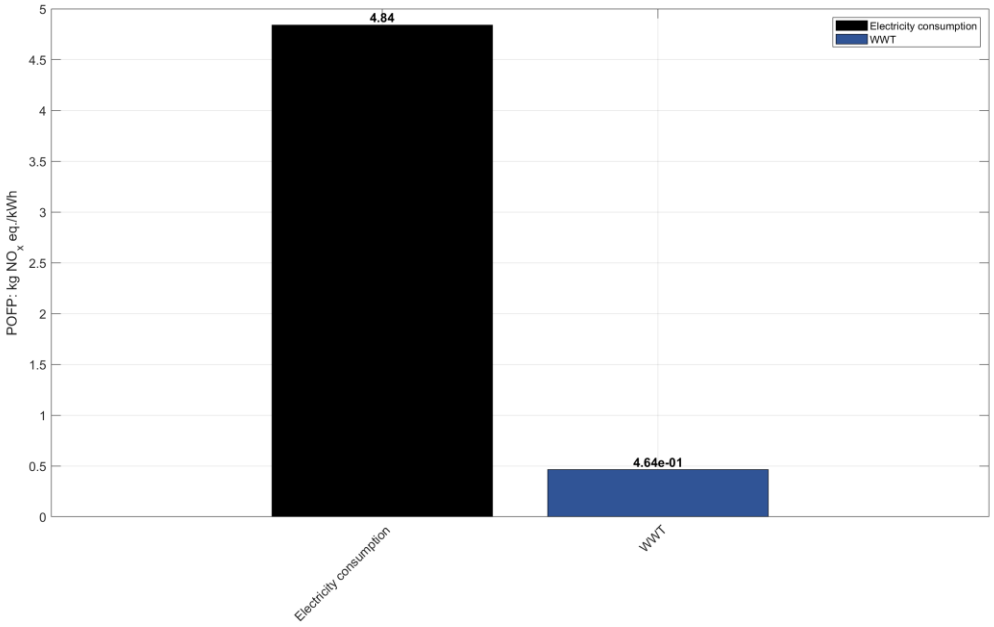

a.

b.

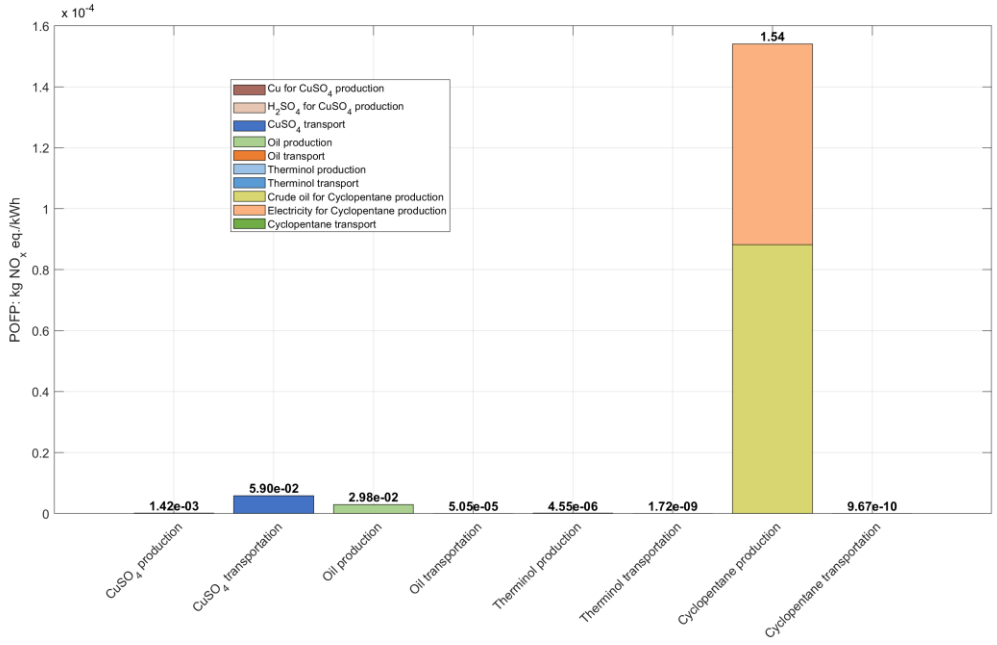

Figure 21. *$POFP_{ecosystem}$ of Use Case 2 – The charging phase: a) major contributors and b) minor contributors*

In the discharging phase, $POFP_{ecosystem}$ decreases to -2.75 kg NO_x eq./kWh, primarily due to the electricity generated at this stage (see Figure 22a). Positive contributions arise from water consumption, $CuSO_4$ and cyclopentane production, respectively, as well as other processes as detailed in Figure 22b. The reduction relative to the charging phase indicates that ozone precursor formation is substantially lower during discharge; however, WWT continues to play a significant role. This highlights the potential for further emissions reduction by adopting alternative or improved water treatment strategies.

a.

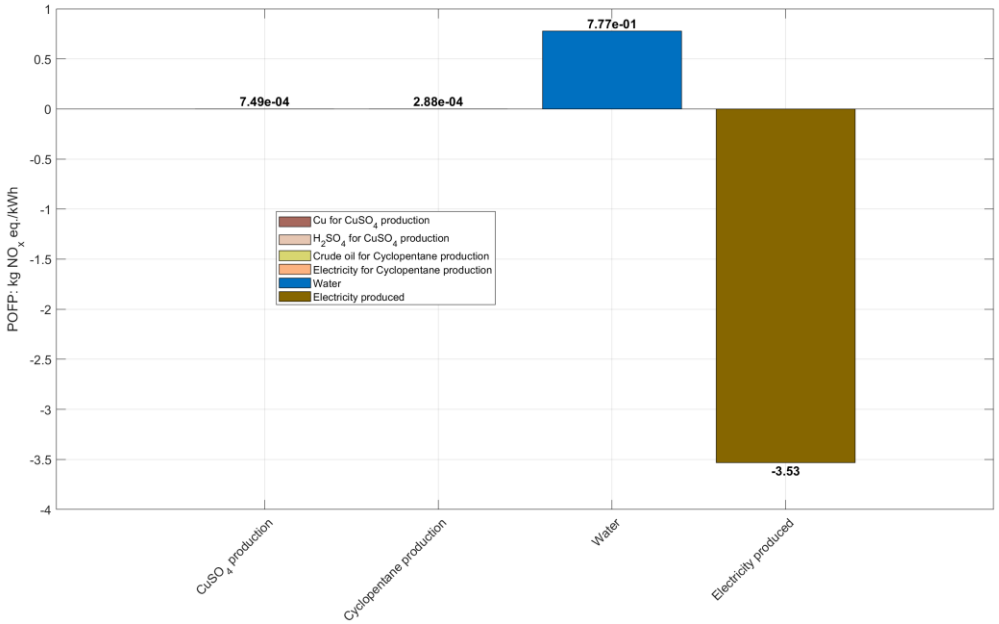

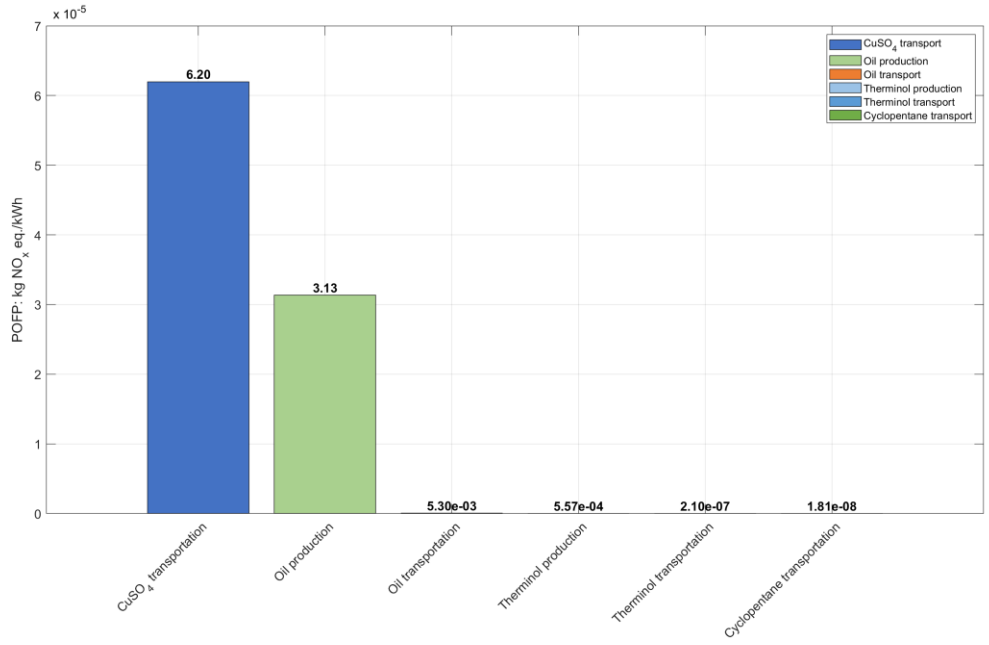

Figure 22. *$POFP_{ecosystem}$ of Use Case 2 – The discharging phase: a) major contributors and b) minor contributors*

$POFP_{ecosystem}$ associated with plant construction is very low, reaching a total of $8.19 \cdot 10^{-6}$ kg NO_x eq./kWh. The impact scores registered are because the primary contributor is the utilization of a polyethylene tank, as presented in Figure 23. These results indicate that construction represents only a minor source of $POFP_{ecosystem}$ relative to operational stages. While material selection can slightly reduce $POFP_{ecosystem}$, the primary focus for mitigation should remain on electricity and chemical production during system operation.

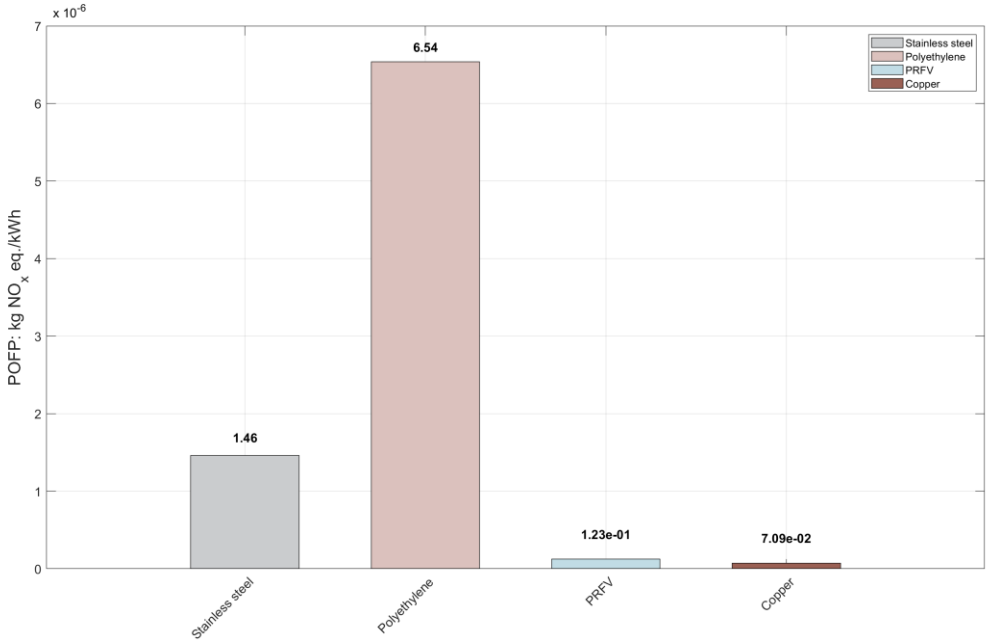

Figure 23. *$POFP_{ecosystem}$ of Use Case 2 – The plant construction*

3.2.9. **Stratospheric Ozone Depletion Potential (ODP)**

During the charging phase, ODP impact is $2.50 \cdot 10^{-7}$ kg CFC-11 eq./kWh, with electricity consumption as the primary contributor due to fossil-based emissions. Other lower contributions arise from Therminol V66 and cyclopentane transportation, as well as oil production. These results indicate that emissions of ozone-depleting substances are highly concentrated in electricity production, suggesting that reducing halogenated emissions during energy generation would be the most effective strategy for lowering ODP in the charging phase.

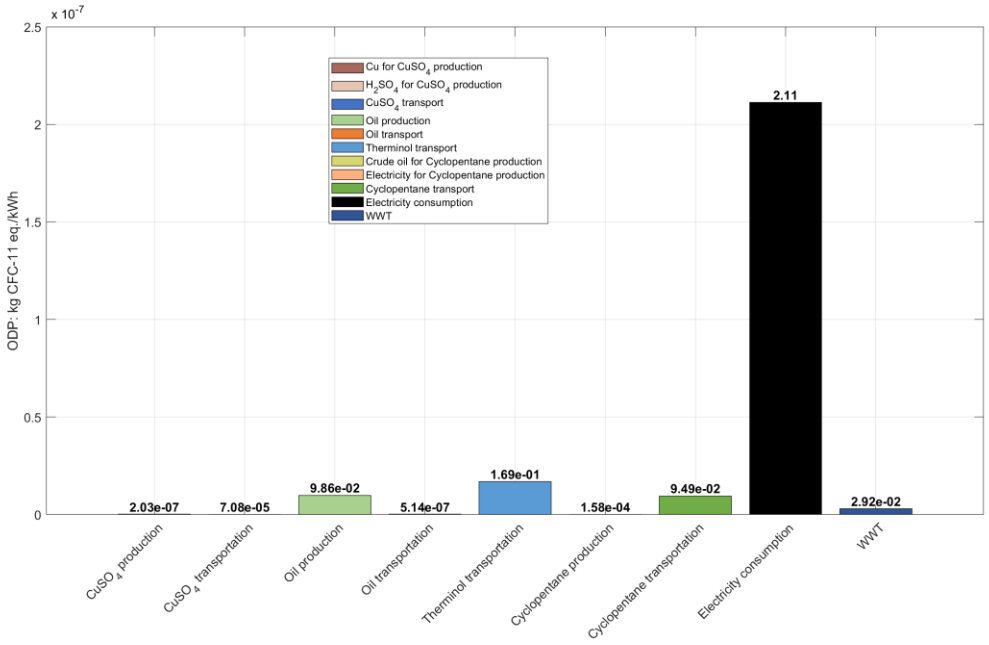

Figure 24. *ODP of Use Case 2 – The charging phase*

In the discharging phase, total ODP score reaches $1.75 \cdot 10^{-7}$ kg CFC-11 eq./kWh, with Therminol V66 transportation and oil production ranking as first and secondary contributors (Figure 25). Other minor contributions arise from $CuSO_4$ production and transport, oil production and transport, as well as cyclopentane supply. The electricity production clearly offsets the total value of this KPI.

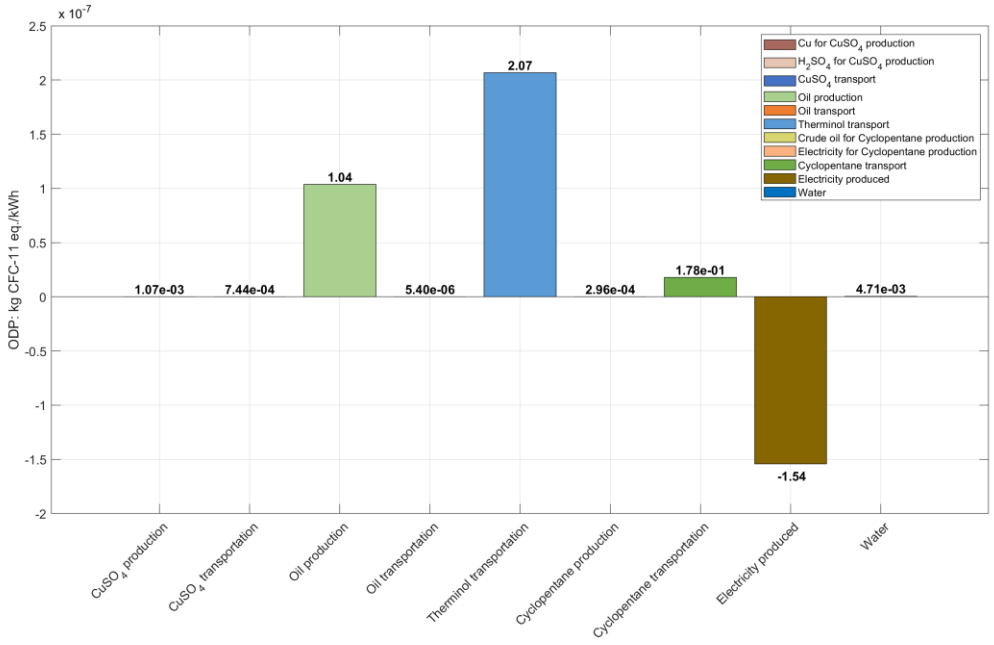

Figure 25. *ODP of Use Case 2 – The discharging phase*

The ODP impact scores associated with plant construction are negligible compared to the others, summing a total of $1.24 \cdot 10^{-9}$ kg CFC eq./kWh, as seen in Figure 26. The primary contributors are polyethylene and stainless-steel components, although, as a total, their impacts remain minimal. Other materials, including copper and fiberglass, PRFV, have virtually no effect. This shows that the construction phase does not significantly affect the ODP impact category. Therefore, mitigation efforts should focus on operational chemical production rather than tank material selection.

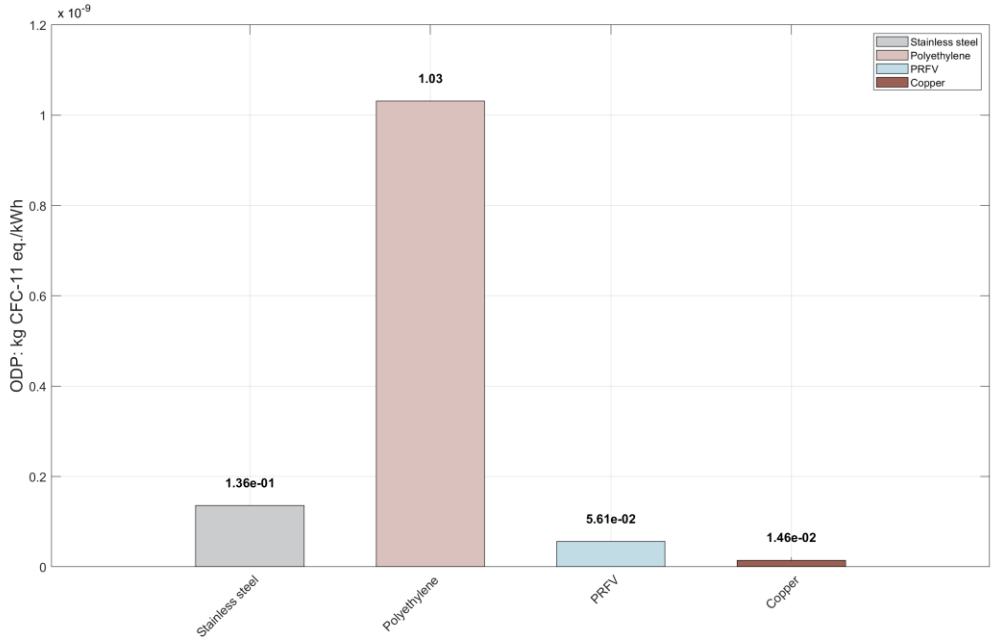

Figure 26. *ODP of Use Case 2 – The plant construction*

3.2.10. **Terrestrial Acidification Potential (TAP)**

The charging phase results in $5.79 \cdot 10^{-4}$ kg SO_2 eq./kWh, being primarily driven by electricity consumption. The impact during the discharging phase is slightly higher at $4.23 \cdot 10^{-4}$ kg SO_2 eq./kWh. Construction-related impacts are minimal, with a total of $9.77 \cdot 10^{-6}$ kg SO_2 eq./kWh.

3.2.11. **Terrestrial Ecotoxicity Potential (TETP)**

The charging phase contributes $7.21 \cdot 10^{-2}$ kg 1.4-DB eq./kWh, while the discharging step nearly offsets the impact of the charging, providing a negative impact score of $-5.13 \cdot 10^{-2}$ kg 1.4-DB eq./kWh. Electricity consumption is the primary driver for the charging step, while electricity generation provides the negative offset during the discharging phase. Construction-related impact reaches a total of $9.90 \cdot 10^{-1}$ kg 1.4-DB eq./kWh.

3.2.12. **Use Case 2 – Main conclusions**

The following is a summary of the key findings in Use Case 2:

- GWP reaches ist highest impact scores during the charging phase, compared to the discharging step and construction stage, primarily due to electricity imports from the grid mix. Negative values observed during discharging stem from electricity generation.
- FDP impact during charging is also largely driven by electricity imports, while the discharging phase provides a fossil-resource credit through displaced grid generation.
- TETP is mainly driven by the plant construction subsystem, particularly due to copper manufacturing.
- In the context of this Use Case, operational benefits from discharging are substantial; however, design and material choices during construction can impose significant ecotoxicty burdens.

3.3. Use Case 3 – Ružomberok Paper Mill Plant – Results and discussions

Table 7 shows the results for the LCA study in Use Case 3, considering the study's assumptions and limitations. It is worth mentioning that, in the context of this specific Use Case, Novec 649 has been considered as the reference fluid for the analysis, with the aim of exploring alternatives among the range of potentially applicable fluids (e.g., cyclopentane). In this way, the report paves the way for future evaluations and optimizations, depending on future requirements and technological developments.

Table 7. LCA results for Use Case 3

KPI	Units	Charging	Discharging	Plant construction
GWP	kg CO_2 eq./kWh	$1.58 \cdot 10^{-1}$	$-6.23 \cdot 10^{-2}$	$3.90 \cdot 10^{-4}$
FDP	kg oil eq./kWh	$4.49 \cdot 10^{-2}$	$-1.54 \cdot 10^{-2}$	$9.65 \cdot 10^{-5}$
FETP	kg 1.4-DB eq./kWh	$2.52 \cdot 10^{-5}$	$1.20 \cdot 10^{-5}$	$3.68 \cdot 10^{-8}$
FEP	kg P eq./kWh	$3.43 \cdot 10^{-5}$	$1.58 \cdot 10^{-4}$	$5.39 \cdot 10^{-10}$
HTP_{cancer}	kg 1.4-DB eq./kWh	$4.76 \cdot 10^{-4}$	$5.29 \cdot 10^{-4}$	$4.82 \cdot 10^{-4}$
$HTP_{non\text{-}cancer}$	kg 1.4-DB eq./kWh	$7.50 \cdot 10^{-2}$	$3.66 \cdot 10^{-1}$	$1.63 \cdot 10^{-5}$
MDP	kg Cu eq./kWh	$4.56 \cdot 10^{-3}$	$2.62 \cdot 10^{-2}$	$1.05 \cdot 10^{-5}$
$POFP_{ecosystem}$	kg NO_x eq./kWh	10.70	$-4.79 \cdot 10^{-2}$	$7.27 \cdot 10^{-7}$
ODP	kg CFC eq./kWh	$1.53 \cdot 10^{-7}$	$2.84 \cdot 10^{-7}$	$6.91 \cdot 10^{-11}$
TAP	kg SO_2 eq./kWh	$5.52 \cdot 10^{-4}$	$1.64 \cdot 10^{-3}$	$2.24 \cdot 10^{-6}$
TETP	kg 1.4-DB eq./kWh	$6.69 \cdot 10^{-2}$	$2.04 \cdot 10^{-1}$	$3.48 \cdot 10^{-4}$

Details, comments, and discussions regarding the main sub-processes influencing the most pertinent effect indicators in this Use Case scenario are included in the following section.

3.3.1. Global Warming Potential (GWP)

The total GWP during the charging phase amounts $1.58 \cdot 10^{-1}$ kg CO_2 eq./kWh, with electricity import from the grid mix as the primary contributor at $1.42 \cdot 10^{-1}$ kg CO_2 eq./kWh (Figure 27a). Additional contributions arise from the production of $CuSO_4$ ($1.17 \cdot 10^{-2}$ kg CO_2 eq./kWh), Therminol V66 production ($2.29 \cdot 10^{-3}$ kg CO_2 eq./kWh), and Novec 649 production process ($2.03 \cdot 10^{-3}$ kg CO_2 eq./kWh), though these are considerably smaller. Minor impacts from municipal WWT and chemical transportation (Figure 27b), each below $1 \cdot 10^{-3}$ kg CO_2 eq./kWh, are shown as well. Overall, the obtained results indicate that operational electricity demand is the main driver of climate change impacts during the charging phase of Use Case 3, while the relatively small role of chemical production highlights the potential for further reductions through the adoption of low-carbon electricity sources.

a.

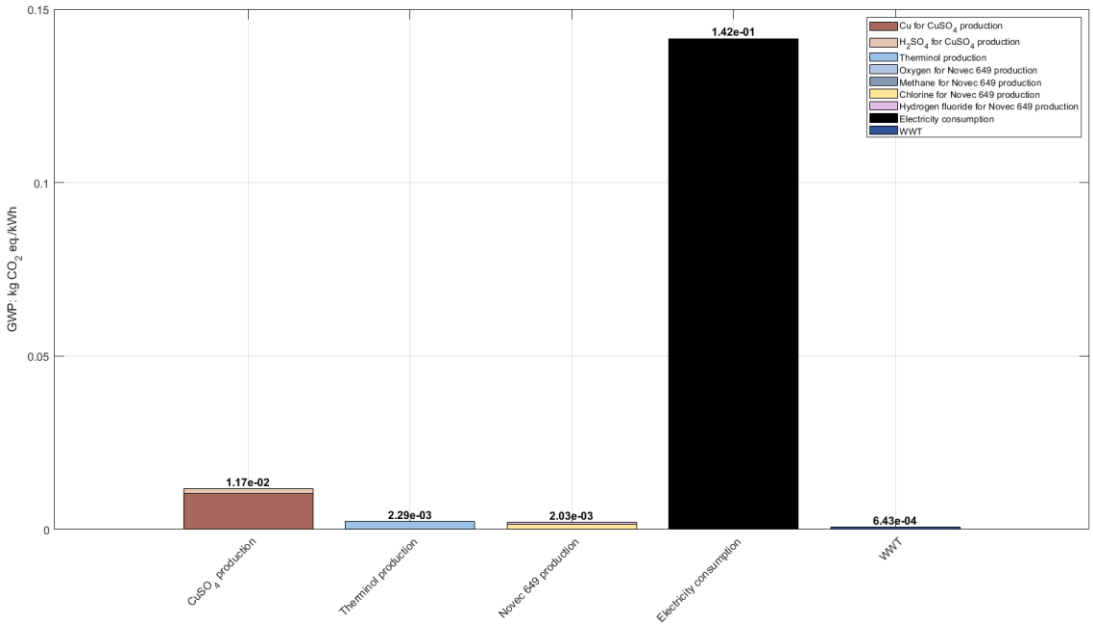

b.

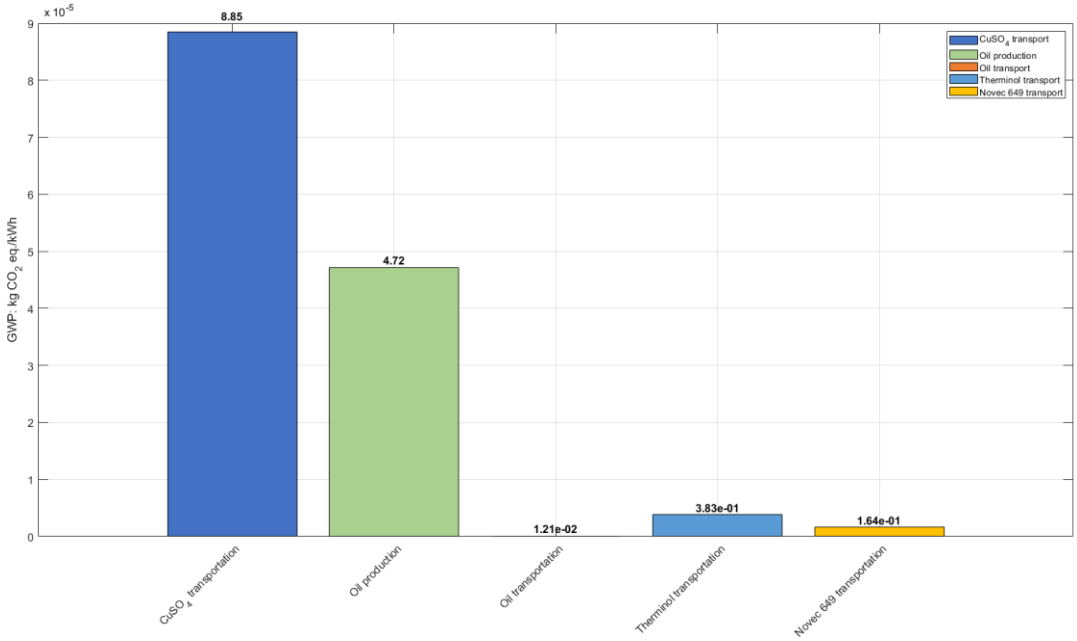

Figure 27. *GWP of Use Case 3 – The charging phase: a) major contributors and b) minor contributors*

During the discharging phase, the total GWP impact score is negative ($-6.23 \cdot 10^{-2}$ kg CO_2 eq./kWh), reflecting a net offset effect mainly due to electricity generation (Figure 28). Among the contributors, $CuSO_4$ production has the highest impact ($7.26 \cdot 10^{-2}$ kg CO_2 eq./kWh), followed by the Therminol V66 production process ($1.12 \cdot 10^{-2}$kg CO_2 eq./kWh) and minor inputs from other processes. In contrast, electricity generation provides a substantial negative contribution ($-1.49 \cdot 10^{-1}$ kg CO_2 eq./kWh), effectively compensating for the emissions associated to the chemical production sub-processes. Overall, the operational impacts during discharging are determined by the interplay between chemical-related emissions and the offset provided by generated electricity.

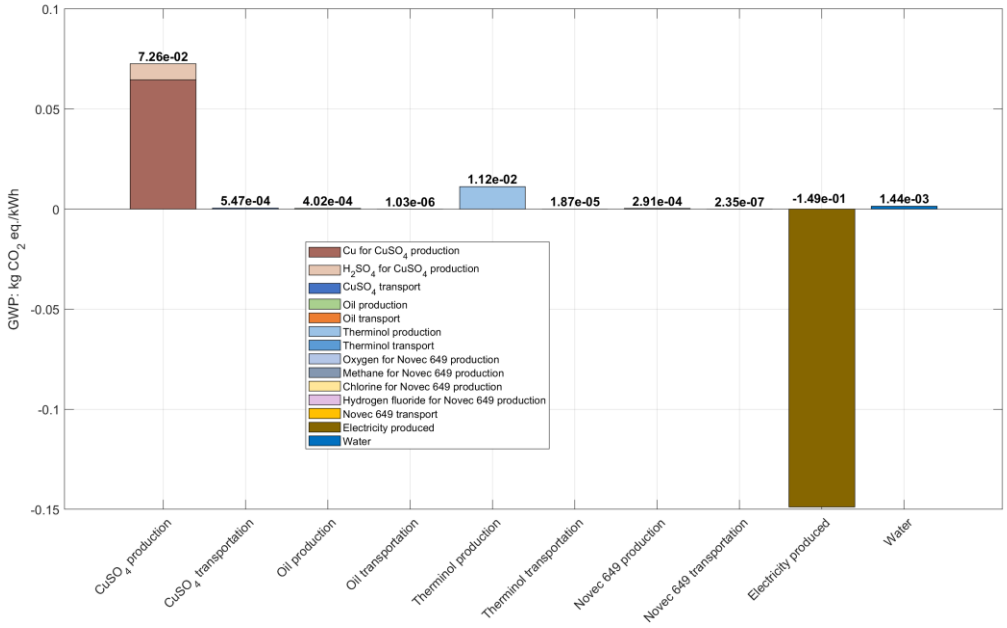

Figure 28. *GWP of Use Case 3 – The discharging phase*

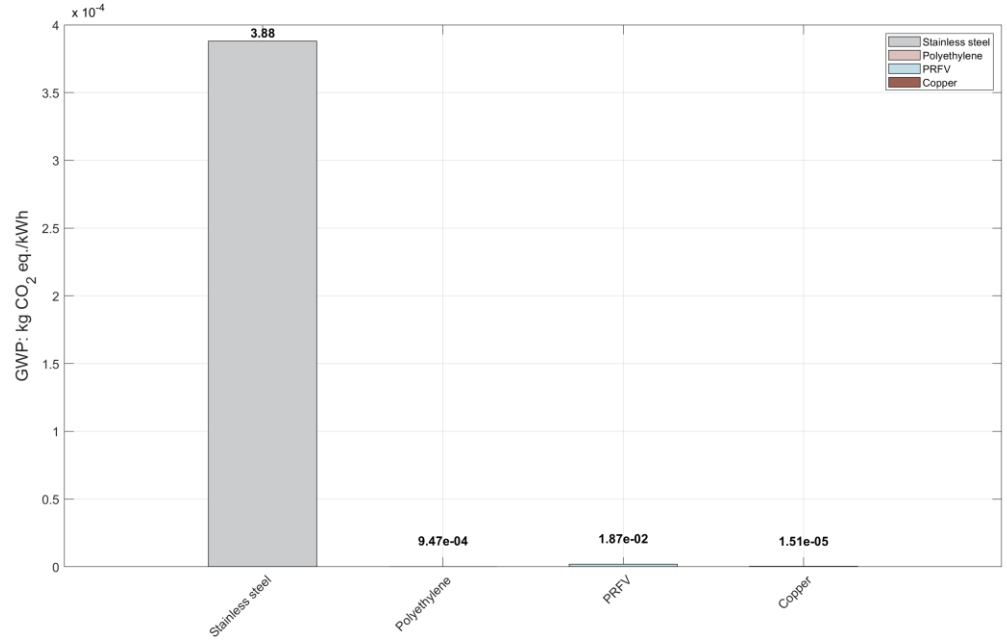

Figure 29. *GWP of Use Case 3 – The plant construction*

Figure 29 shows the impact of plant construction in Use Case 3 and how it influences the overall GWP indicator. Of the total of $3.90 \cdot 10^{-4}$ kg CO_2 eq./kWh, the need for stainless steel has the highest influence ($3.88 \cdot 10^{-4}$ kg CO_2 eq./kWh), the other contributors being minor in comparison.

3.3.2. **Fossil Depletion Potential (FDP)**

During the charging phase, the total FDP amounts to $4.49 \cdot 10^{-2}$ kg oil eq./kWh. The use of electricity from the grid mix stands as the primary contributor ($3.96 \cdot 10^{-2}$ kg oil eq./kWh),

followed by $CuSO_4$ production process ($4.13 \cdot 10^{-3}$ kg oil eq./kWh) and Novec 649 production ($1.01 \cdot 10^{-3}$ kg oil eq./kWh), as shown in Figure 30a. Other contributions such as oil production and WWT are negligible (Figure 30b). These results indicate that fossil resource depletion is primarily driven by the electricity consumption, with chemical feedstocks playing a secondary role. Consequently, mitigation strategies should prioritize reducing the carbon intensity and fossil dependence of electricity supply.

In the discharging step, the total FDP becomes slightly negative ($-1.54 \cdot 10^{-2}$ kg oil eq./kWh), reflecting a net offset due to power generation. $CuSO_4$ production represents the largest positive contributor ($2.56 \cdot 10^{-2}$ kg oil eq./kWh), with minor inputs from Novec 649 and oil production (Figure 31). Electricity production ($-4.17 \cdot 10^{-2}$ kg oil eq./kWh) counterbalances these impacts, while water use adds only a negligible contribution ($4.80 \cdot 10^{-4}$ kg oil eq./kWh).

a.

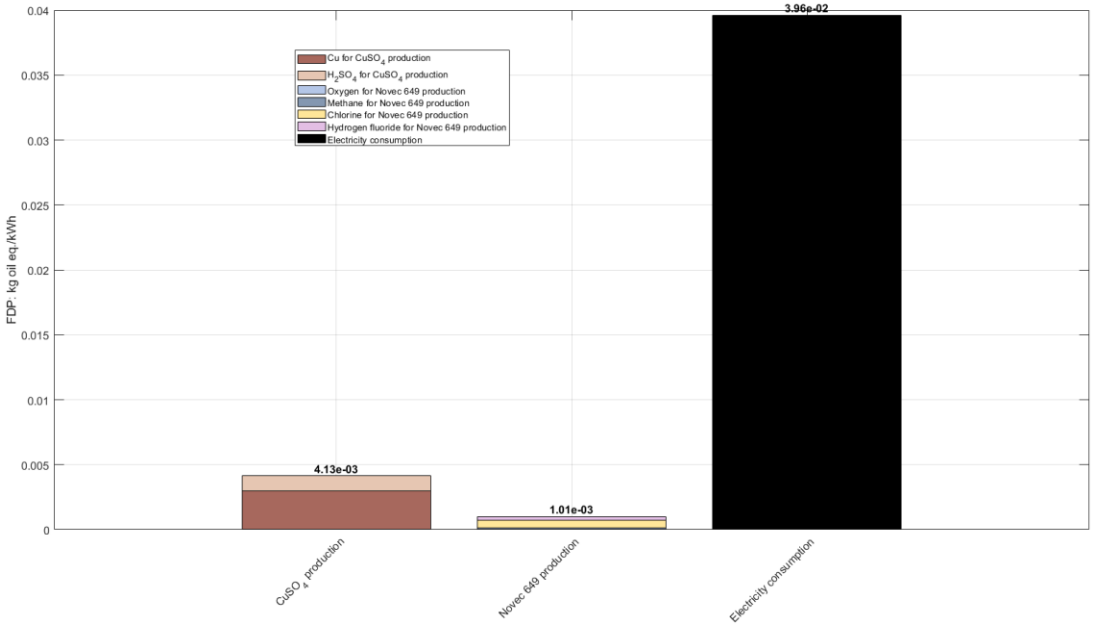

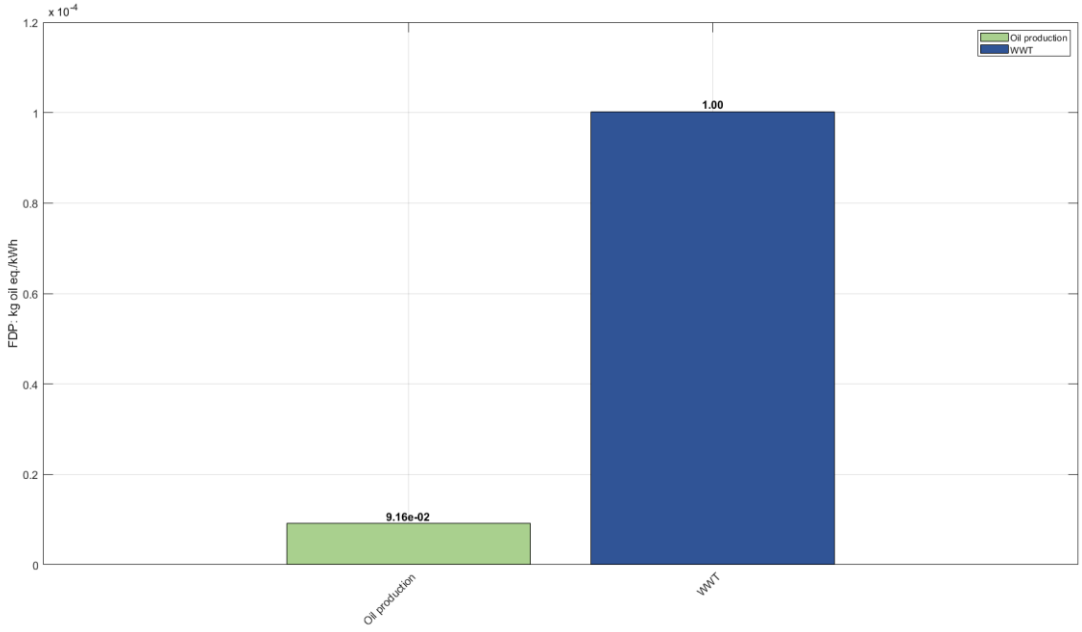

b.

Figure 30. *FDP of Use Case 3 – The charging phase: a) major contributors and b) minor contributors*

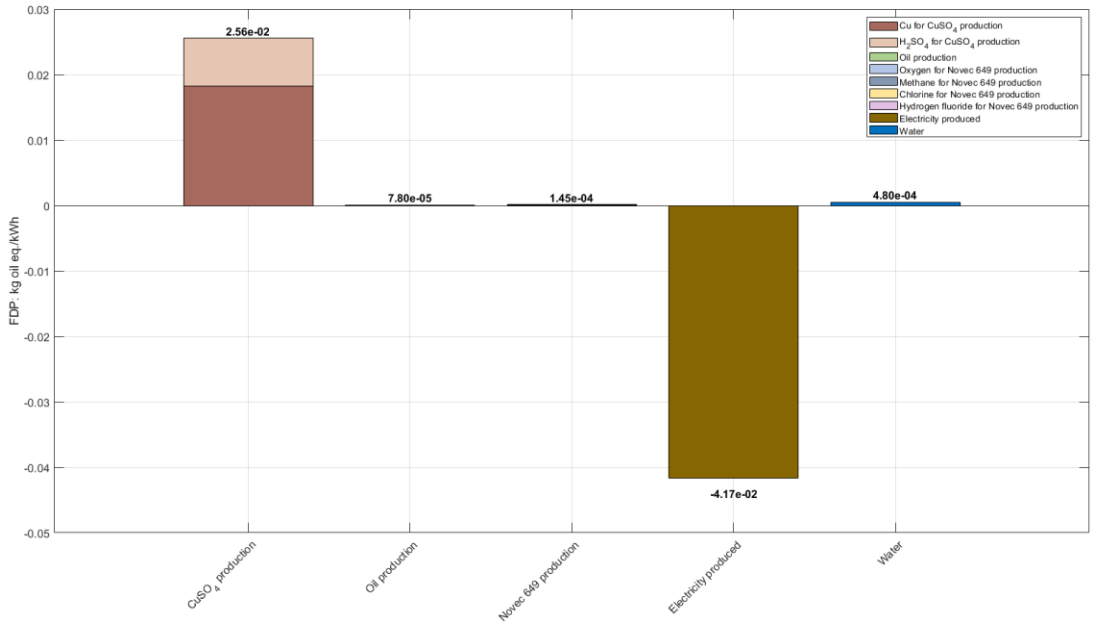

Figure 31. *FDP of Use Case 3 – The discharging phase*

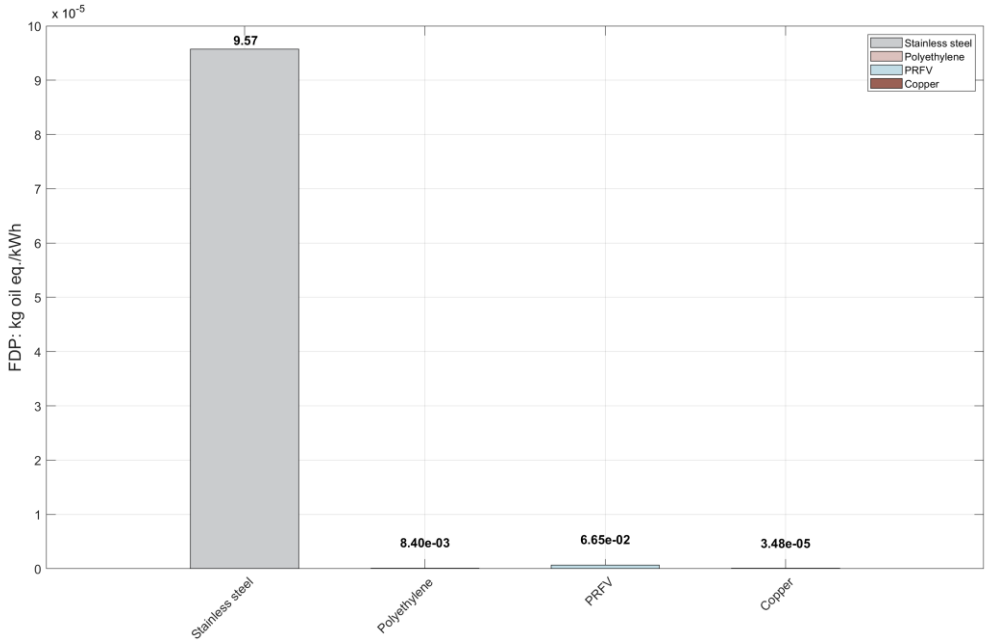

Figure 32. *FDP of Use Case 3 – The plant construction*

The plant construction has a minor contribution to FDP, as represented in Figure 32. For this environmental KPI, the stainless-steel subsystem has the highest contribution, of the total of $9.65 \cdot 10^{-5}$ kg oil eq./kWh, it contributes by $9.57 \cdot 10^{-5}$ kg oil eq./kWh.

3.3.3. **Freshwater Ecotoxicity Potential (FETP)**

During the charging phase, the impact accounts to $2.52 \cdot 10^{-5}$ kg 1.4-DB eq./kWh, driven primarily by electricity generation and $CuSO_4$ production. In the discharging phase, the impact is halved to $1.20 \cdot 10^{-5}$ kg 1.4-DB eq./kWh, with $CuSO_4$ production remaining the dominant contributor. Negative offsets from electricity generation further reduce the overall burden, confirming that discharging consistently exerts a lower impact than the charging phase. The plant construction has a very small contribution of $3.68 \cdot 10^{-8}$ kg 1.4-DB eq./kWh for this KPI.

3.3.4. **Freshwater Eutrophication Potential (FEP)**

Regarding the eutrophication potential, the charging phase results in $3.43 \cdot 10^{-5}$ kg P eq./kWh, almost entirely being dominated by Therminol V66 production ($3.24 \cdot 10^{-5}$ kg P eq./kWh). In the discharging step, the impact increases substantially to $1.58 \cdot 10^{-4}$ kg P eq./kWh, again with Therminol V66 production as the primary contributor ($1.59 \cdot 10^{-4}$ kg P eq./kWh). Although power production introduces a minor negative contribution, it is insufficient to offset Therminol's V66 strong effect, highlighting its consistent impact across both phases. The plant construction has a negligible contribution of $5.39 \cdot 10^{-10}$ kg P eq./kWh for this KPI.

3.3.5. **Human Toxicity Potential cancer (HTP_{cancer})**

Charging contributes by $4.76 \cdot 10^{-4}$ kg 1.4-DB eq./kWh, primarily due to electricity consumption and $CuSO_4$ production. The discharging phase results in a slightly higher value of $5.29 \cdot 10^{-4}$ kg 1.4-DB eq./kWh, with $CuSO_4$ production remaining the dominant contributor. Although electricity generation provides a negative offset, it is insufficient to fully

counterbalance chemical-related impacts, leading to a marginally higher cancer toxicity burden during discharging compared to charging. The plant construction's total contribution of $4.82 \cdot 10^{-4}$ kg 1.4-DB eq./kWh for this KPI is due to the use of stainless steel.

3.3.6. Human Toxicity Potential non-cancer ($HTP_{non\text{-}cancer}$)

For non-cancer human toxicity, both charging and discharging steps show significant burdens. Charging accounts for $7.50 \cdot 10^{-2}$ kg 1.4-DB eq./kWh, largely driven by Therminol V66 and $CuSO_4$ production ($4.96 \cdot 10^{-2}$ kg 1.4-DB eq./kWh and $2.03 \cdot 10^{-2}$ kg 1.4-DB eq./kWh, respectively). Discharging exhibits a substantially higher burden of $3.66 \cdot 10^{-1}$ kg 1.4-DB eq./kWh, dominated by the production of Therminol V66 ($2.43 \cdot 10^{-1}$ kg 1.4-DB eq./kWh) and $CuSO_4$ ($1.25 \cdot 10^{-1}$ kg 1.4-DB eq./kWh), although the electricity generation ($-3.97 \cdot 10^{-3}$ kg 1.4-DB eq./kWh) slightly offsets the total value. Even after accounting for the electricity credits, the discharging phase remains markedly more impactful, establishing non-cancer toxicity as one of the most critical environmental hotspots. The plant construction has an almost negligible contribution of $1.63 \cdot 10^{-5}$ kg 1.4-DB eq./kWh for this KPI.

3.3.7. Metal Depletion Potential (MDP)

During the charging phase, total MDP score amounts to $4.56 \cdot 10^{-3}$ kg Cu eq./kWh, while in the discharging phase it substantially increases to $2.62 \cdot 10^{-2}$ kg Cu eq./kWh. In both phases, charging and discharging, the $CuSO_4$ production ranks as the primary contributor ($4.20 \cdot 10^{-3}$ kg Cu eq./kWh and $2.58 \cdot 10^{-2}$ kg Cu eq./kWh, respectively). These results demonstrate that MDP is strongly associated with the use of Cu-based compounds, with the effect of becoming more pronounced during discharging. The plant construction has an almost negligible contribution of $1.05 \cdot 10^{-5}$ kg Cu eq./kWh for this KPI.

3.3.8. Photochemical Ozone Formation Potential ecosystem ($POFP_{ecosystem}$)

During the charging phase, the total $POFP_{ecosystem}$ amounts to 10.70 kg NO_x eq./kWh, with municipal WWT (9.00 kg NO_x eq./kWh) and electricity import from the grid mix (1.66 kg NO_x eq./kWh) as the primary contributors (Figure 33a). Minor contributions arise from $CuSO_4$ transportation ($1.18 \cdot 10^{-5}$ kg NO_x eq./kWh) and Novec 649 production ($3.80 \cdot 10^{-6}$ kg NO_x eq./kWh), while other chemicals and transport processes remain negligible (Figure 33b). These results indicate that $POFP_{ecosystem}$ is primarily driven by operational activities, particularly wastewater management and electricity demand. The relatively small role of chemical production suggests that targeted improvements in process efficiency and energy sourcing could substantially reduce $POFP_{ecosystem}$. The notably high magnitude of this impact compared to other indicators further underscores the potential risks to local ecosystems from nitrogen oxide emissions.

a.

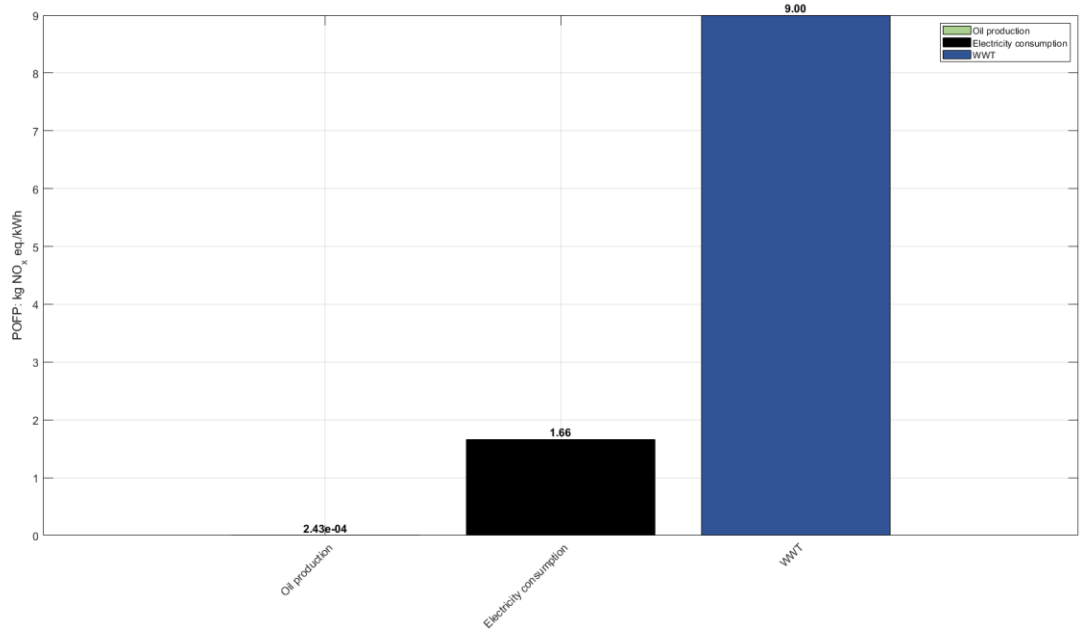

b.

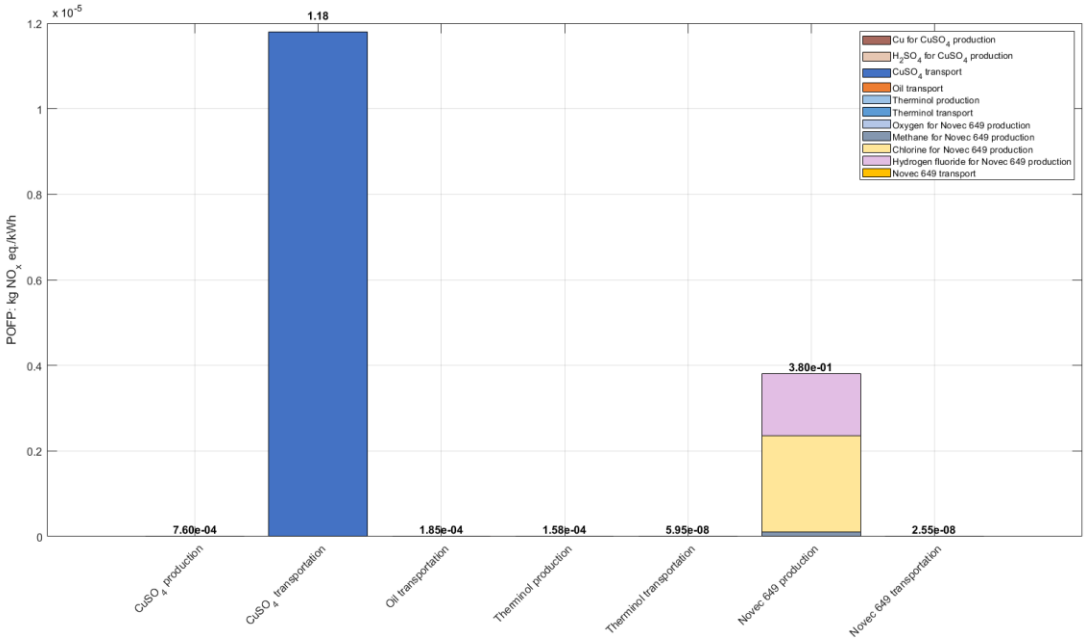

Figure 33. *$POFP_{ecosystem}$ of Use Case 3 – The charging phase: a) major contributors and b) minor contributors*

In the discharging step, total $POFP_{ecosystem}$ becomes negative ($-4.79 \cdot 10^{-2}$ kg NO_x eq./kWh), having water use as the primary contributor (1.70 kg NO_x eq./kWh), however, reflecting a net offset effect mainly due to the electricity generation (-1.75 kg NO_x eq./kWh) (Figure 34a). Positive contributions from Novec 649 production, $CuSO_4$ transport, and oil production are comparatively minor, while other chemical inputs remain as well negligible (Figure 34b). This outcome suggests that under certain operational conditions, the system can function as a net sink for ground-level ozone precursors through the compensatory effects of electricity generation.

a.

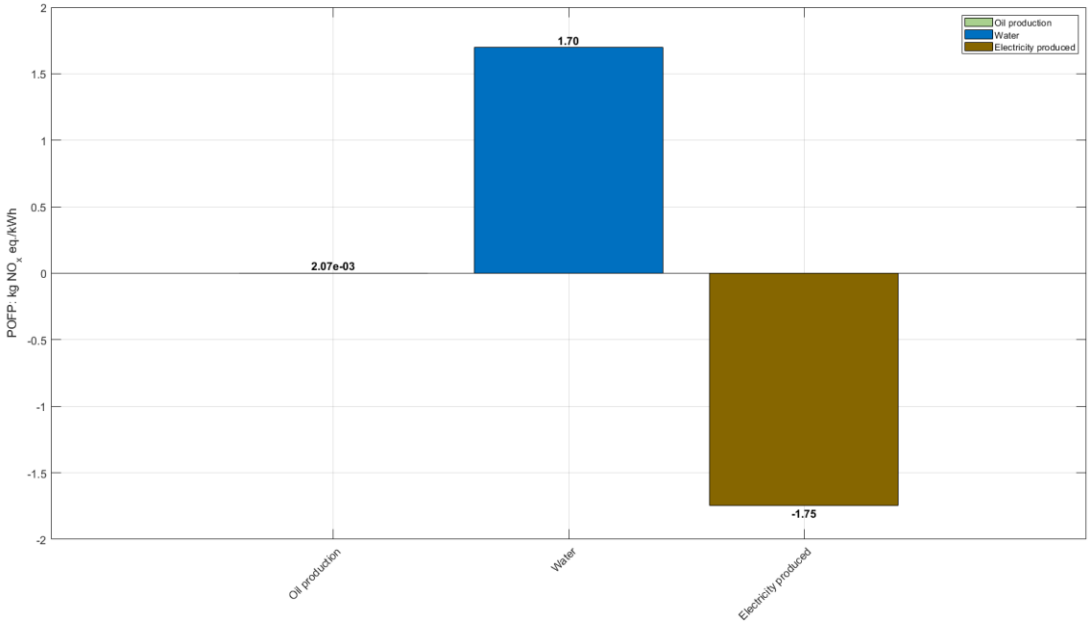

b.

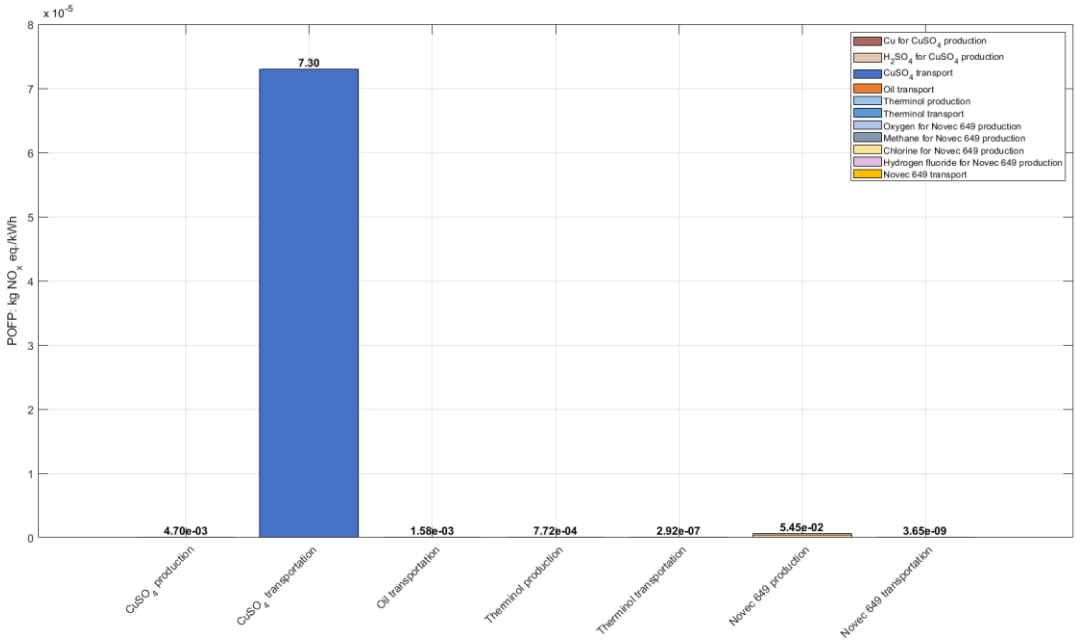

Figure 34. *$POFP_{ecosystem}$ of Use Case 3 – The discharging phase: a) major contributors and b) minor contributors*

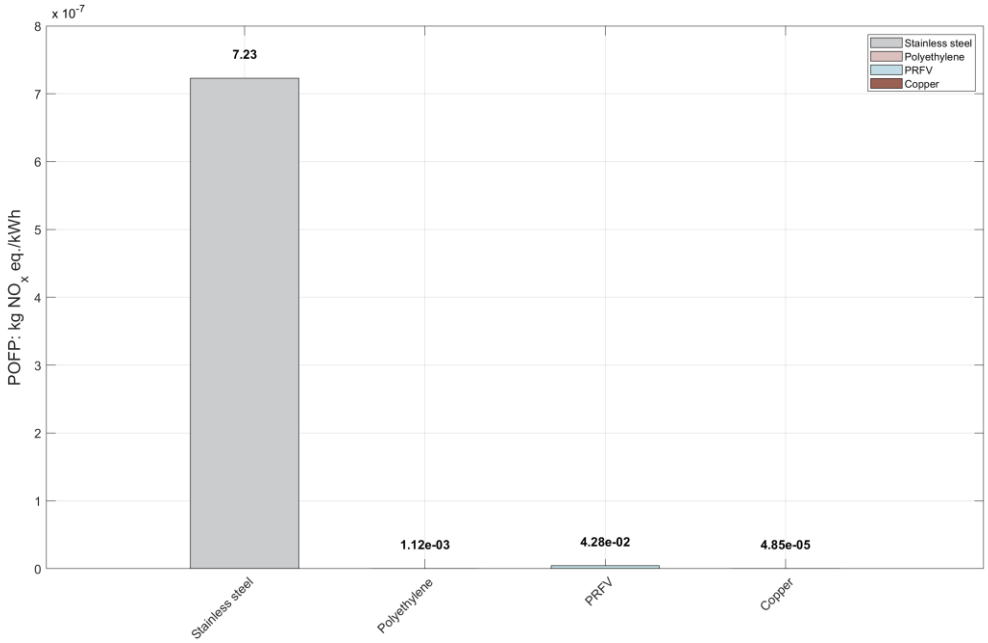

Figure 35. *$POFP_{ecosystem}$ of Use Case 3 – The plant construction*

The plant construction has a minor contribution to FDP, as seen in Figure 35. In this KPI, the stainless-steel subsystem has the largest contribution, of the total of $7.27 \cdot 10^{-7}$ kg NO_x eq./kWh, it has $7.23 \cdot 10^{-7}$ kg NO_x eq./kWh.

3.3.9. **Stratospheric Ozone Depletion Potential (ODP)**

The total ODP impact score during the charging phase is very low, amounting to $1.53 \cdot 10^{-7}$ kg CFC-11 eq./kWh. Contributions are shared among the import of electricity from the grid mix, Therminol V66 transportation, as well as Novec 649 and $CuSO_4$ production (Figure 36). The Therminol V66 transport along with electricity consumption account for the largest share ($5.84 \cdot 10^{-8}$ kg CFC-11 eq./kWh and $5.80 \cdot 10^{-8}$ kg CFC-11 eq./kWh, respectively), while other transport processes and municipal WWT have lower effects. These results suggest that ODP is minimal during charging, with halogenated chemical emissions from Therminol V66 and Novec 649 representing the most relevant, though minor contributors. From a mitigation perspective, replacing or optimizing the use of halogenated compounds could further reduce this impact.

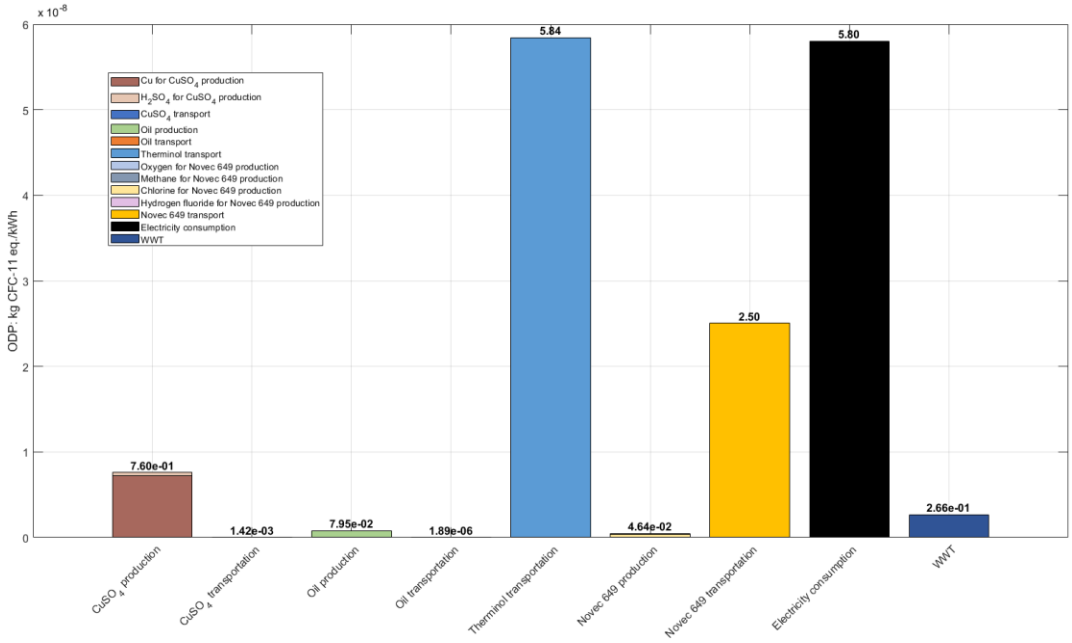

Figure 36. *ODP of Use Case 3 – The charging phase*

In the discharging phase, the total ODP increases slightly to $2.84 \cdot 10^{-7}$ kg CFC-11 eq./kWh. The largest contribution comes from Therminol V66 transportation ($2.86 \cdot 10^{-7}$ kg CFC-11 eq./kWh), while $CuSO_4$ and oil production add only minor amounts (Figure 37).

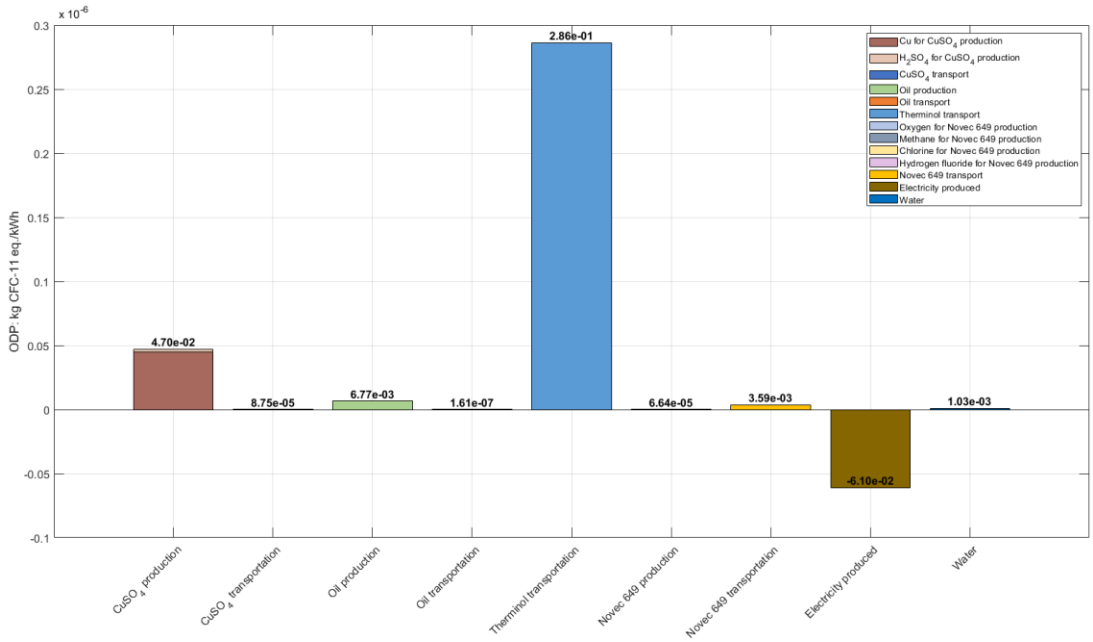

Figure 37. *ODP of Use Case 3 – The discharging phase*

Electricity generation slightly offsets the burden ($-6.10 \cdot 10^{-8}$ kg CFC-11 eq./kWh), reflecting either low-halogen processes or compensatory effects. Overall, although discharging shows a marginally higher ODP compared to charging, the absolute values remain very low. This confirms that ODP is not a significant environmental concern for the system.

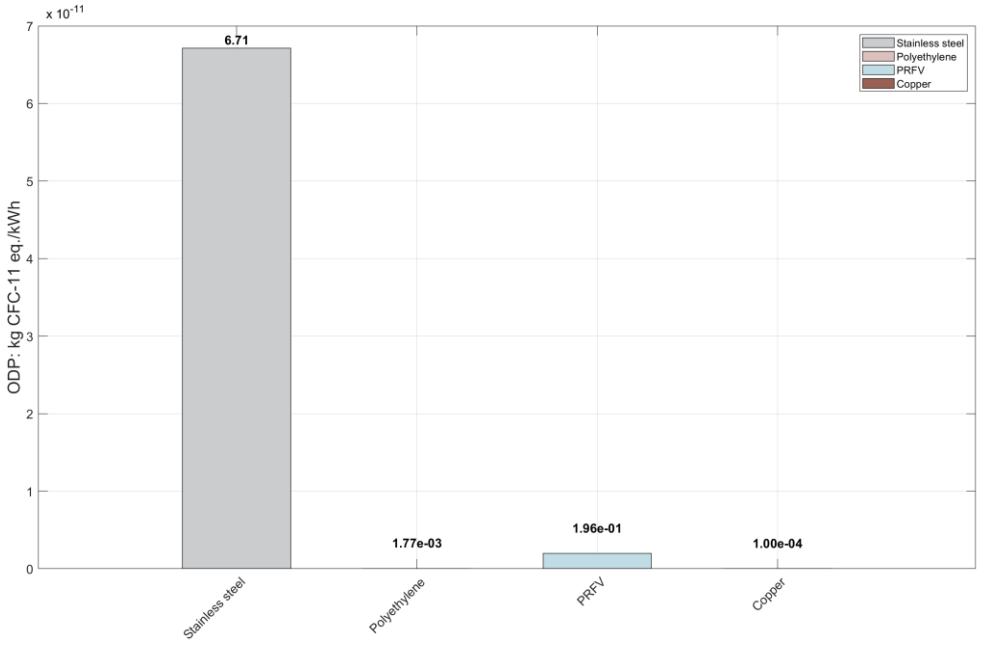

Figure 38. *ODP of Use Case 3 – The plant construction*

The plant construction has a minor contribution to FDP, as seen in Figure 38. For this KPI as well, the stainless-steel subsystem has the biggest contribution, from the total of $6.91 \cdot 10^{-11}$ kg CFC eq./kWh, it has $6.71 \cdot 10^{-11}$ kg CFC eq./kWh.

3.3.10. **Terrestrial Acidification Potential (TAP)**

For the terrestrial acidification potential, the charging step generates $5.52 \cdot 10^{-4}$ kg SO_2 eq./kWh, primarily driven by Therminol V66 production ($1.51 \cdot 10^{-4}$ kg SO_2 eq./kWh) and electricity consumption ($1.31 \cdot 10^{-4}$ kg SO_2 eq./kWh). In the discharging step, the impact nearly triples to $1.64 \cdot 10^{-3}$ kg SO_2 eq./kWh, with major contributions from Therminol V66 production ($7.40 \cdot 10^{-4}$ kg SO_2 eq./kWh) and $CuSO_4$ production. While electricity credits provide some offset, they are insufficient to counterbalance the substantial burden from the chemical manufacturing. The plant construction has a negligible contribution of $2.24 \cdot 10^{-6}$ kg SO_2 eq./kWh for this KPI.

3.3.11. **Terrestrial Ecotoxicity Potential (TETP)**

Terrestrial ecotoxicity potential during the charging phase accounts for $6.69 \cdot 10^{-2}$ kg 1.4-DB eq./kWh, with $CuSO_4$ production ($3.77 \cdot 10^{-2}$ kg 1.4-DB eq./kWh), electricity consumption ($2.83 \cdot 10^{-2}$ kg 1.4-DB eq./kWh), and Novec 649 production ($7.76 \cdot 10^{-4}$ kg 1.4-DB eq./kWh) as the main contributors. In contrast, discharging exhibits a markedly higher burden of 0.204 kg 1.4-DB eq./kW, primarily driven by $CuSO_4$ production (0.233 kg 1.4-DB eq./kWh). Negative contributions from electricity generation (–0.030 kg 1.4-DB eq./kWh) partially offset this value but are insufficient to change the overall outcome. These findings confirm $CuSO_4$ production as the primary driver of terrestrial ecotoxicity, particularly during the discharging phase. Plant construction exhibits a small contribution of nearly $3.50 \cdot 10^{-4}$ kg 1.4-DB eq./kWh.

3.3.12. **Use Case 3 – Main conclusions**

The following is a summary of the investigation's key outcome:

- Electricity consumption – and thus grid imports – represents the largest contributor to total GWP during charging, whereas the discharging phase generates climate credits through electricity production.
- FDP in the charging phase is primarily linked to electricity requirements, while the discharging phase offers only a modest offset.
- $CuSO_4$ production is the leading contributor to MDP, with higher MDP values in the discharging phase compared to charging, underscoring the role of chemical compounds as a critical hotspot.
- Overall, $CuSO_4$ production imposes greater resource and toxicity burdens than infrastructure, and although discharging credits improve certain key performance indicators (KPIs), they do not mitigate the impacts associated with metal use.

3.4. **Use Case 4 – Alfa Acciai Steel Production – Results and discussions**

Table 8 presents the LCA results for the Use Case 4, taking into account the study's limitations and assumptions.

Table 8. LCA results for Use Case 4

KPI	Units	Charging	Discharging	Plant construction
GWP	kg CO_2 eq./kWh	$5.75 \cdot 10^{-1}$	$-4.54 \cdot 10^{-1}$	$1.07 \cdot 10^{-4}$
FDP	kg oil eq./kWh	$1.74 \cdot 10^{-1}$	$-1.40 \cdot 10^{-1}$	$2.70 \cdot 10^{-5}$
FETP	kg 1.4-DB eq./kWh	$4.07 \cdot 10^{-5}$	$-2.20 \cdot 10^{-5}$	$2.21 \cdot 10^{-8}$
FEP	kg P eq./kWh	$1.49 \cdot 10^{-5}$	$9.27 \cdot 10^{-5}$	$1.48 \cdot 10^{-10}$
HTP_{cancer}	kg 1.4-DB eq./kWh	$2.04 \cdot 10^{-4}$	$-1.11 \cdot 10^{-4}$	$1.30 \cdot 10^{-4}$
$HTP_{non\text{-}cancer}$	kg 1.4-DB eq./kWh	$4.84 \cdot 10^{-2}$	$1.25 \cdot 10^{-1}$	$9.53 \cdot 10^{-6}$
MDP	kg Cu eq./kWh	$1.21 \cdot 10^{-3}$	$-4.36 \cdot 10^{-4}$	$2.90 \cdot 10^{-6}$
$POFP_{ecosystem}$	kg NO_x eq./kWh	4.98	-2.79	$2.00 \cdot 10^{-7}$
ODP	kg CFC eq./kWh	$2.40 \cdot 10^{-7}$	$4.88 \cdot 10^{-8}$	$2.04 \cdot 10^{-11}$
TAP	kg SO_2 eq./kWh	$5.51 \cdot 10^{-4}$	$2.56 \cdot 10^{-4}$	$6.12 \cdot 10^{-7}$
TETP	kg 1.4-DB eq./kWh	$6.69 \cdot 10^{-2}$	$-5.31 \cdot 10^{-2}$	$1.51 \cdot 10^{-4}$

Information, comments, and discussions regarding the main sub-processes influencing the most pertinent effect indicators for this Use Case scenario are included in the section that follows.

3.4.1. **Global Warming Potential (GWP)**

During the charging phase, the total GWP amounts to $5.75 \cdot 10^{-1}$ kg CO_2 eq./kWh, with electricity consumption overwhelmingly dominating the impact, accounting for approximately 99% of the total score (see Figure 39a). Other contributors, including WWT or Cyclopentane and Therminol V66 production, respectively, together represent less than 1% (Figure 39b), while raw materials transportation step is negligible, with an impact below 0.01% of the overall footprint. These findings emphasize that the selection of the energy source is the key determinant of climate performance during charging phase.

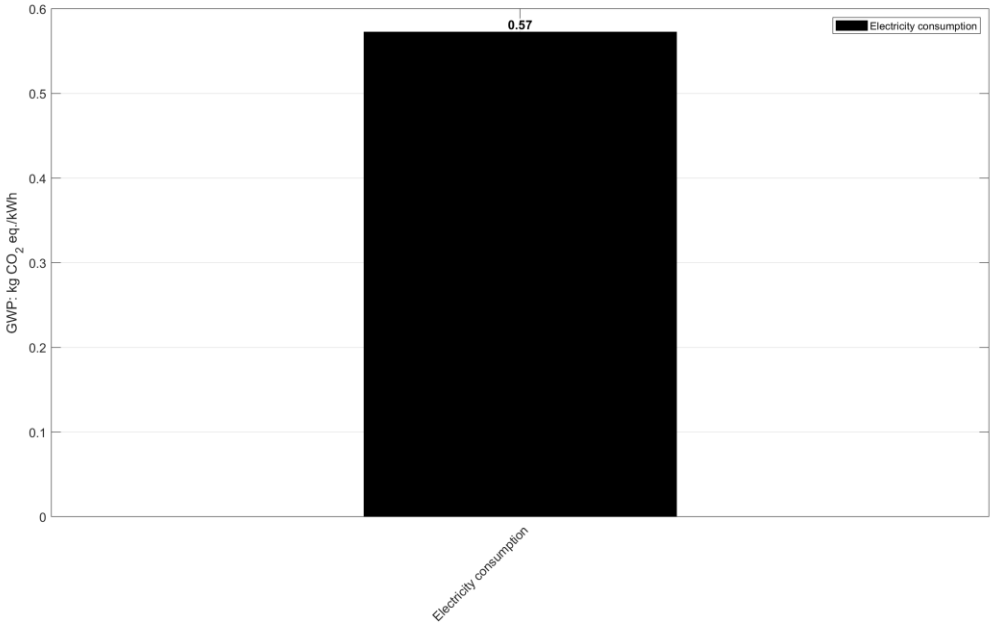

a.

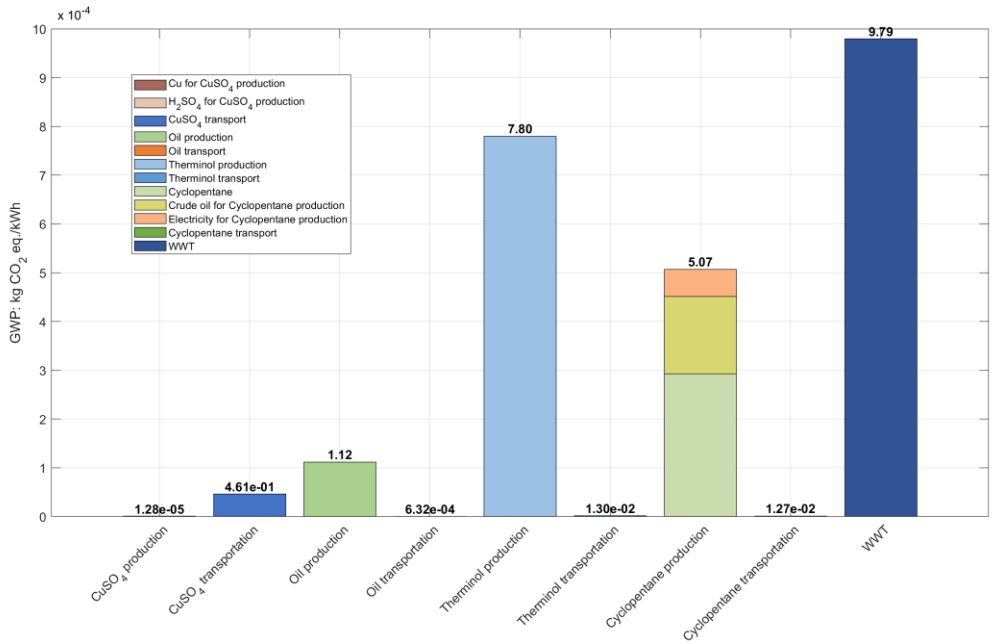

b.

Figure 39. *GWP of Use Case 4 – The charging phase: a) major contributors and b) minor contributors*

During the discharging phase, the total GWP decreases to $-4.54 \cdot 10^{-1}$ kg CO_2 eq./kWh. The negative contribution comes from the electricity generation which offsets other process' emissions (Figure 40a). Minor contributions from oil and Therminol V66 production account for less than 1% (Figure 40b), while transportation and water use remain negligible, mirroring the charging phase. Overall, the discharging phase results in negative GWP impact score, primarily due to partial energy recovery and associated negative grid emissions. This demonstrates that operational strategies play a decisive role in shaping the net climate impact of the storage cycle.

a.

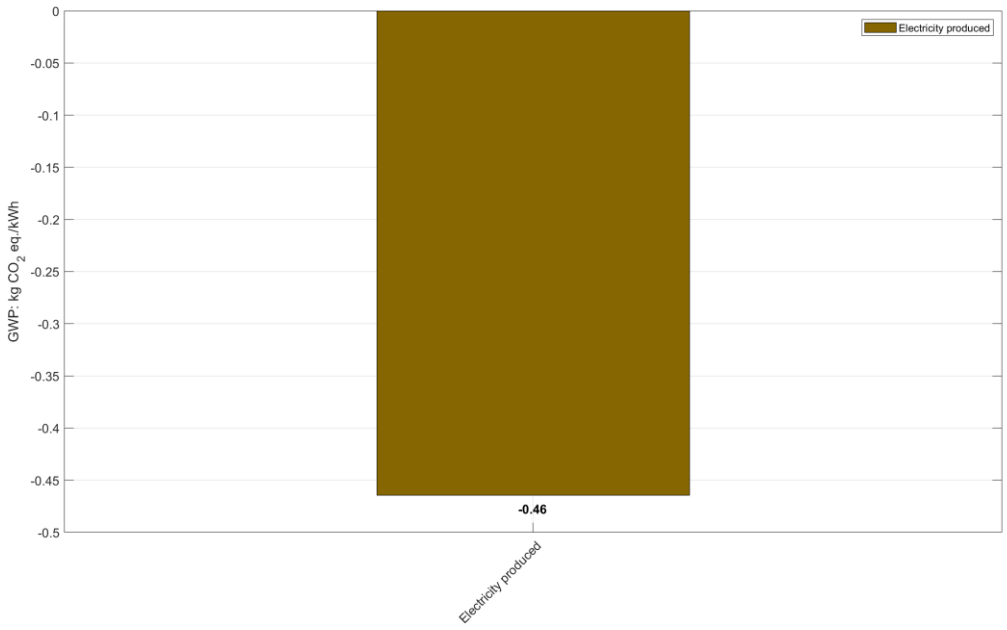

b.

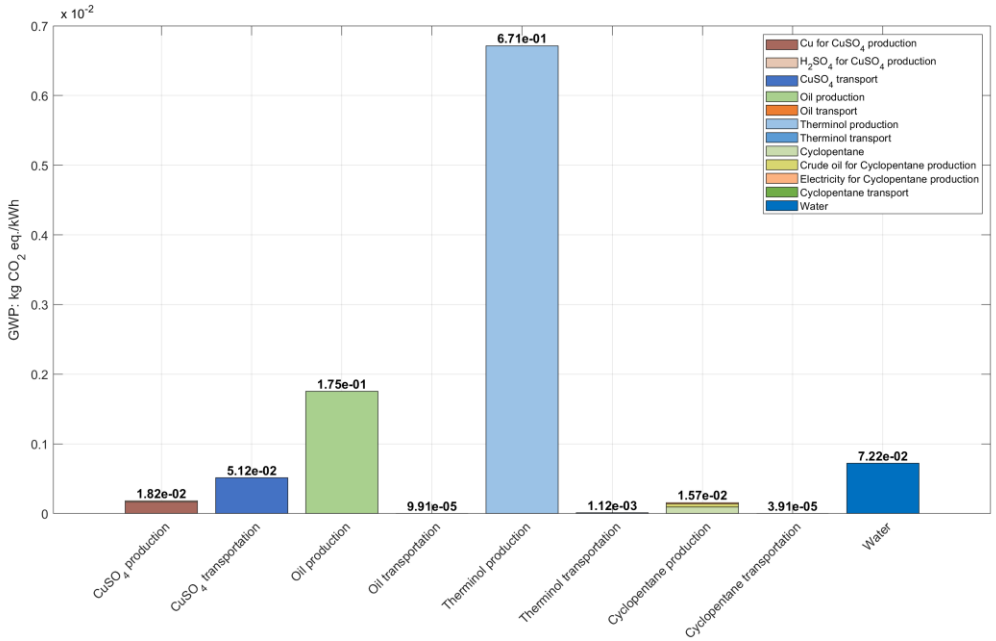

Figure 40. GWP of Use Case 4 – The discharging phase: *a) major contributors and b) minor contributors*

The contribution of plant construction towards total GWP is negligible, having a total of $1.07 \cdot 10^{-4}$ kg CO_2 eq./kWh. As shown in Figure 41, stainless steel ranks as the primary contributor, while polyethylene, copper, and fiberglass (PRFV) show very low impact. This confirms that the construction phase exerts minimal influence on the life-cycle GWP compared to operational stages, indicating that optimization efforts should instead target electricity sourcing.

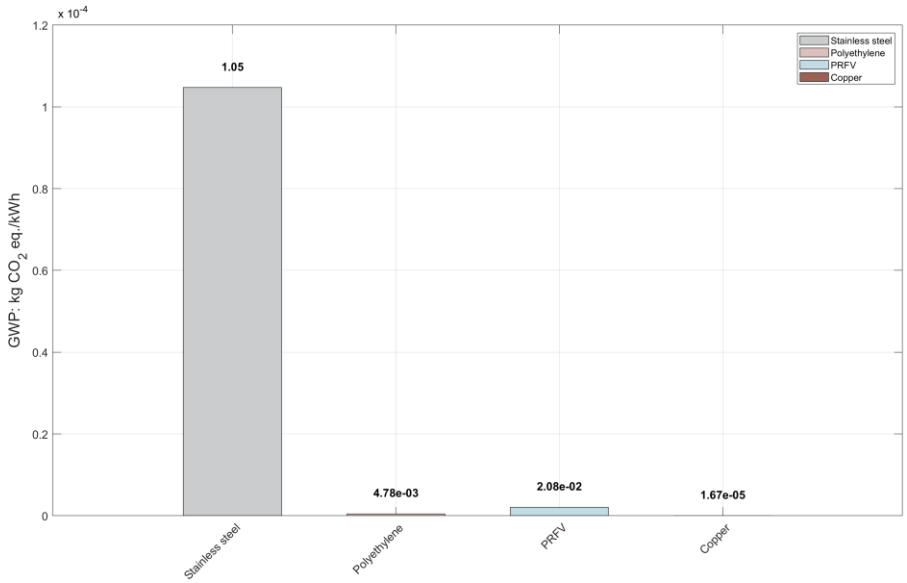

Figure 41. *GWP of Use Case 4 – The plant construction*

3.4.2. **Fossil Depletion Potential (FDP)**

During the charging phase, total FDP impact amounts to $1.74 \cdot 10^{-1}$ kg oil eq./kWh, largely driven by the electricity consumption, which accounts for around 99% of the total impact (Figure 42). The production processes of $CuSO_4$, oil, and cyclopentane, together with municipal WWT, account collectively for less than 1%, while transportation processes are virtually negligible. The results indicate that opting for energy sources with lower fossil intensity can significantly reduce FDP, thereby confirming that the charging phase is particularly sensitive to this selection.

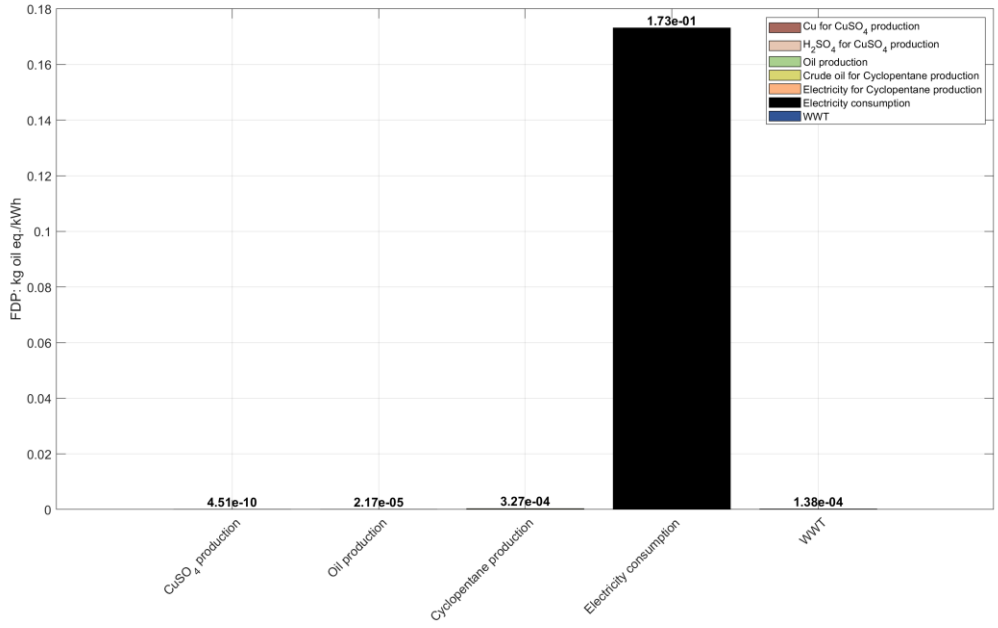

Figure 42. *FDP of Use Case 4 – The charging phase*

During the discharging phase, total FDP decreases to $-1.40 \cdot 10^{-1}$ kg oil eq./kWh, registering negative contribution due to the electricity production, which partially offsets fossil fuel demand (Figure 43), while minor contributions arise from oil, cyclopentane production and water treatment. The negative grid-related impact demonstrates the potential of energy recovery or low-carbon electricity in reducing fossil depletion during discharge. Transportation remains negligible, underscoring that raw material processing is the primary driver of fossil depletion. These results demonstrate that both operational efficiency and material selection are decisive in shaping fossil resource consumption across the storage cycle.

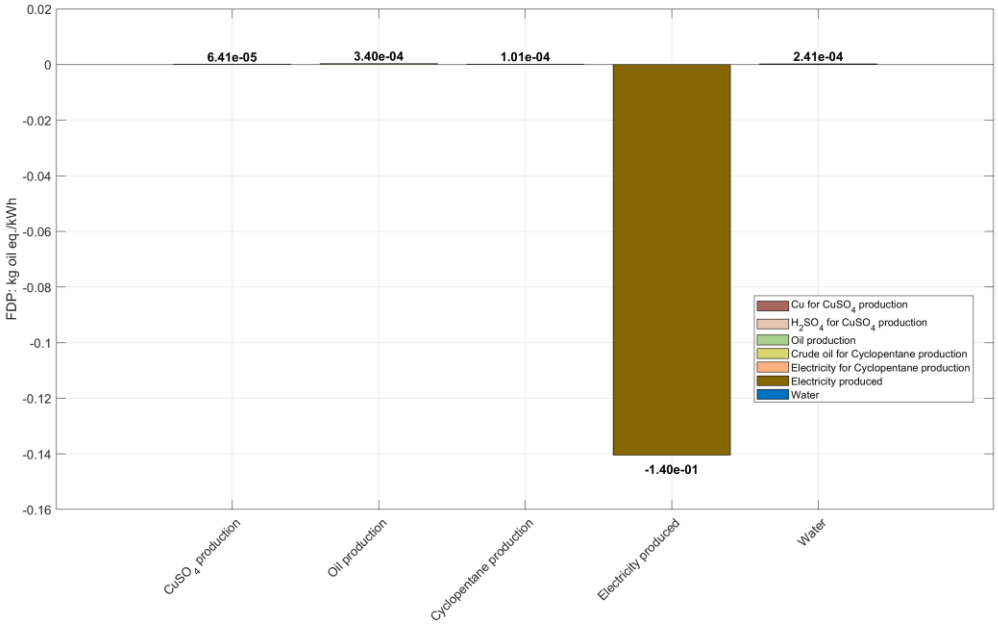

Figure 43. *FDP of Use Case 4 – The discharging phase*

Plant construction accounts for a negligible total FDP of $2.70 \cdot 10^{-5}$ kg oil eq./kWh, with stainless steel being the only material with a measurable contribution (Figure 44). Other materials, such as polyethylene, copper, and fiberglass (PRFV), exhibit low detectable impact. Consequently, the FDP associated with plant infrastructure is minimal compared to the operational stages, indicating that construction exerts an almost negligible influence on the overall systems' FDP.

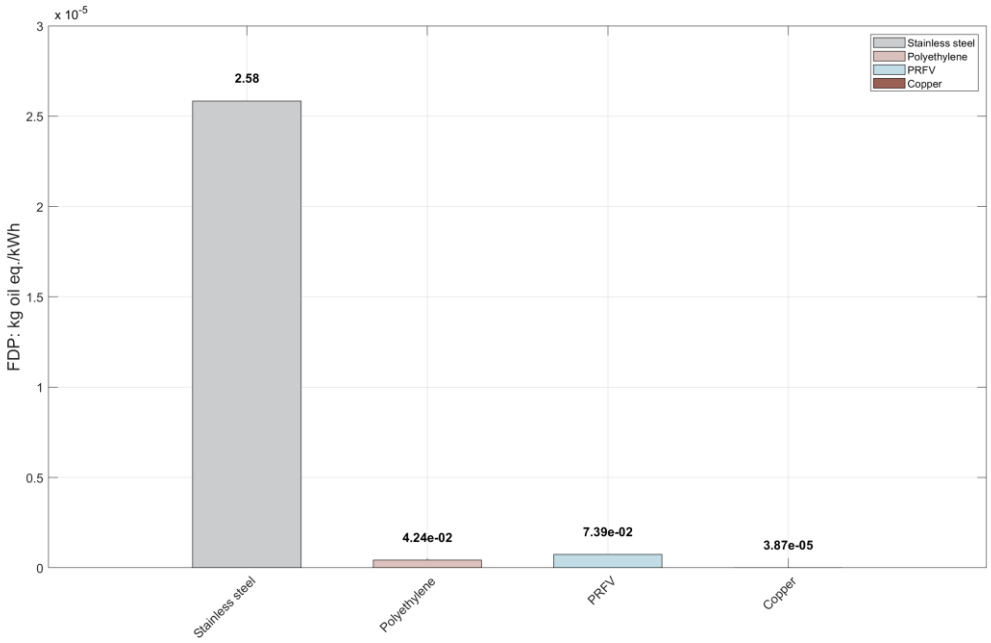

Figure 44. *FDP of Use Case 4 – The plant construction*

3.4.3. **Freshwater Ecotoxicity Potential (FETP)**

During the charging phase, freshwater ecotoxicity reaches a value of $4.07 \cdot 10^{-5}$ kg 1.4-DB eq./kWh, with electricity consumption identified as the main contributor ($2.98 \cdot 10^{-5}$ kg 1.4-DB eq./kWh). In the discharging phase, the impact decreases to $-2.20 \cdot 10^{-5}$ kg 1.4-DB eq./kWh, primarily driven by the energy production ($-2.42 \cdot 10^{-5}$ kg 1.4-DB eq./kWh) and water consumption ($1.72 \cdot 10^{-6}$ kg 1.4-DB eq./kWh). Contributions from plant construction are negligible ($2.21 \cdot 10^{-8}$ kg 1.4-DB eq./kWh). Overall, these results highlight the electricity source as the dominant factor influencing aquatic toxicity.

3.4.4. **Freshwater Eutrophication Potential (FEP)**

Freshwater eutrophication during the charging phase amounts to $1.49 \cdot 10^{-5}$ kg P eq./kWh, primarily driven by Therminol V66 ($1.10 \cdot 10^{-5}$ kg P eq./kWh) and electricity consumption ($3.20 \cdot 10^{-6}$ kg P eq./kWh). In the discharging phase, the impact slightly increases to $9.27 \cdot 10^{-5}$ kg P eq./kWh, with similar contributions from chemical production processes and water consumption. Plant construction exerts a negligible influence, with impacts of $1.48 \cdot 10^{-10}$ kg P eq./kWh.

3.4.5. **Human Toxicity Potential cancer (HTP_{cancer})**

For human toxicity (cancer effects), the charging phase contributes $2.04 \cdot 10^{-4}$ kg 1.4-DB eq./kWh, predominantly from electricity consumption ($1.50 \cdot 10^{-4}$ kg 1.4-DB eq./kWh). During

discharging, the impact decreases to $-1.11 \cdot 10^{-4}$ kg 1.4-DB eq./kWh, as a result of energy generation. Plant construction contributes only marginally ($1.30 \cdot 10^{-4}$ kg 1.4-DB eq./kWh), and it is primarily due to stainless steel components.

3.4.6. Human Toxicity Potential non-cancer ($HTP_{non\text{-}cancer}$)

During the charging phase, the $HTP_{non\text{-}cancer}$ impact score amounts to $4.84 \cdot 10^{-2}$ kg 1.4-DB eq./kWh, primarily influenced by electricity consumption ($2.93 \cdot 10^{-2}$ kg 1.4-DB eq./kWh) and Therminol V66 production ($1.69 \cdot 10^{-2}$ kg 1.4-DB eq./kWh). In the discharging phase, the impact increases to $1.25 \cdot 10^{-1}$ kg 1.4-DB eq./kWh, with Therminol V66 production emerging as the dominant contributor ($1.45 \cdot 10^{-1}$ kg 1.4-DB eq./kWh). Negative emissions arise due to electricity generation during this step. Plant construction contributes only marginally ($9.53 \cdot 10^{-6}$ kg 1.4-DB eq./kWh), confirming that non-carcinogenic toxicity is strongly driven by Therminol production during both charging and discharging phases.

3.4.7. Metal Depletion Potential (MDP)

For the MDP, as reported in Table 8, the charging phase contributes $1.21 \cdot 10^{-3}$ kg Cu eq./kWh, largely attributable to energy consumption ($1.20 \cdot 10^{-3}$ kg Cu eq./kWh). In contrast, the discharging phase exhibits a negative impact of $-4.36 \cdot 10^{-4}$ kg Cu eq./kWh, mainly due to electricity generation ($-9.72 \cdot 10^{-4}$ kg Cu eq./kWh). Plant construction impacts remain negligible ($2.90 \cdot 10^{-6}$ kg Cu eq./kWh). Overall, energy source is identified as the dominant driver of metal depletion, particularly during charging.

3.4.8. Photochemical Ozone Formation Potential ecosystem ($POFP_{ecosystem}$)

During the charging phase, the total $POFP_{ecosystem}$ amounts to 4.98 kg NO_x eq./kWh, with electricity consumption and municipal WWT representing the dominant contributors, jointly accounting for approximately 99% of the overall score (Figure 45a). Cyclopentane production adds a minor yet measurable share ($3.14 \cdot 10^{-4}$ kg NO_x eq./kWh), while other sources, including $CuSO_4$, oil, and Therminol V66 production, remain negligible (<0.01%) (Figure 45b). Transportation impacts are insignificant. These results emphasize the fact that operational energy use and wastewater management are the principal drivers of $POFP_{ecosystem}$ during charging, underscoring the potential for substantial reductions through cleaner electricity supply and optimized WWT technologies.

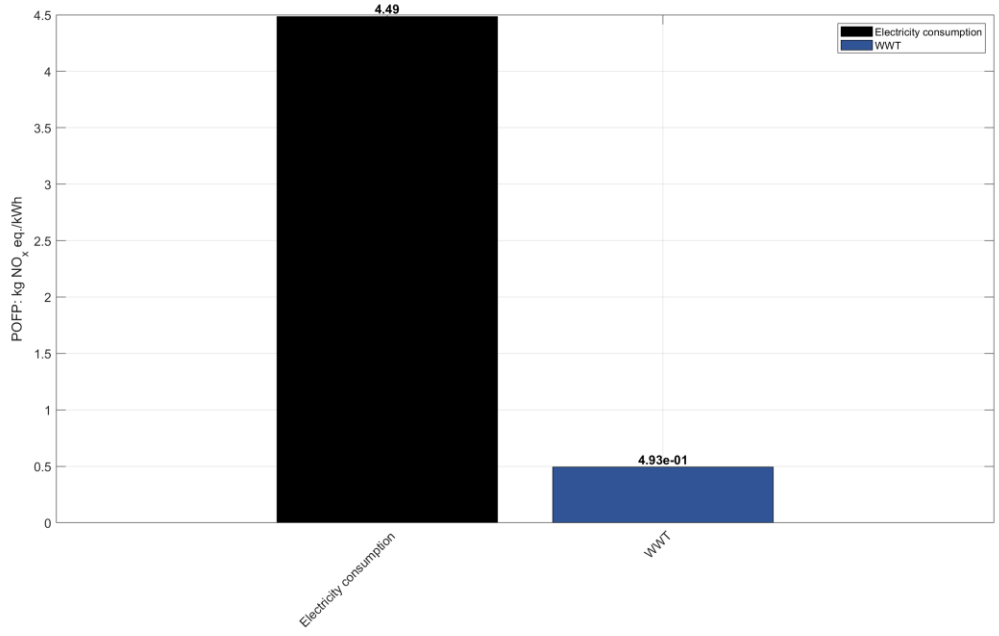

a.

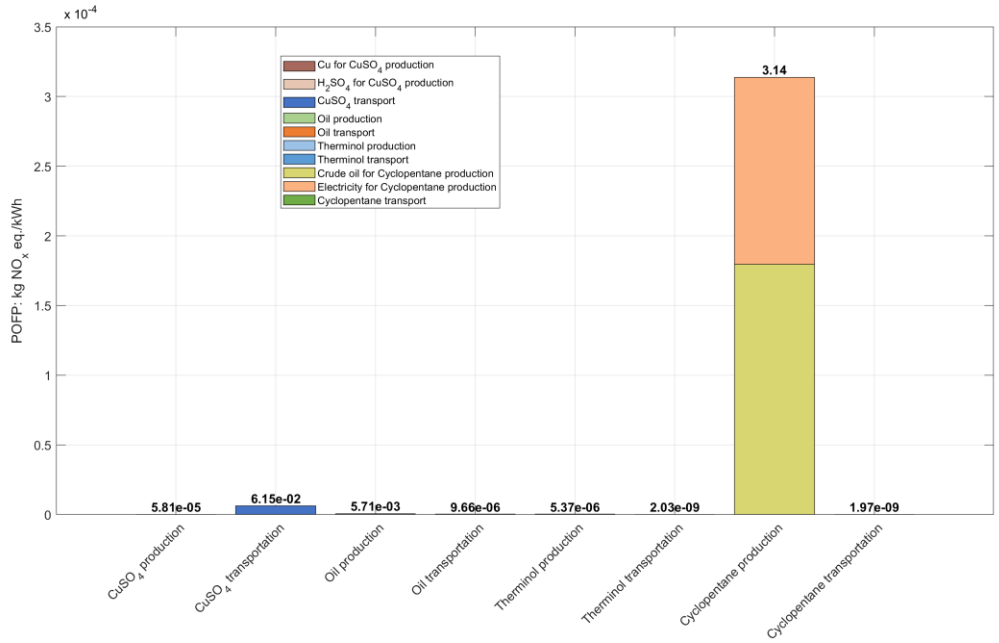

b.

Figure 45. *$POFP_{ecosystem}$ of Use Case 4 – The charging phase: a) major contributors and b) minor contributors*

In the discharging phase, the total $POFP_{ecosystem}$ is -2.79 kg NO_x eq./kWh, primarily due to the negative contribution of electricity generation, which offsets emissions associated with water usage (Figure 46a). Minor positive contributions also arise from $CuSO_4$ transportation, as well as oil and cyclopentane production (Figure 46b). The net negative outcome indicates an overall offset of NO_x emissions, demonstrating the potential of operational strategies and energy recovery to substantially mitigate, or even reverse, photochemical smog impacts. Transport-related contributions remain insignificant.

a.

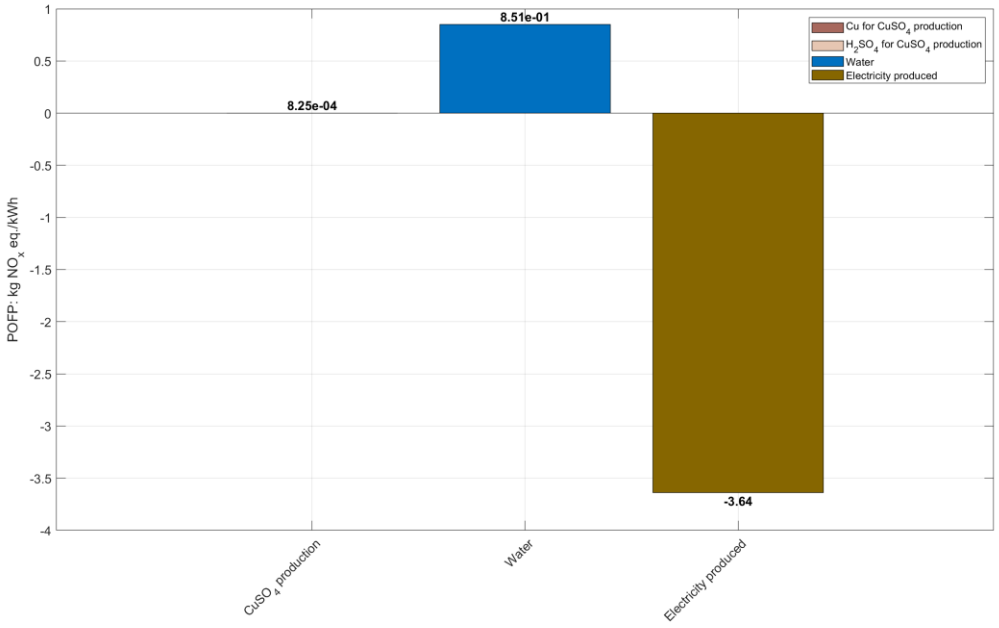

b.

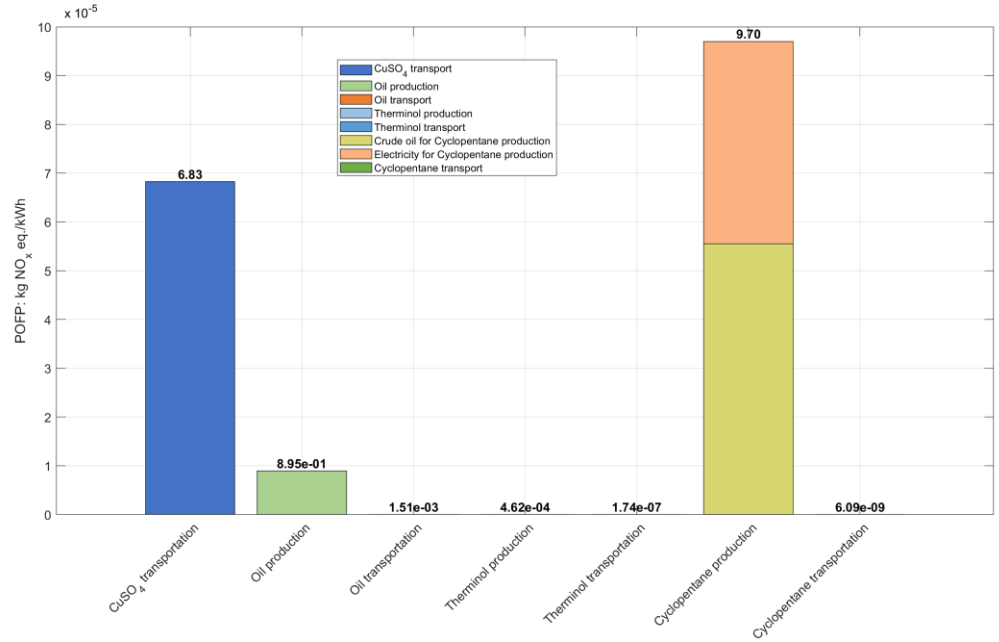

Figure 46. *$POFP_{ecosystem}$ of Use Case 4 – The discharging phase: a) major contributors and b) minor contributors*

Plant construction contributes only minimally to $POFP_{ecosystem}$ ($2.00 \cdot 10^{-7}$ kg NO_x eq./kWh), with stainless steel identified as the main contributor (see Figure 47). Other construction materials (e.g, polyethylene, PRFV, copper) exhibit virtually no measurable impact. These findings confirm that infrastructure plays a negligible role in photochemical smog formation, indicating that mitigation strategies should instead prioritize reducing operational emissions, particularly those linked with energy use and WWT.

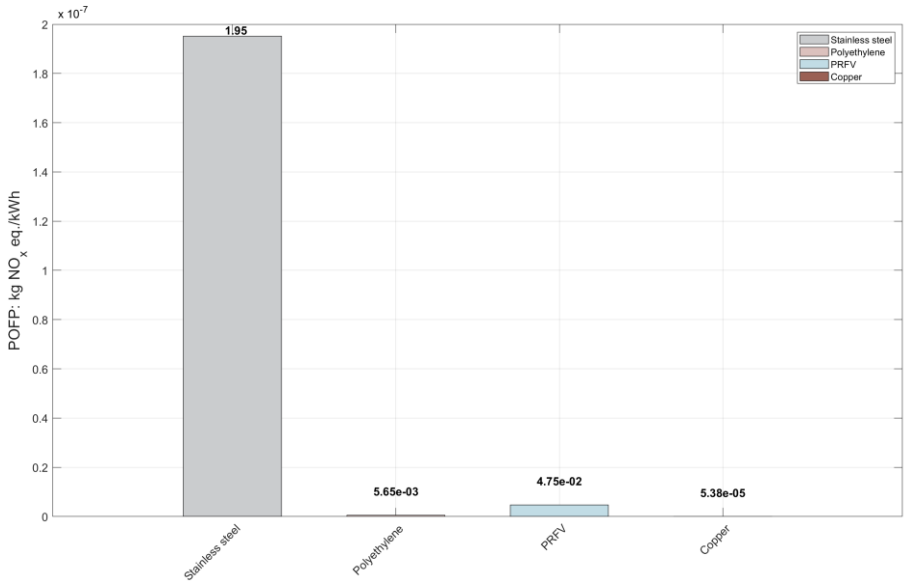

Figure 47. *$POFP_{ecosystem}$ of Use Case 4 – The plant construction*

3.4.9. **Stratospheric Ozone Depletion Potential (ODP)**

In the charging phase, the overall ODP amounts to $2.40 \cdot 10^{-7}$ kg CFC-11 eq./kWh, with energy consumption representing the dominant contributor, accounting for nearly 97% of the total impact. Minor contributions arise from materials' transportation (Figure 48a), while chemical production processes exert a negligible influence (Figure 48b). These results highlight the strong sensitivity of ODP to the choice of energy source.

a.

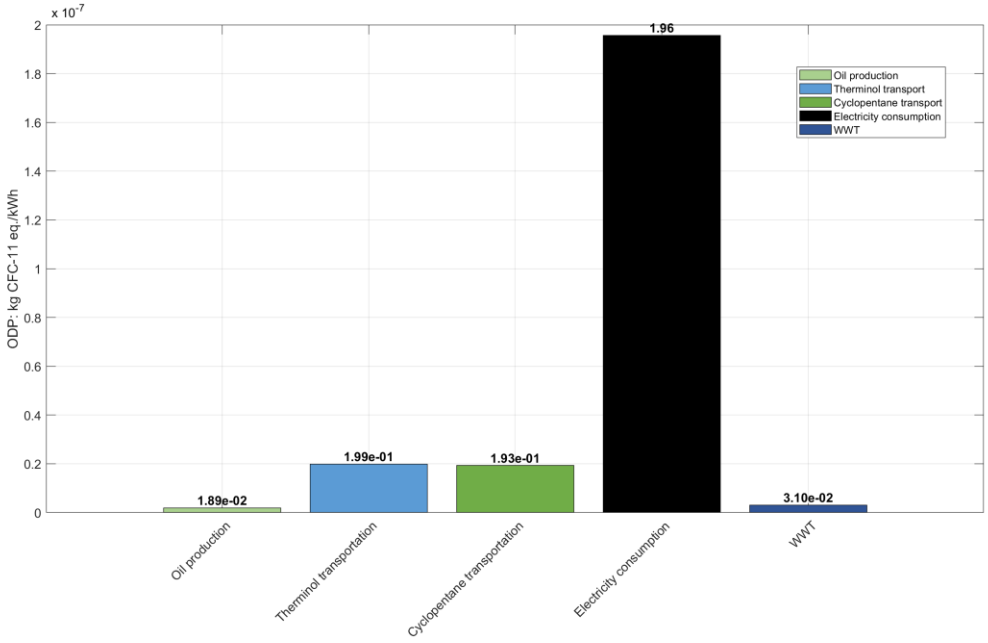

b.

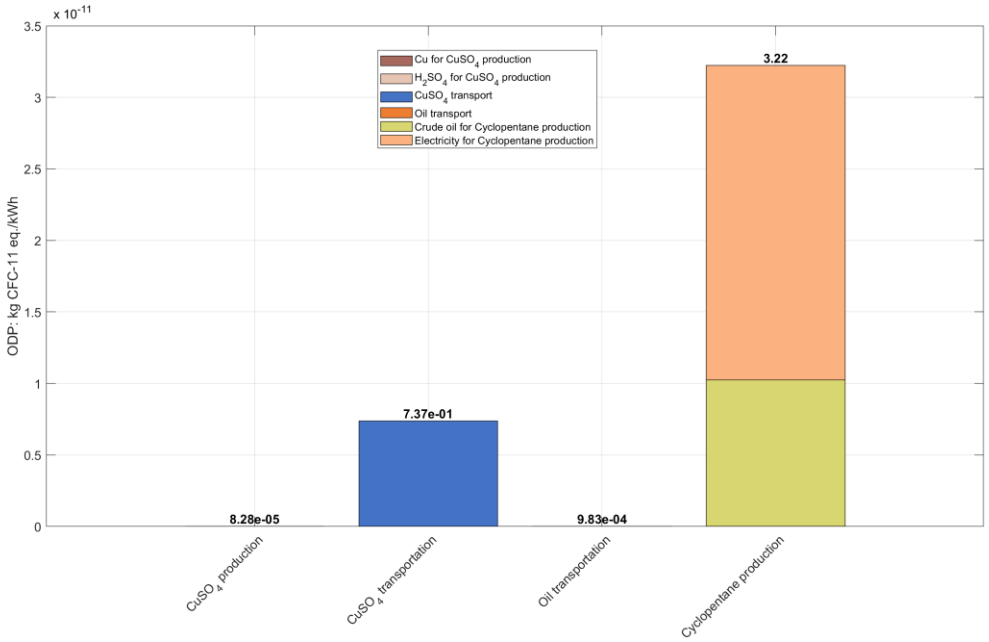

Figure 48. *ODP of Use Case 4 – The charging phase: a) major contributors and b) minor contributors*

During discharging, the total ODP decreases slightly to $4.88 \cdot 10^{-8}$ kg CFC-11 eq./kWh, primarily due to offsets from cyclopentane production. In this phase as well, chemical transportation exerts a noticeable influence on the overall value (Figure 49). This indicates that although operational management can moderately reduce ODP through energy-related offsets, material supply chains also play a relevant role. Overall, discharging contributes marginally less to ODP than charging, largely because of the partial compensation provided by system electricity generation.

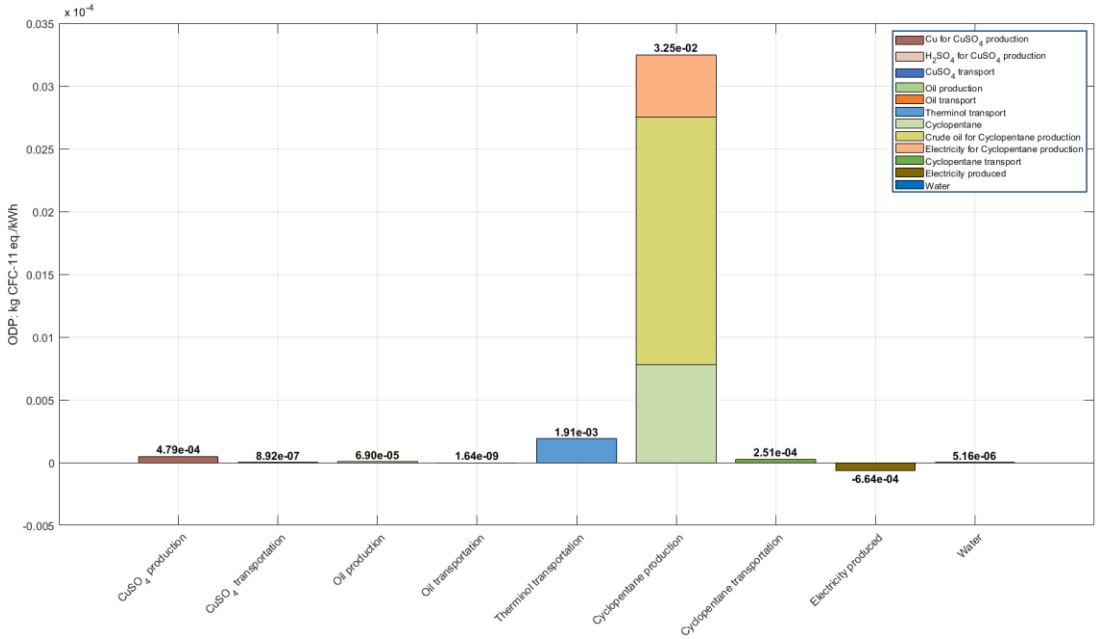

Figure 49. *ODP of Use Case 4 – The discharging phase*

The construction phase shows an almost negligible ODP of $2.04 \cdot 10^{-11}$ kg CFC eq./kWh, with stainless steel identified as the primary contributor (see Figure 50). These results confirm that infrastructure has a minimal role in ODP compared with operational phases, suggesting that mitigation strategies should target operational chemical use and supply chains rather than construction materials.

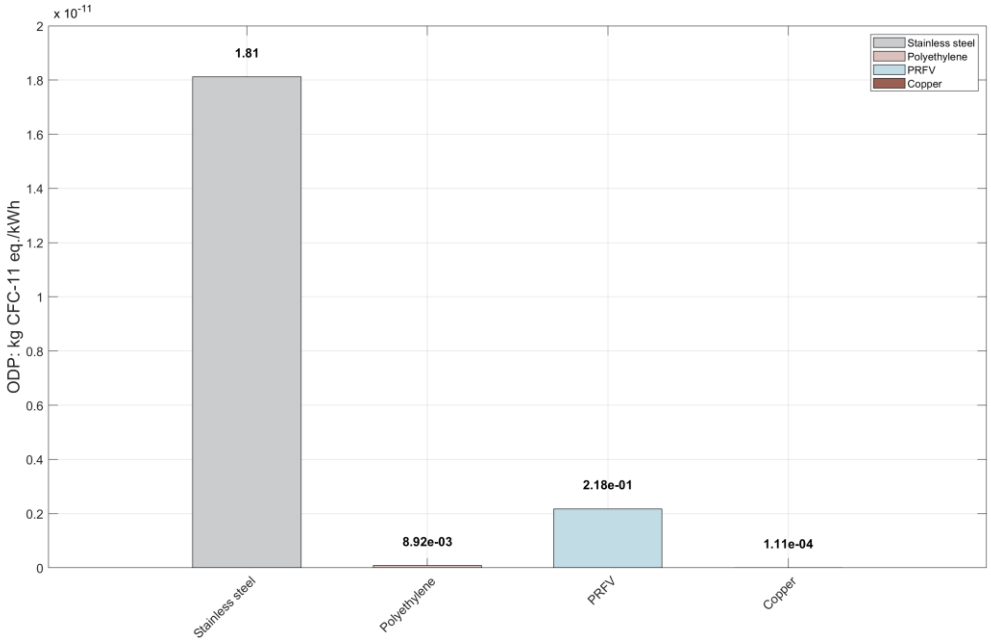

Figure 50. *ODP of Use Case 4 – The plant construction*

3.4.10. **Terrestrial Acidification Potential (TAP)**

In the charging phase, terrestrial acidification potential reaches $5.51 \cdot 10^{-4}$ kg SO_2 eq./kWh, overwhelmingly driven by energy requirements ($4.11 \cdot 10^{-4}$ kg SO_2 eq./kWh). The discharging phase results in a slightly lower value of $2.56 \cdot 10^{-4}$ kg SO_2 eq./kWh, influenced by water consumption and partially offset by electricity generation. Plant construction contributes negligibly ($6.12 \cdot 10^{-7}$ kg SO_2 eq./kWh), confirming that acidification is almost entirely linked to operational activities.

3.4.11. **Terrestrial Ecotoxicity Potential (TETP)**

For TETP, the charging phase contributes $6.69 \cdot 10^{-2}$ kg 1.4-DB eq./kWh, nearly all of which originates from electricity consumption ($6.66 \cdot 10^{-2}$ kg 1.4-DB eq./kWh). In contrast, the discharging phase yields a negative score of $-5.31 \cdot 10^{-2}$ kg 1.4-DB eq./kWh, primarily due to the offset from electricity production (–$5.40 \cdot 10^{-2}$ kg 1.4-DB eq./kWh). Contributions from plant construction remain minimal ($1.51 \cdot 10^{-4}$ kg 1.4-DB eq./kWh).

3.4.12. **Use Case 4 – Main conclusions**

This section is a summary of the key findings in Use Case 4:

- GWP during charging is primarily influenced by electricity consumption, while the discharging phase produces a net negative GWP through electricity generation.

- FDP in the charging phase is driven by electricity demand, whereas the discharging phase delivers fossil-resource credits by offsetting grid electricity.
- $HTP_{non\text{-}cancer}$ is largely associated with Therminol V66 production in both charging and discharging phases. Although electricity consumption during charging contributes to this category, the electricity generating during discharging does not sufficiently compensate for the toxicity impacts linked to Therminol V66 manufacturing.
- In the context of this specific Use Case, electricity consumption emerges as the dominant factor for GWP and FDP, while Therminol V66 and other materials are the primary contributors to toxicity-related impacts.

3.5. Use Case 5 – Holzkirchen Facility – Results and discussions

Table 9 presents the LCA results for the Use Case 5, considering the limitations and assumptions used in the study.

Table 9. LCA results for Use Case 5

KPI	Units	Charging	Discharging	Plant construction
GWP	kg CO_2 eq./kWh	$5.41 \cdot 10^{-1}$	$-4.09 \cdot 10^{-1}$	$1.85 \cdot 10^{-4}$
FDP	kg oil eq./kWh	$1.63 \cdot 10^{-1}$	$-1.28 \cdot 10^{-1}$	$4.71 \cdot 10^{-5}$
FETP	kg 1.4-DB eq./kWh	$3.91 \cdot 10^{-5}$	$-2.00 \cdot 10^{-5}$	$1.07 \cdot 10^{-7}$
FEP	kg P eq./kWh	$1.45 \cdot 10^{-5}$	$1.79 \cdot 10^{-4}$	$2.53 \cdot 10^{-10}$
HTP_{cancer}	kg 1.4-DB eq./kWh	$1.95 \cdot 10^{-4}$	$-1.01 \cdot 10^{-4}$	$2.14 \cdot 10^{-4}$
$HTP_{non\text{-}cancer}$	kg 1.4-DB eq./kWh	$4.64 \cdot 10^{-2}$	$2.58 \cdot 10^{-1}$	$4.55 \cdot 10^{-5}$
MDP	kg Cu eq./kWh	$1.14 \cdot 10^{-3}$	$-3.54 \cdot 10^{-4}$	$5.07 \cdot 10^{-6}$
$POFP_{ecosystem}$	kg NO_x eq./kWh	4.71	-2.48	$3.50 \cdot 10^{-7}$
ODP	kg CFC eq./kWh	$2.39 \cdot 10^{-7}$	$2.11 \cdot 10^{-7}$	$4.31 \cdot 10^{-11}$
TAP	kg SO_2 eq./kWh	$5.25 \cdot 10^{-4}$	$6.86 \cdot 10^{-4}$	$1.04 \cdot 10^{-6}$
TETP	kg 1.4-DB eq./kWh	$6.30 \cdot 10^{-2}$	$-4.86 \cdot 10^{-2}$	$5.83 \cdot 10^{-4}$

Information, comments, and discussions regarding the main sub-processes that exhibit the largest influence on the main impact indicators are included in the section that follows.

3.5.1. Global Warming Potential (GWP)

During the charging phase, the total GWP is almost entirely determined by electricity consumption, which accounts for roughly $5.39 \cdot 10^{-1}$ kg CO_2 eq./kWh out of the total of $5.41 \cdot 10^{-1}$ kg CO_2 eq./kWh (Figure 51a). In comparison, the production and transportation of other chemicals exert only minor influences (Figure 51b). These results highlight the energy-intensive nature of the charging phase and underscore the critical role of energy source selection in mitigating CO_2 emissions. Small contributions from municipal WWT and oil production illustrate additional system-level impacts, though on a marginal scale.

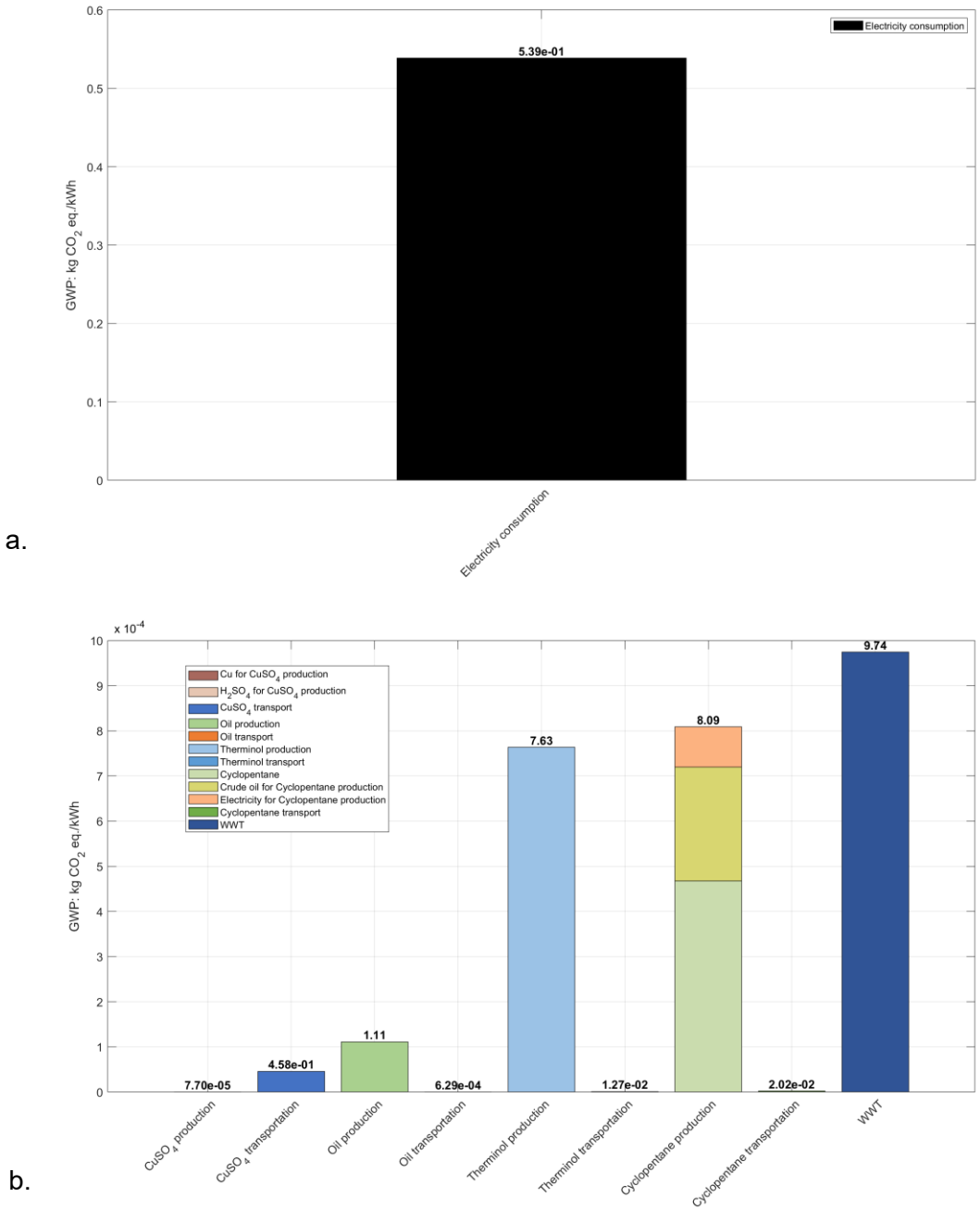

Figure 51. *GWP of Use Case 5 – The charging phase: a) major contributors and b) minor contributors*

By contrast, the discharging phase results in a net negative GWP of $-4.09 \cdot 10^{-1}$ kg CO_2 eq./kWh, primarily driven by the electricity supplied back to the grid, which more than compensates for emissions associated with Therminol V66 production (Figure 52a). Minor positive contributions from chemicals production and water use are observed, (see Figure 52b), but they remain negligible relative to the electricity credit. This net negative outcome suggests that the discharging process can provide a temporary climate benefit, particularly in grids with high carbon intensity. It also highlights the potential of energy storage systems to operate as carbon mitigation tools, contingent on system boundaries and local grid composition. Overall, the

negative GWP underscores the importance of energy recovery and efficient dispatch as key mechanisms for reducing life-cycle emissions and advancing the system's broader sustainability goals.

a.

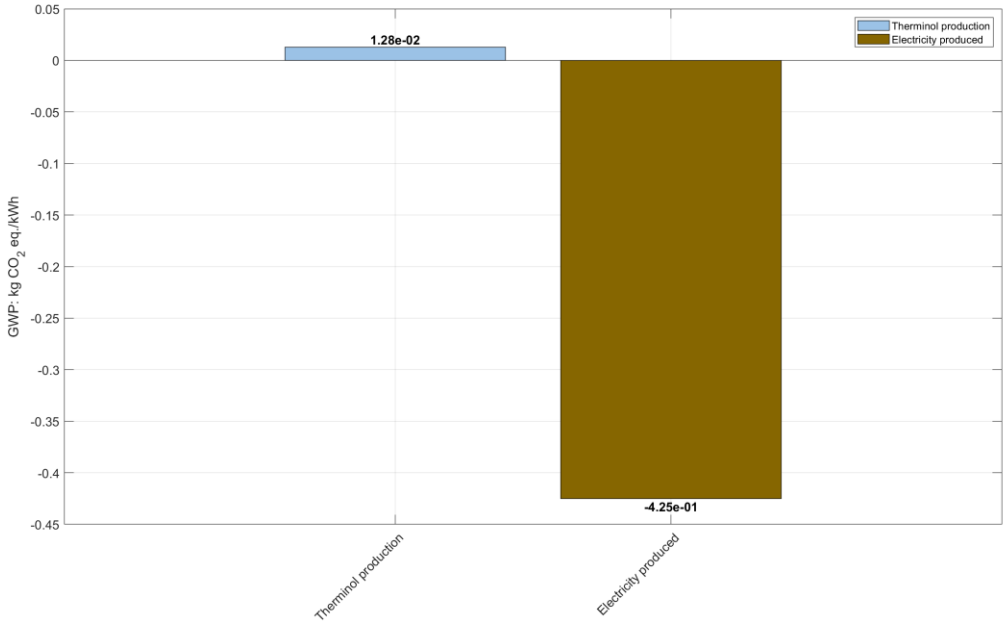

b.

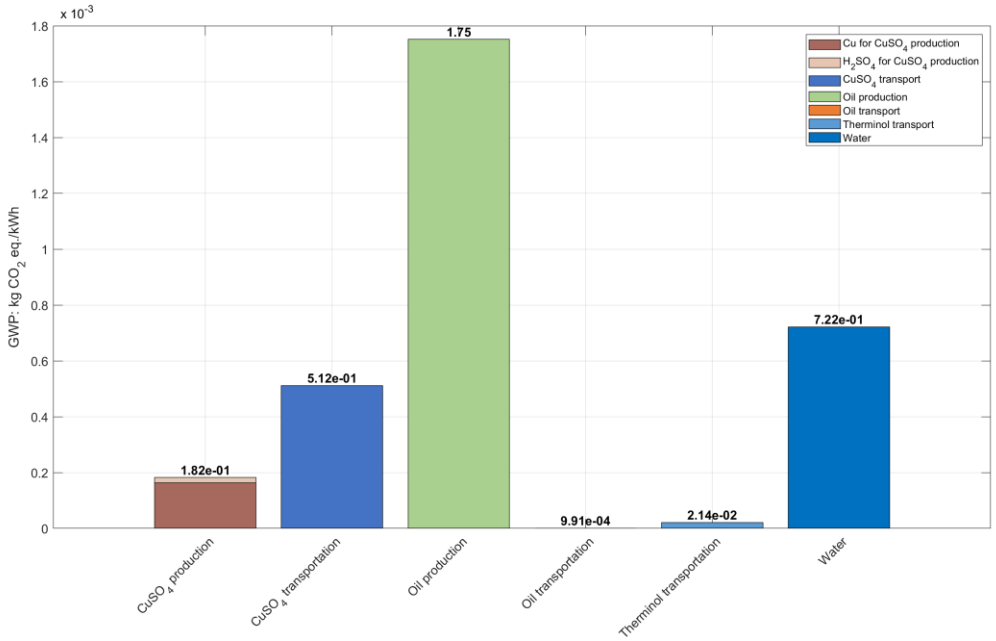

Figure 52. *GWP of Use Case 5 – The discharging phase: a) major contributors and b) minor contributors*

The GWP associated with plant construction is minimal ($1.85 \cdot 10^{-4}$ kg CO_2 eq./kWh), with stainless steel as the main contributor (see Figure 53). Other materials, including polyethylene, copper, and fiberglass, have only minor impacts on climate change. These results confirm that the infrastructure footprint of the energy storage system is negligible compared with operational emissions during both charging and discharging phases. Consequently, mitigation strategies should focus primarily on the operational stages rather than on construction.

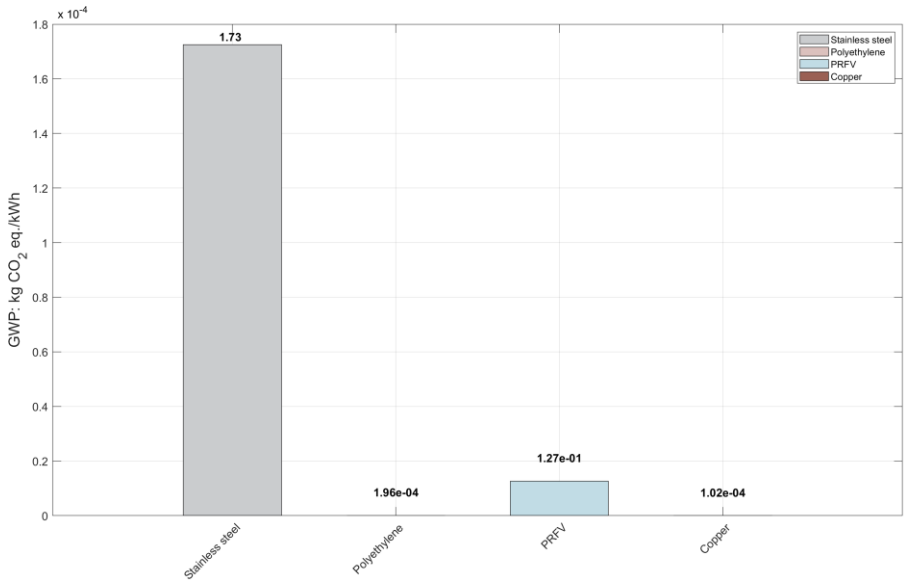

Figure 53. *GWP of Use Case 5 – The plant construction*

3.5.2. **Fossil Depletion Potential (FDP)**

As shown in Figure 54, FDP impact during the charging phase is predominantly driven by the electricity consumption (nearly $1.63 \cdot 10^{-1}$ kg oil eq./kWh), while contributions from other production and transport processes are negligible. This indicates that fossil resource depletion is largely determined by electricity use, highlighting the importance of sourcing renewable energy to reduce FDP impacts. Minor contributions from municipal WWT further illustrate the limited yet systemic role of auxiliary processes in fossil resource consumption.

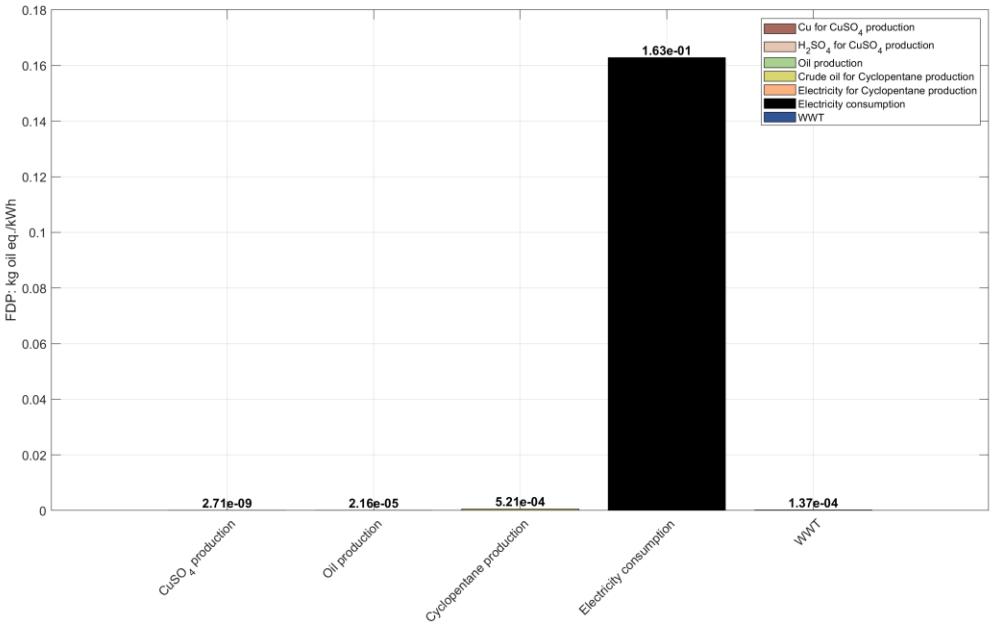

Figure 54. *FDP of Use Case 5 – The charging phase*

During the discharging step, the FDP becomes slightly negative ($-1.28 \cdot 10^{-1}$ kg oil eq./kWh), primarily due to electricity generation, which offsets fossil resource use elsewhere. Other processes, including $CuSO_4$ and oil production as well as water consumption, exhibit low

positive contributions relative to the energy credit (Figure 55). The negligible impact of transport and other chemicals confirms that operational electricity flows are the main drivers of FDP during discharging. These results underscore that the environmental performance of the discharge phase is highly sensitive to the characteristics of the electricity grid.

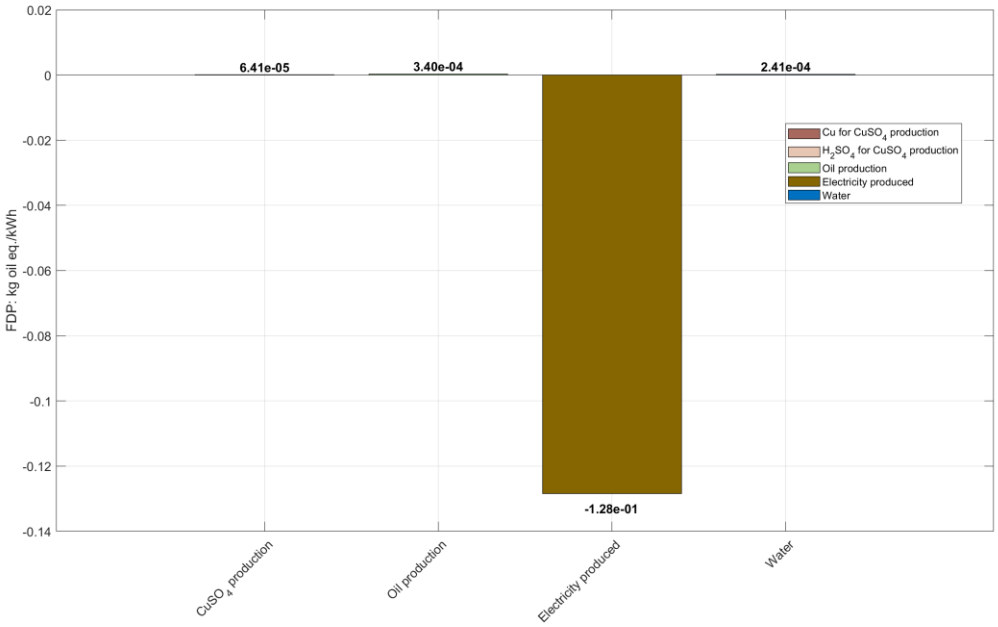

Figure 55. *FDP of Use Case 5 – The discharging phase*

The FDP associated with plant construction is extremely low ($4.71 \cdot 10^{-5}$ kg oil eq./kWh), with stainless steel as the major contributor (Figure 56). Contributions from polymeric materials and other structural components are minor or negligible. This indicates that the fossil resource footprint of the infrastructure is minimal compared to the operational phases. Accordingly, mitigation strategies should focus on the selection of energy sources during charging rather than on construction. Overall, plant construction does not constitute a significant contributor to fossil depletion in this Use Case configuration.

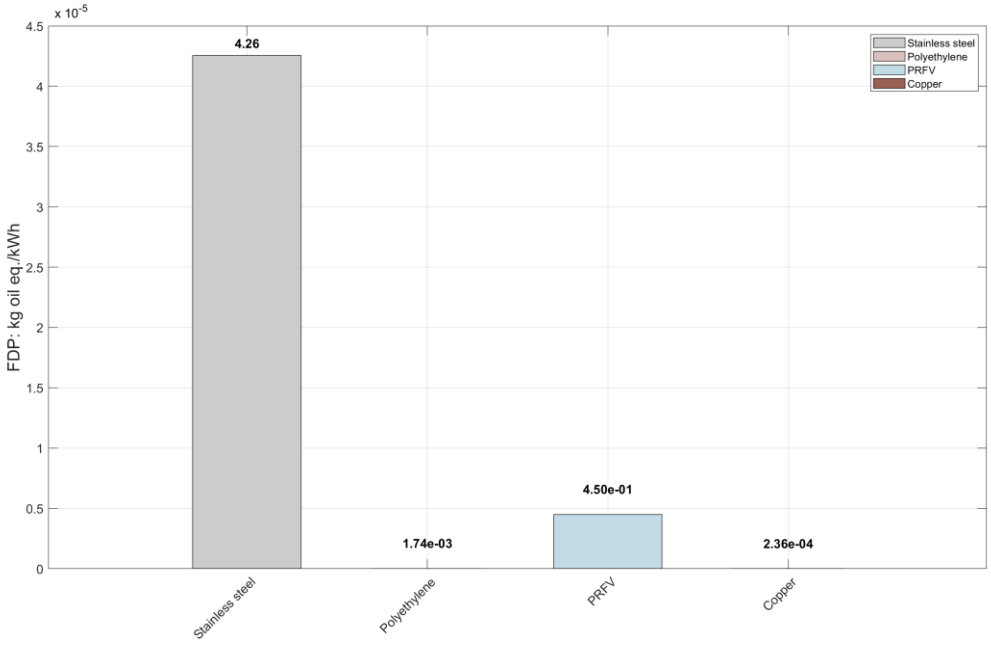

Figure 56. *FDP of Use Case 5 – The plant construction*

3.5.3. **Freshwater Ecotoxicity Potential (FETP)**

In terms of FETP, the charging phase contributes $3.91 \cdot 10^{-5}$ kg 1.4-DB eq./kWh, with electricity generation ($2.81 \cdot 10^{-5}$ kg 1.4-DB eq./kWh) and municipal WWT ($1.05 \cdot 10^{-5}$ kg 1.4-DB eq./kWh) as the primary drivers. During discharging, the contribution is negative ($-2.00 \cdot 10^{-5}$ kg 1.4-DB eq./kWh), while the construction phase has a negligible impact ($1.07 \cdot 10^{-7}$ kg 1.4-DB eq./kWh). Overall, freshwater ecotoxicity is predominantly influenced by the electricity generation and WWT during charging, with plant construction playing an almost insignificant role.

3.5.4. **Freshwater Eutrophication Potential (FEP)**

During charging, FEP amounts to $1.45 \cdot 10^{-5}$ kg P eq./kWh, mainly due to Therminol V66 production ($1.08 \cdot 10^{-5}$ kg P eq./kWh). In the discharging phase, the impact increases to a value of $1.79 \cdot 10^{-4}$ kg P eq./kWh, having again Therminol V66 production as the main contributor ($1.81 \cdot 10^{-4}$ kg P eq./kWh). Plant construction has negligible influence on the overall FEP performance ($2.53 \cdot 10^{-10}$ kg P eq./kWh). Therefore, these results indicate that Therminol V66 production represents a persistent hotspot for FEP across both charging and discharging phases.

3.5.5. **Human Toxicity Potential cancer (HTP_{cancer})**

During charging, cancer-related toxicity reaches $1.95 \cdot 10^{-4}$ kg 1.4-DB eq./kWh, largely driven by electricity consumption ($1.42 \cdot 10^{-4}$ kg 1.4-DB eq./kWh). In the discharging phase, the impact decreases to $-1.01 \cdot 10^{-4}$ kg 1.4-DB eq./kWh, with $CuSO_4$ production ($2.05 \cdot 10^{-6}$ kg 1.4-DB eq./kWh) as the main contributor, fully offset by the credit from electricity generation ($-1.12 \cdot 10^{-4}$ kg 1.4-DB eq./kWh). Plant construction contributes with $2.14 \cdot 10^{-4}$ kg 1.4-DB eq./kWh. Overall, cancer-related toxicity is dominated by electricity generation during charging and by $CuSO_4$ production during discharging, while in the plant construction stage, it is mainly influenced by the usage of stainless steel.

3.5.6. **Human Toxicity Potential non-cancer ($HTP_{non-cancer}$)**

During charging, non-cancer human toxicity totals $4.64 \cdot 10^{-2}$ kg 1.4-DB eq./kWh, with contributions from Therminol V66 production ($1.65 \cdot 10^{-2}$ kg 1.4-DB eq./kWh) and electricity consumption ($2.76 \cdot 10^{-2}$ kg 1.4-DB eq./kWh). In the discharging phase, the impact increases to $2.58 \cdot 10^{-1}$ kg 1.4-DB eq./kWh, predominantly driven by Therminol V66 production ($2.77 \cdot 10^{-1}$ kg 1.4-DB eq./kWh), and partially offset by electricity generation ($-2.17 \cdot 10^{-2}$ kg 1.4-DB eq./kWh). Contributions from plant construction are negligible ($4.55 \cdot 10^{-5}$ kg 1.4-DB eq./kWh).

3.5.7. **Metal Depletion Potential (MDP)**

In regards to MDP impact indicator, the charging phase contributes $1.14 \cdot 10^{-3}$ kg Cu eq./kWh, mainly due to the electricity consumption ($1.13 \cdot 10^{-3}$ kg Cu eq./kWh). Discharging results in a net negative impact of $-3.54 \cdot 10^{-4}$ kg Cu eq./kWh, largely due to the electricity production process ($-8.89 \cdot 10^{-4}$ kg Cu eq./kWh). Construction impacts remain minimal ($5.07 \cdot 10^{-6}$ kg Cu eq./kWh). Overall, electricity use emerges as the main driver of MDP across both operational phases.

3.5.8. **Photochemical Oxidant Formation Potential ecosystem ($POFP_{ecosystem}$)**

During the charging phase, the total $POFP_{ecosystem}$ impact amounts to 4.71 kg NO_x eq./kWh, with electricity consumption ranking as the primary contributor (4.22 kg NO_x eq./kWh) and municipal WWT as the second-largest source (0.49 kg NO_x eq./kWh) (Figure 57a). Cyclopentane production provides a minor contribution (approximately $5.01 \cdot 10^{-4}$ kg NO_x eq./kWh), while other chemicals and transport processes are negligible (Figure 57b). These results indicate that indirect emissions from energy use and wastewater management are the main drivers of $POFP_{ecosystem}$. The high $POFP_{ecosystem}$ underscores the importance of low-emission electricity sources and improved WWT technologies, consistent with previous cases. Minor contributors highlight that chemical feedstock selection has a relatively small influence on ozone formation compared with operational energy-related processes. Overall, the charging phase presents substantial opportunities for mitigating smog-forming emissions.

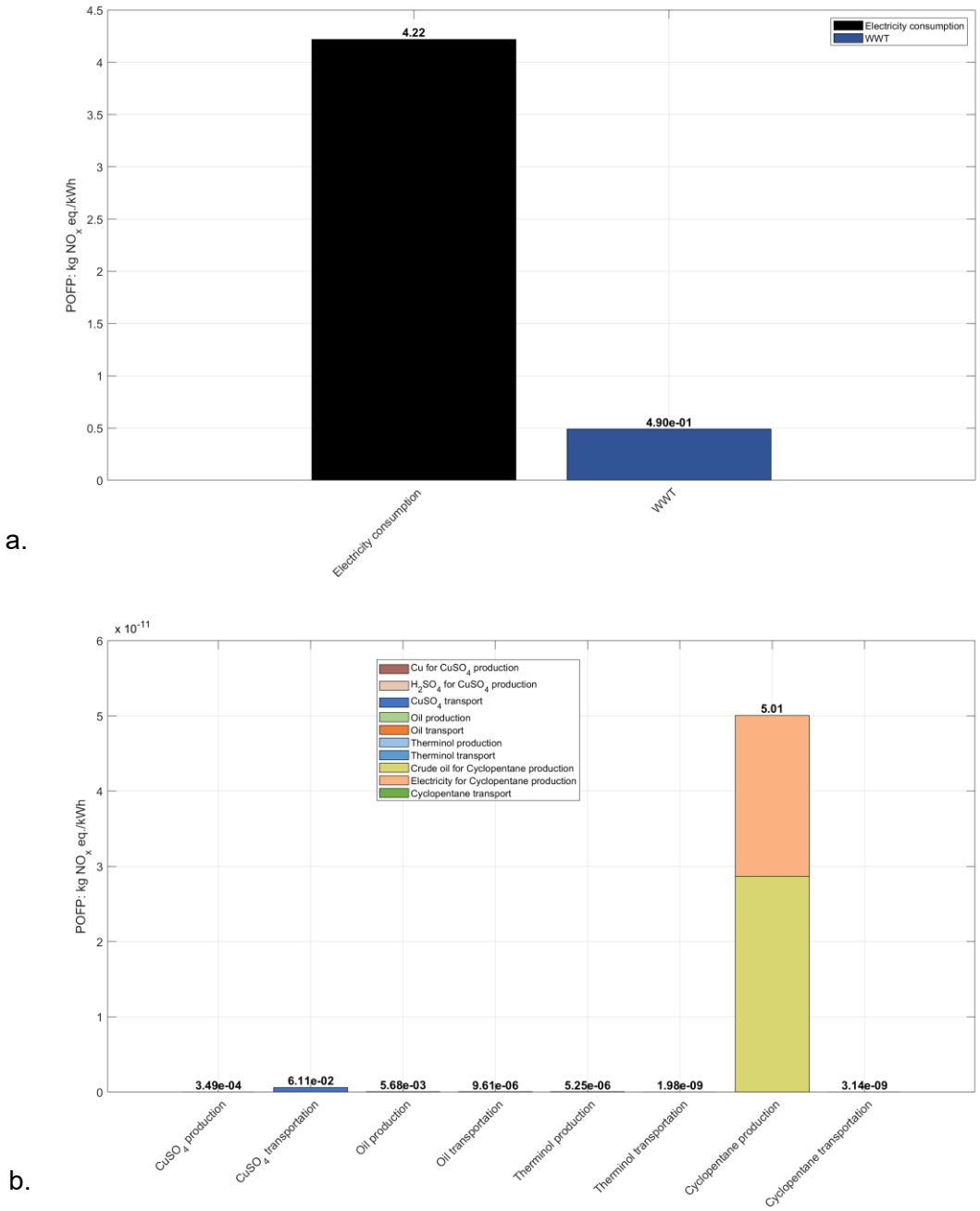

Figure 57. *$POFP_{ecosystem}$ of Use Case 5 – The charging phase: a) major contributors and b) minor contributors*

During discharging, the total $POFP_{ecosystem}$ reaches -2.48 kg NOx eq./kWh, largely due to the electricity credit (-3.33 kg NO_x eq./kWh), which offsets emissions from water use (0.851 kg NO_x eq./kWh) and $CuSO_4$ production (Figure 58a). This result indicates that energy recovery during discharging can effectively mitigate photochemical ozone formation, particularly in electricity grids characterized by high NO_x intensity. Transport processes exhibit minor contributions (Figure 58b). Overall, these results underscore the potential of energy storage systems to serve as mitigation tools not only for climate change but also for reducing smog precursors.

a.

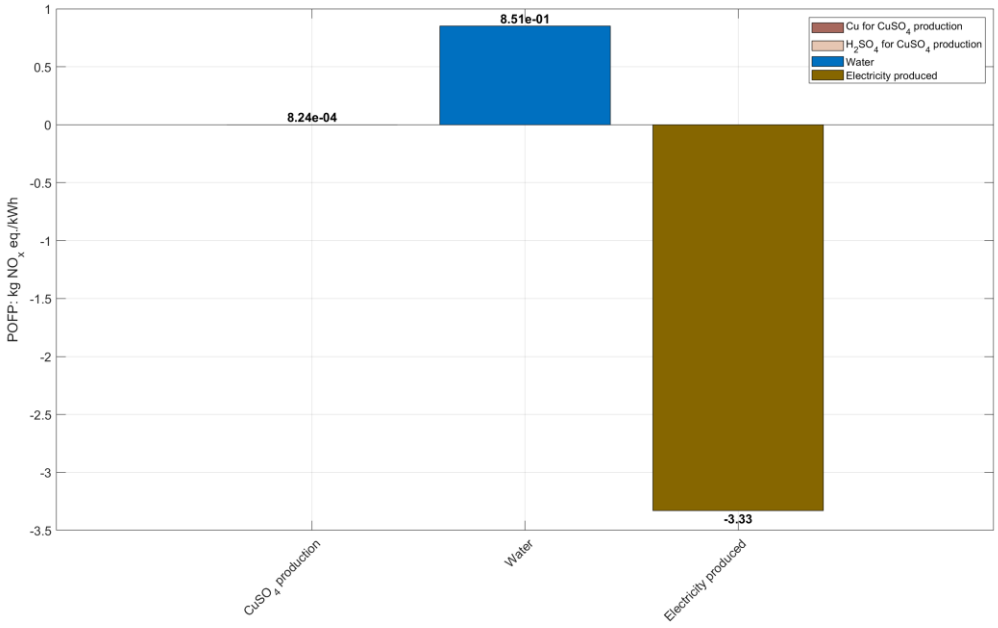

b.

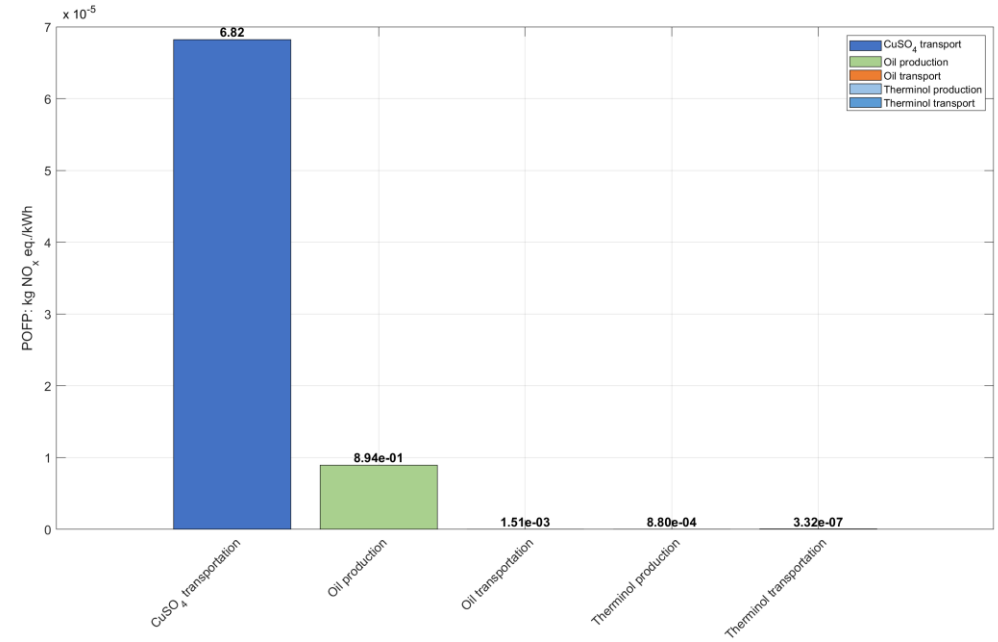

Figure 58. *$POFP_{ecosystem}$ of Use Case 5 – The discharging phase: a) major contributors and b) minor contributors*

The POFP associated with plant construction is minimal ($3.50 \cdot 10^{-7}$ kg NO_x eq./kWh), primarily with contributions from stainless steel and PRFV (Figure 59). Other construction materials, including polyethylene and copper, contribute negligibly. These results indicate that the infrastructure-related share of $POFP_{ecosystem}$ is insignificant compared with operational emissions. Accordingly, mitigation strategies should focus on the operational phase in Use Case 5.

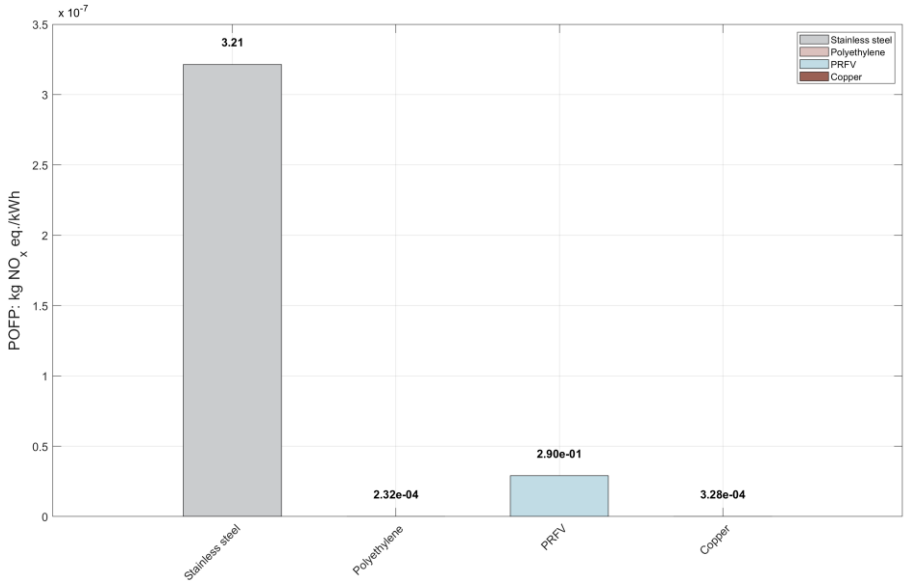

Figure 59. *$POFP_{ecosystem}$ of Use Case 5 – The plant construction*

3.5.9. **Stratospheric Ozone Depletion Potential (ODP)**

As illustrated in Figure 60, the total ODP value during the charging phase reaches $2.39 \cdot 10^{-7}$ kg CFC-11 eq./kWh, with electricity consumption ranking as the primary contributor ($1.84 \cdot 10^{-7}$ kg CFC-11 eq./kWh). Contributions from other chemicals production and transport processes are considerably smaller, with $CuSO_4$ production being nearly negligible. These results indicate that the ODP environmental impact indicator is predominantly driven by the energy use rather than the specific feedstock chemicals. Minor contributions from other materials suggest that selecting low-ODP chemicals can further reduce the overall impact.

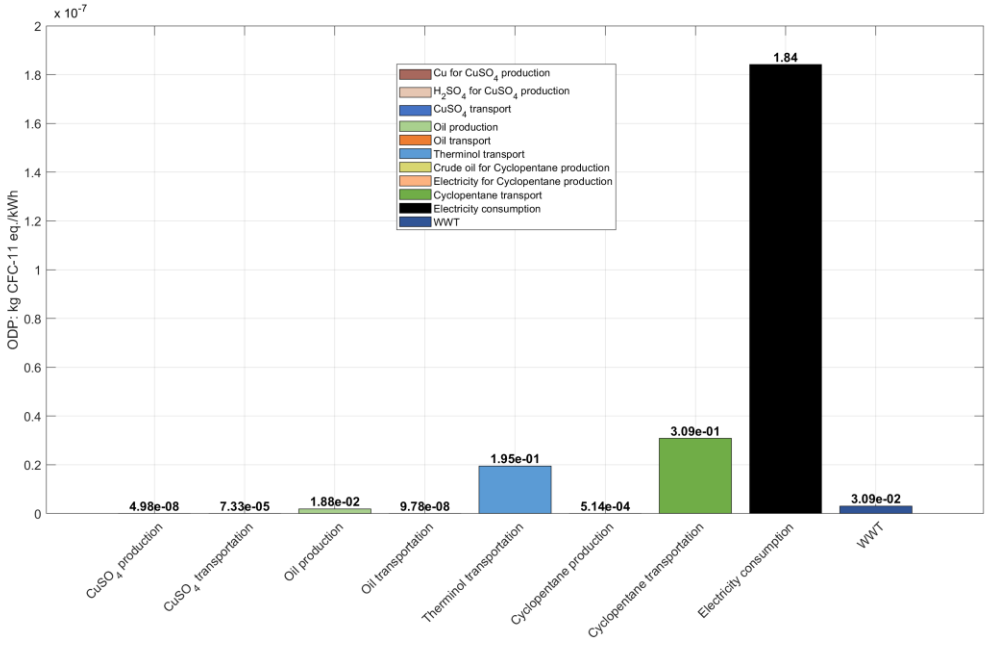

Figure 60. *ODP of Use-Case 5 – The charging phase*

During discharging, the ODP impact score reaches $2.11 \cdot 10^{-7}$ kg CFC-11 eq./kWh, with minor contributions from Therminol V66 transportation (see Figure 61). The negative effect of electricity generation slightly offsets emissions; however, the overall ODP remains positive. These findings highlight that the discharging phase has a minimal effect on ODP.

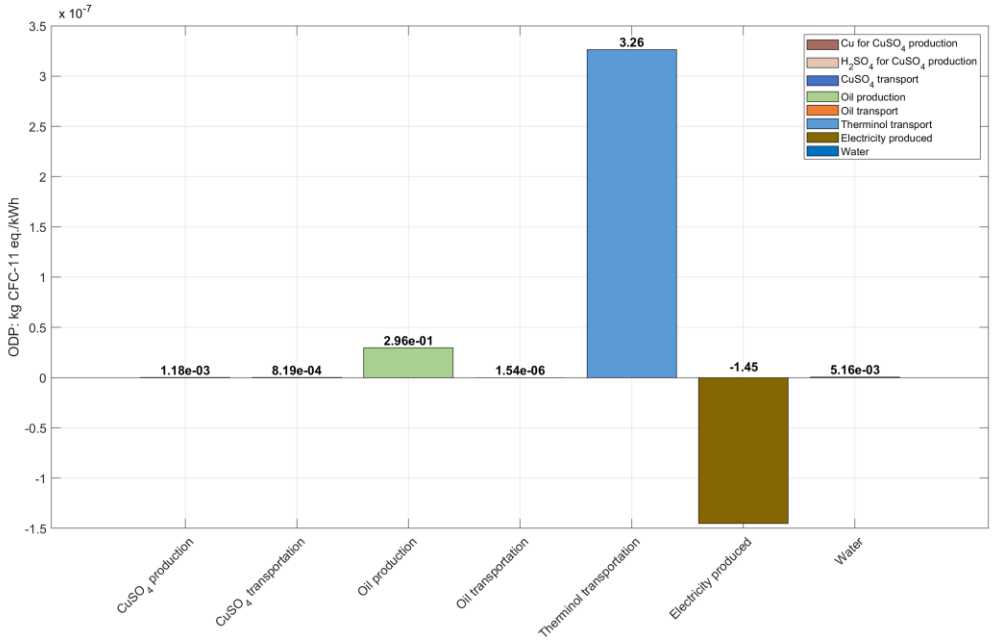

Figure 61. *ODP of Use-Case 5 – The discharging phase*

The ODP associated with plant construction amounts to $4.31 \cdot 10^{-11}$ kg CFC eq./kWh, with only trace contributions from stainless steel and PRFV (Figure 62). Polyethylene and copper have no measurable influence on ODP. These negligible values indicate that infrastructure choices do not meaningfully affect stratospheric ozone depletion. Therefore, mitigation efforts should focus entirely on electricity source selection and operational chemical management. Overall, these results confirm that plant construction is essentially irrelevant for ODP impacts.

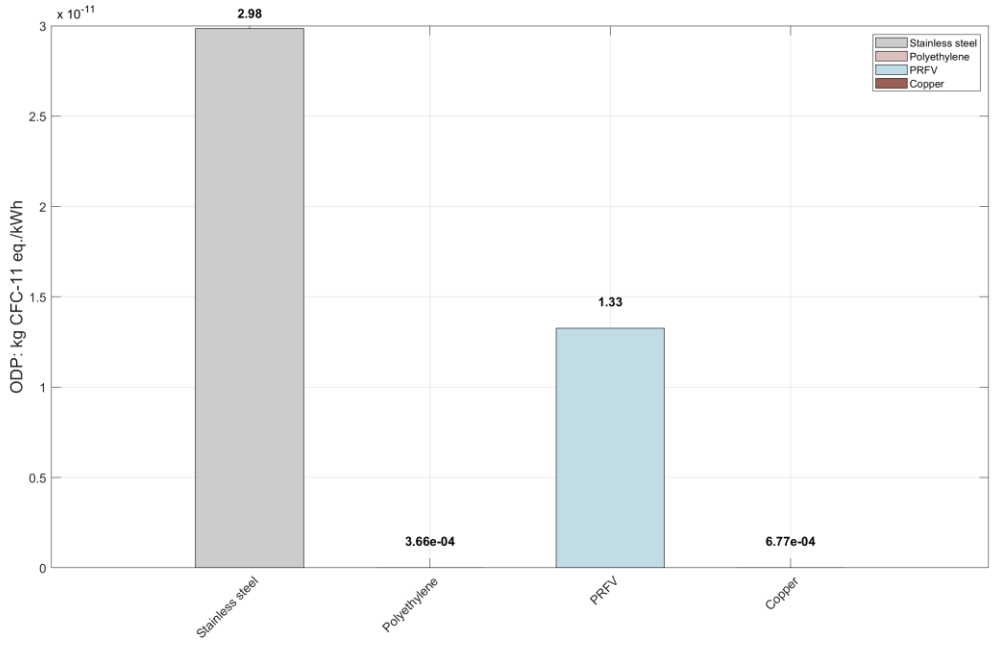

Figure 62. *ODP of Use Case 5 – The plant construction*

3.5.10. **Terrestrial Acidification Potential (TAP)**

During charging, TAP impact score reaches $5.25 \cdot 10^{-4}$ kg SO_2 eq./kWh, almost entirely driven by electricity consumption ($3.87 \cdot 10^{-4}$ kg SO_2 eq./kWh). In the discharging phase, the TAP indicator increases to $6.86 \cdot 10^{-4}$ kg SO_2 eq./kWh, primarily due to Therminol V66 production and water use. Contributions from plant construction are negligible ($1.04 \cdot 10^{-6}$ kg SO_2 eq./kWh).

3.5.11. **Terrestrial Ecotoxicity Potential (TETP)**

The TETP impact during charging reached $6.30 \cdot 10^{-2}$ kg 1.4-DB eq./kWh, largely attributable to electricity consumption ($6.26 \cdot 10^{-2}$ kg 1.4-DB eq./kWh). In discharging phase, TETP shows a negative impact of $-4.86 \cdot 10^{-2}$ kg 1.4-DB eq./kWh, mainly due to the credit from electricity generation ($-4.94 \cdot 10^{-2}$ kg 1.4-DB eq./kWh). Plant construction impacts are minimal in this case as well ($5.83 \cdot 10^{-4}$ kg 1.4-DB eq./kWh).

3.5.12. **Use Case 5 – Main conclusions**

The following is a summary of the main findings in Use Case 5:

- Electricity consumption and imports from the grid represent the largest share of GWP during charging, whereas the discharging phase yields negative GWP values through power generation.
- A similar trend is observed for FDP: charging is dominated by electricity imports, while discharging provides fossil-resource credits from electricity production.
- $HTP_{non\text{-}cancer}$ is consistently driven by Therminol V66 production, highlighting chemical manufacturing as a significant operational hotspot, even in the context of geothermal resource use.

- Overall, in geothermal-based DHC, the net environmental outcome is strongly shaped by upstream chemical production (e.g., Therminol V66) and the characteristics of grid electricity required during charging.

3.6. Use Case 6 – POLIMI Campus Energy Network – Results and discussions

Table 10 shows the LCA results in Use Case 6 scenario, taking into account the study's limitations and assumptions. Regarding this particular Use Case, it is important to emphasize that Novec 649 has been used as the reference fluid for the study, with the aim of exploring alternatives among the range of potentially applicable fluids (e.g., Solstice 1233zd). The study therefore provides a basis for future assessments and improvements, contingent on future need and technology advancements.

Information, comments, and discussions regarding the main subprocesses influencing the most pertinent effect indicators for this Use Case scenario are included in the section that follows.

Table 10. LCA results for Use Case 6

KPI	Units	Charging	Discharging	Plant construction
GWP	kg CO_2 eq./kWh	$2.85 \cdot 10^{-1}$	$1.36 \cdot 10^{-1}$	$3.34 \cdot 10^{-1}$
FDP	kg oil eq./kWh	$9.82 \cdot 10^{-2}$	$8.25 \cdot 10^{-2}$	$9.19 \cdot 10^{-2}$
FETP	kg 1.4-DB eq./kWh	$9.16 \cdot 10^{-5}$	$4.23 \cdot 10^{-5}$	$3.78 \cdot 10^{-1}$
FEP	kg P eq./kWh	$5.12 \cdot 10^{-6}$	$1.54 \cdot 10^{-7}$	$6.08 \cdot 10^{-7}$
HTP_{cancer}	kg 1.4-DB eq./kWh	$1.32 \cdot 10^{-3}$	$1.07 \cdot 10^{-3}$	$3.61 \cdot 10^{-1}$
$HTP_{non\text{-}cancer}$	kg 1.4-DB eq./kWh	$1.14 \cdot 10^{-1}$	$2.08 \cdot 10^{-1}$	161.11
MDP	kg Cu eq./kWh	$2.32 \cdot 10^{-2}$	$4.13 \cdot 10^{-2}$	$1.07 \cdot 10^{-1}$
$POFP_{ecosystem}$	kg NO_x eq./kWh	49.01	-1.76	$1.27 \cdot 10^{-3}$
ODP	kg CFC eq./kWh	$9.65 \cdot 10^{-7}$	$2.14 \cdot 10^{-6}$	$9.68 \cdot 10^{-8}$
TAP	kg SO_2 eq./kWh	$1.79 \cdot 10^{-3}$	$1.79 \cdot 10^{-3}$	$6.72 \cdot 10^{-3}$
TETP	kg 1.4-DB eq./kWh	$2.59 \cdot 10^{-1}$	$4.04 \cdot 10^{-1}$	1809.41

3.6.1. Global Warming Potential (GWP)

During the charging phase, the total GWP impact amounts to $2.85 \cdot 10^{-1}$ kg CO_2 eq./kWh, and it is primarily influenced by the electricity import from the grid (0.15 kg CO_2 eq./kWh), followed by the Novec 649 production ($6.74 \cdot 10^{-2}$ kg CO_2 eq./kWh) (Figure 63a). As observed in Figure 63a, $CuSO_4$ production ($6.31 \cdot 10^{-2}$ kg CO_2 eq./kWh) and municipal WWT ($3.38 \cdot 10^{-3}$ kg CO_2 eq./kWh) rank third and fourth. Transport processes have negligible contributions when compared to material production. Figure 63a highlights that the electricity use, Novec 649 and $CuSO_4$ production are the primary contributors, while Figure 63b shows low, yet non-negligible impacts from other processes such as oil production and material transportation. Overall, the results emphasize decarbonization of the electricity supply as key to reduce the GWP.

a.

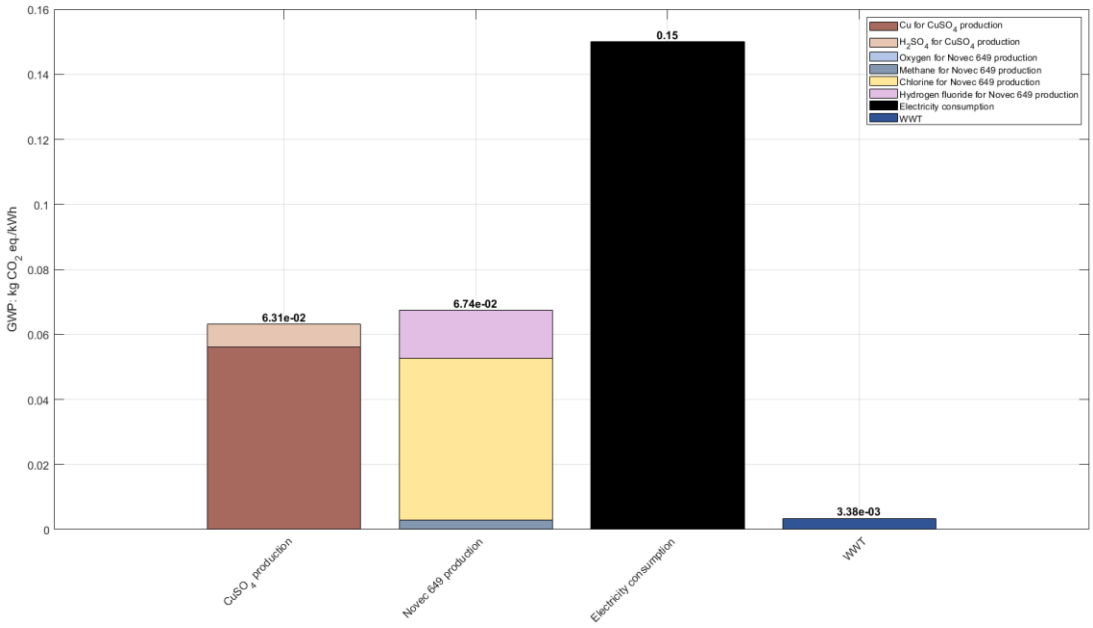

b.

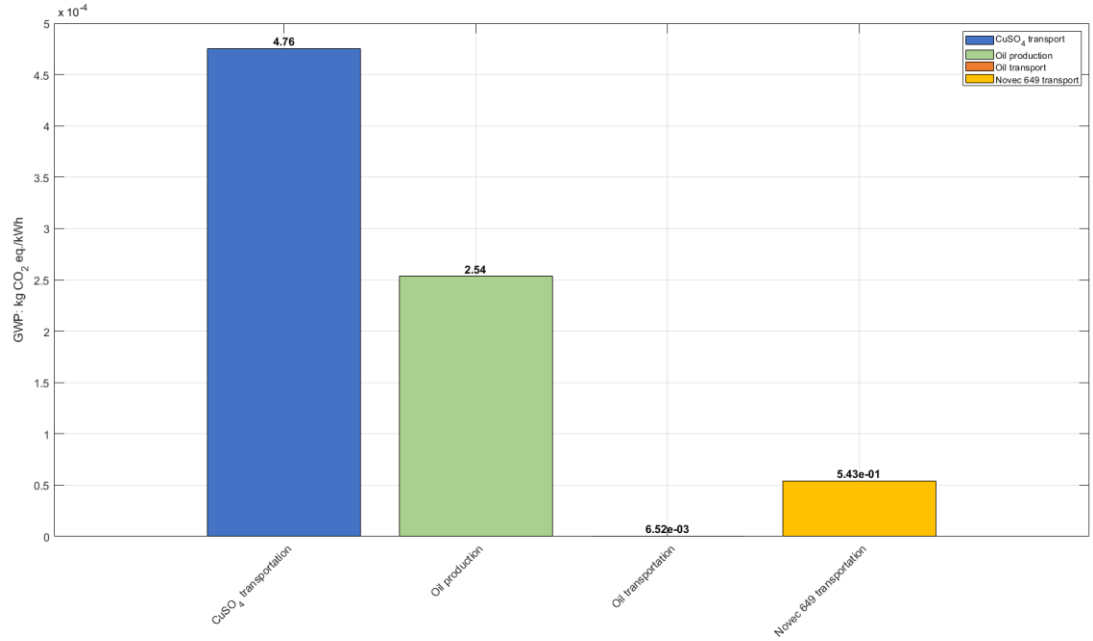

Figure 63. *GWP of Use Case 6 – The charging phase: a) major contributors and b) minor contributors*

During the discharging phase, the GWP score is reduced to $1.36 \cdot 10^{-1}$ kg CO_2 eq./kWh. Novec 649 and $CuSO_4$ production ($1.69 \cdot 10^{-1}$ kg CO_2 eq./kWh and $1.15 \cdot 10^{-1}$ kg CO_2 eq./kWh, respectively) are the largest contributors. Nevertheless, their impacts are partly offset by the negative contribution obtained due to the electricity produced ($-1.5 \cdot 10^{-1}$ kg CO_2 eq./kWh). This negative balance indicates an avoided burden effect due to power generation, which substantially improves the climate profile of this phase. Transport contributions remain small, with $CuSO_4$, oil, and Novec 649 transport contributing $0.87 \cdot 10^{-3}$ kg CO_2 eq./kWh, $0.64 \cdot 10^{-3}$ kg CO_2 eq./kWh and $0.14 \cdot 10^{-3}$ kg CO_2 eq./kWh, respectively. Figure 64a shows that Novec 649 and $CuSO_4$ production rank as first and second contributors, while emphasizing as well the

role of avoided electricity burdens. Figure 64b highlights the impact of transport processes. This demonstrates that discharging allows for compensatory effects, thus reducing the overall burden.

a.

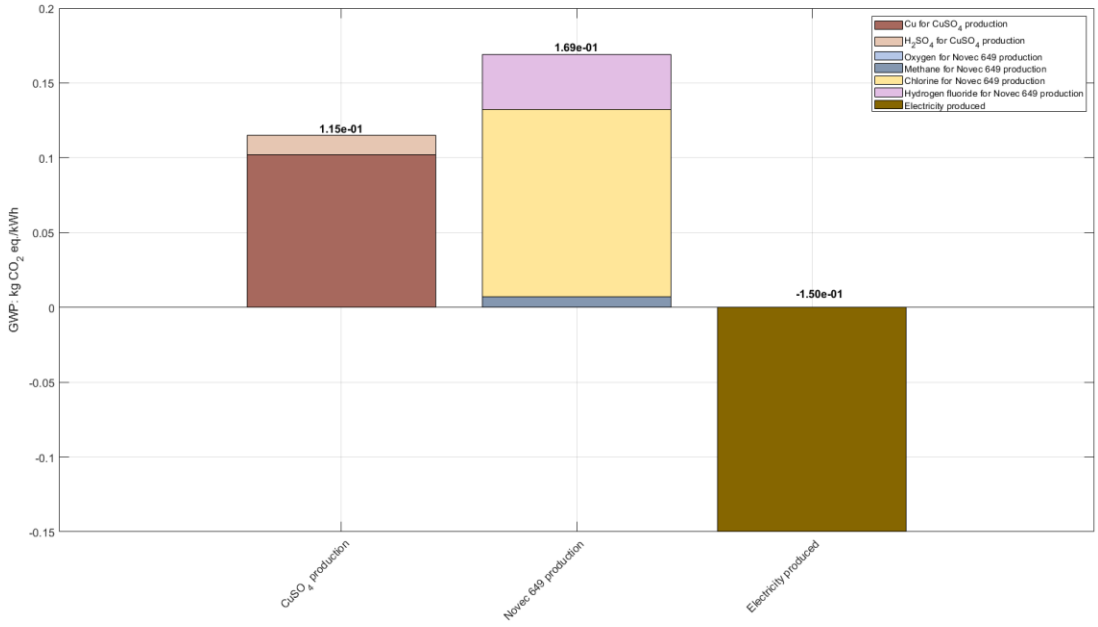

b.

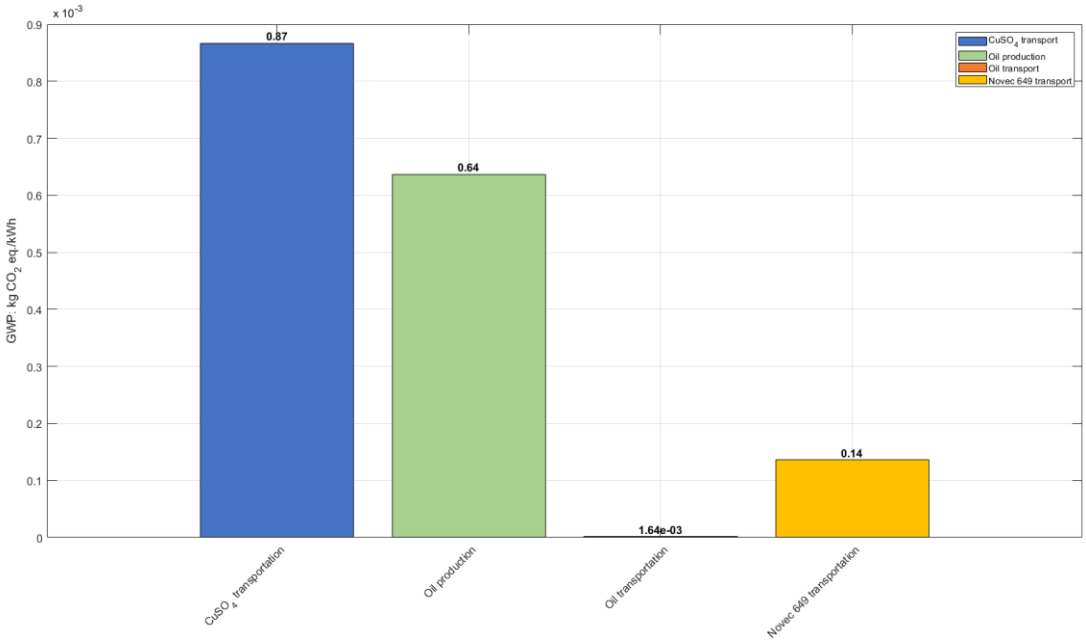

Figure 64. *GWP of Use Case 6 – The discharging phase: a) major contributors and b) minor contributors*

For the plant construction, the GWP impact score is significantly higher ($3.34 \cdot 10^{-1}$ kg CO_2 eq./kWh) compared to both operational stages. This is primarily driven by platinum production ($2.92 \cdot 10^{-1}$ kg CO_2 eq./kWh), which accounts for the majority of the impact due to its highly energy-intensive extraction and refining.

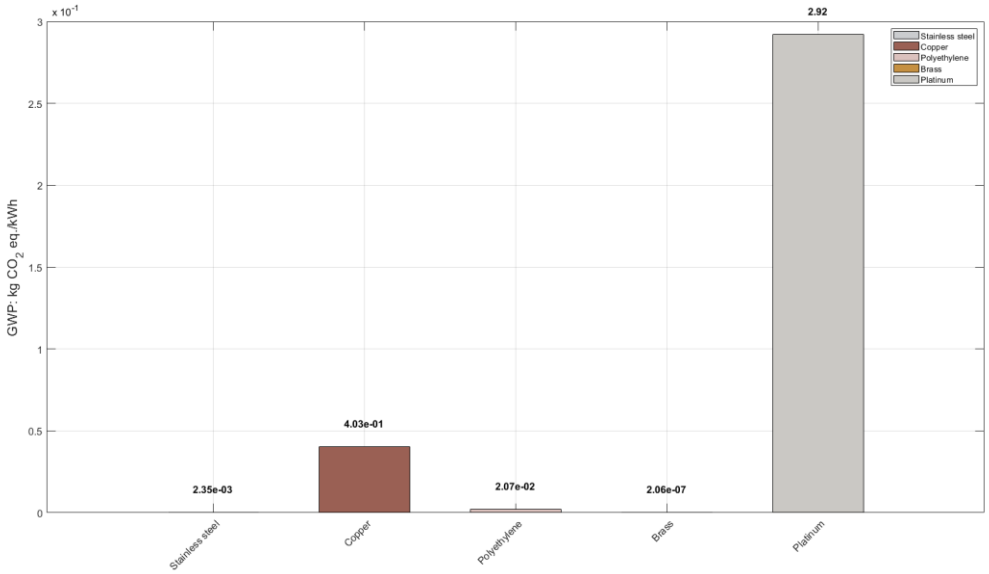

Figure 65. GWP of Use Case 6 – The plant construction

Additional relevant contributions include copper cathode production ($4.03 \cdot 10^{-2}$ kg CO_2 eq./kWh) and plastic production ($2.07 \cdot 10^{-3}$ kg CO_2 eq./kWh). Steel and brass inputs contribute only marginally. Unlike the charging and discharging phases, there are no avoided burdens in this stage, and the impacts are solely driven by material demand. Figure 65 highlights that construction-related emissions may represent a long-term hotspot in cumulative life cycle impacts if system replacement rates are high.

3.6.2. **Fossil Depletion Potential (FDP)**

Fossil depletion impact during charging reaches $9.82 \cdot 10^{-2}$ kg oil eq./kWh, with the largest contributions arising from $CuSO_4$ production ($6.31 \cdot 10^{-2}$ kg oil eq./kWh), electricity import from the grid mix ($4.20 \cdot 10^{-2}$ kg oil eq./kWh), and Novec 649 production ($3.34 \cdot 10^{-2}$ kg oil eq./kWh) (Figure 66a). The WWT process adds a small contribution ($5.26 \cdot 10^{-4}$ kg oil eq./kWh), while oil-related processes remain negligible (Figure 66b). The results reveal a balanced distribution of fossil resource demand between material production and electricity use. Figure 66a identifies $CuSO_4$ production, electricity use, and Novec 649 production as key contributors, while Figure 66b highlights minor yet impactful contributions from WWT and oil production. This indicates that fossil resource dependency in the charging phase is structurally tied both to electricity use and refrigerant production, making substitution strategies crucial for future reductions.

The discharging phase exhibits a slightly lower FDP value, amounting to $8.25 \cdot 10^{-2}$ kg oil eq./kWh. This phase is primarily dominated by Novec 649 production ($8.39 \cdot 10^{-2}$ kg oil eq./kWh) and $CuSO_4$ production ($4.05 \cdot 10^{-2}$ kg oil eq./kWh). However, the negative contribution due to the electricity produced ($-4.20 \cdot 10^{-2}$ kg oil eq./kWh) offsets part of the material-related impacts. This again demonstrates the importance of avoiding burdens during energy discharge, which significantly improves the net fossil resource balance. Transport and wastewater contributions are negligible, as depicted in Figure 67.

a.

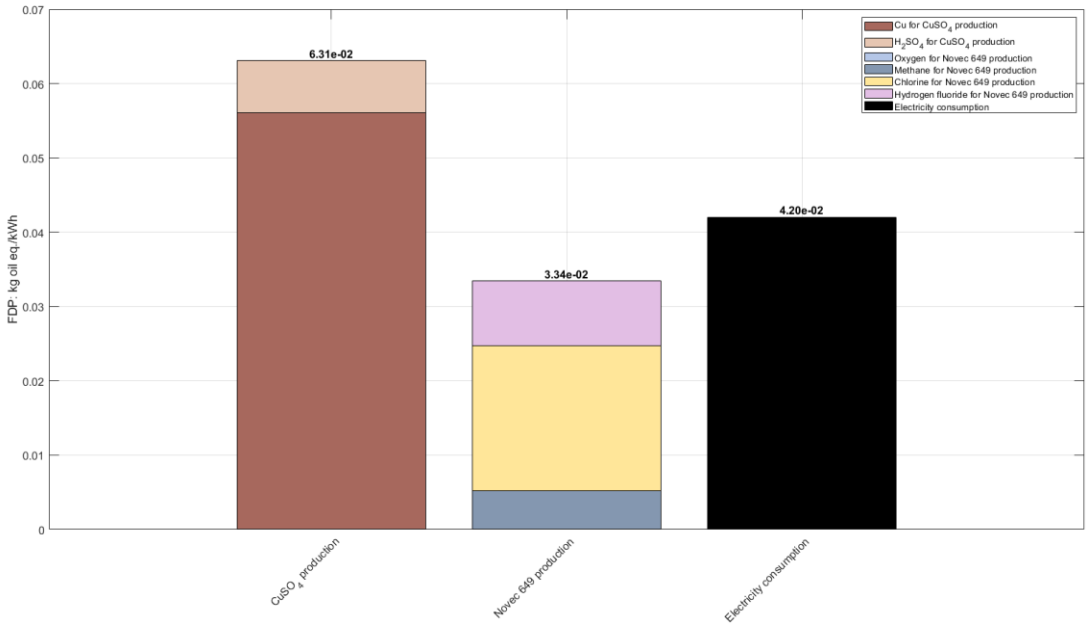

b.

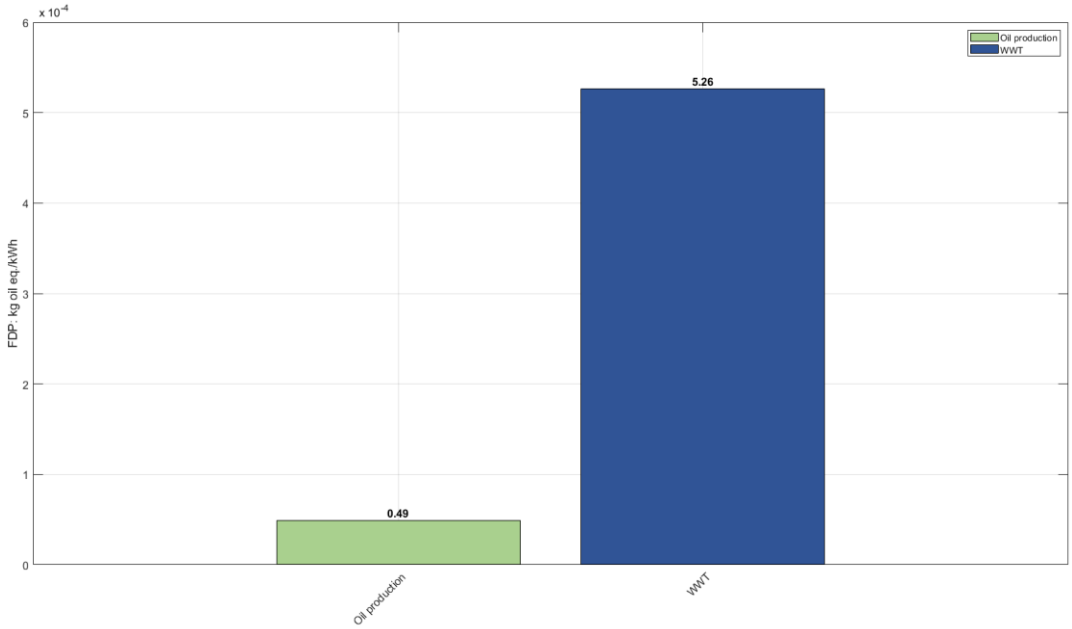

Figure 66. *FDP of Use Case 6 – The charging phase: a) major contributors and b) minor contributors*

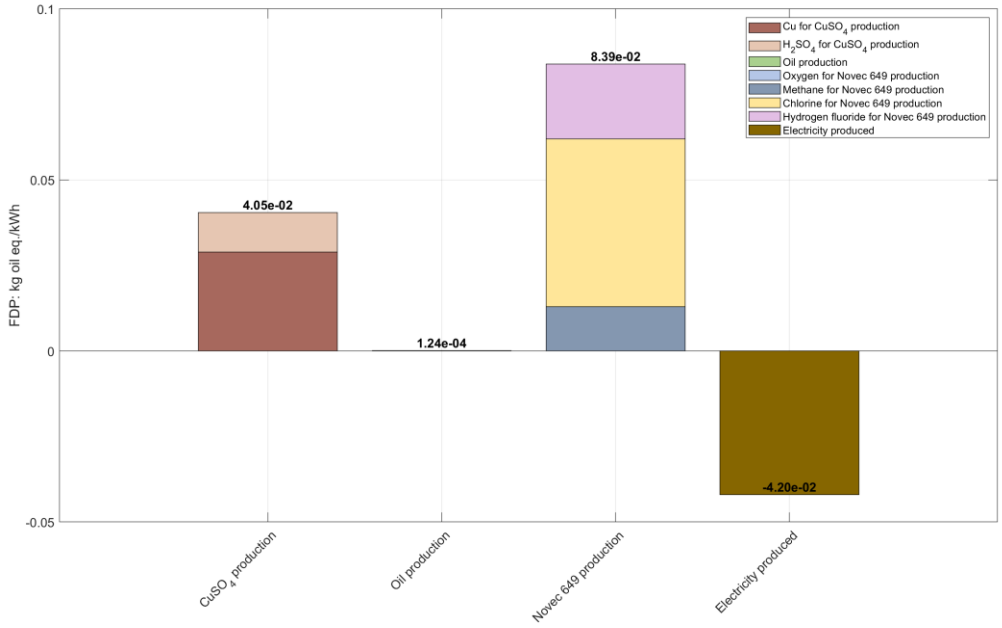

Figure 67. *FDP of Use Case 6 – The discharging phase*

Plant construction results in a total FDP impact score of $9.19 \cdot 10^{-2}$ kg oil eq./kWh, which is close to that obtained in the charging phase (Figure 68). The single largest contributor is the platinum production process ($8.07 \cdot 10^{-2}$ kg oil eq./kWh), thus reflecting the high fossil energy demand in precious metal mining and processing. Minor contributions come from copper production ($9.31 \cdot 10^{-3}$ kg oil eq./kWh) and plastics ($1.84 \cdot 10^{-3}$ kg oil eq./kWh). Steel and brass play only a minor role here. This phase is therefore highly material-dependent, especially with regard to scarce and energy-intensive metals. Future reductions may require the substitution of platinum with less fossil-intensive alternatives.

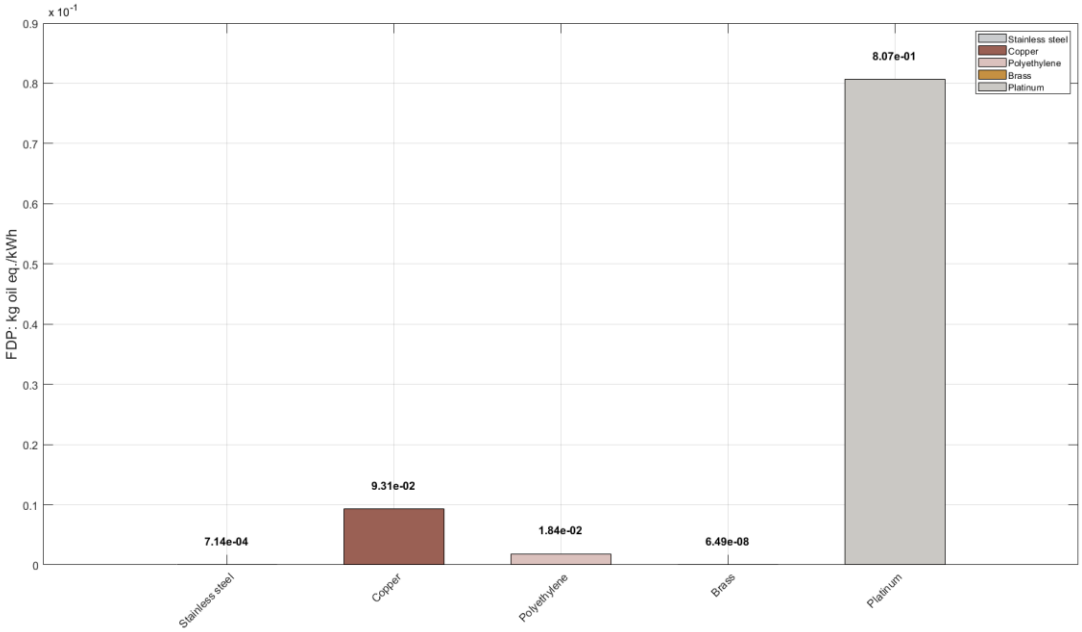

Figure 68. *FDP of Use-Case 6 – The plant construction*

3.6.3. **Freshwater Ecotoxicity Potential (FETP)**

In the charging phase, wastewater treatment ($5.26 \cdot 10^{-5}$ kg 1.4-DB eq./kWh) and $CuSO_4$ ($1.80 \cdot 10^{-5}$ kg 1.4-DB eq./kWh) dominate, resulting in a total impact score of $9.16 \cdot 10^{-5}$ kg 1.4-DB eq./kWh. The discharging phase leads to $4.23 \cdot 10^{-5}$ kg 1.4-DB eq./kWh, with $CuSO_4$ production as the main contributor ($3.27 \cdot 10^{-5}$ kg 1.4-DB eq./kWh). By contrast, plant construction shows much larger burden ($3.78 \cdot 10^{-1}$ kg 1.4-DB eq./kWh), entirely dominated by copper production (0.378 kg 1.4-DB eq./kWh). Hence, ecotoxicity is almost exclusively linked to copper-intensive plant components.

3.6.4. **Freshwater Eutrophication Potential (FEP)**

During the charging step, the system reaches a total of $5.12 \cdot 10^{-6}$ kg P eq./kWh, with municipal WWT as the key driver ($3.23 \cdot 10^{-6}$ kg P eq./kWh). In discharging phase, avoided emissions from electricity generation ($-1.22 \cdot 10^{-6}$ kg P eq./kWh) reduce the total impact score up to $1.54 \cdot 10^{-7}$ kg P eq./kWh. Plant construction contributes by $6.08 \cdot 10^{-7}$ kg P eq./kWh, mainly from platinum production ($3.74 \cdot 10^{-7}$ kg P eq./kWh).

3.6.5. **Human Toxicity Potential cancer (HTP_{cancer})**

The charging phase results in a total of $1.32 \cdot 10^{-3}$ kg 1.4-DB eq./kWh, and it is primarily due to the $CuSO_4$ production and electricity consumption ($7.10 \cdot 10^{-4}$ kg 1.4-DB eq./kWh and $3.10 \cdot 10^{-4}$ kg 1.4-DB eq./kWh, respectively). During the discharging step, credits from electricity generation reduce the overall burden up to $1.07 \cdot 10^{-3}$ kg 1.4-DB eq./kWh. However, $CuSO_4$ production stands as the primary contributor ($1.30 \cdot 10^{-3}$ kg 1.4-DB eq./kWh). Plant construction adds $3.61 \cdot 10^{-1}$ kg 1.4-DB eq./kWh, with copper production ($3.60 \cdot 10^{-1}$ kg 1.4-DB eq./kWh) as the overwhelming contributor.

3.6.6. **Human Toxicity Potential non-cancer ($HTP_{non\text{-}cancer}$)**

The charging step leads to a total of $1.14 \cdot 10^{-1}$ kg 1.4-DB eq./kWh, driven by $CuSO_4$ production ($1.09 \cdot 10^{-1}$ kg 1.4-DB eq./kWh). During the discharge, the impact increases up to $2.08 \cdot 10^{-1}$ kg 1.4-DB eq./kWh, and it is once again dominated by $CuSO_4$ production ($1.98 \cdot 10^{-1}$ kg 1.4-DB eq./kWh). Plant construction has a disproportionately high burden (161.11 kg 1.4-DB eq./kWh), overwhelmingly due to copper production (161.10 kg 1.4-DB eq./kWh). This highlights the toxicity-related concerns of copper-based infrastructure.

3.6.7. **Metal Depletion Potential (MDP)**

For the MDP indicator, the charging step yields a total impact score of $2.32 \cdot 10^{-2}$ kg Cu eq./kWh, having $CuSO_4$ production as the primary contributor ($2.24 \cdot 10^{-2}$ kg Cu eq./kWh). The discharging increases the burden to a value of $4.13 \cdot 10^{-2}$ kg Cu eq./kWh due to $CuSO_4$ manufacture leading to $4.10 \cdot 10^{-2}$ kg Cu eq./kWh. Plant construction adds $1.07 \cdot 10^{-1}$ kg Cu eq./kWh, with platinum production ($8.40 \cdot 10^{-2}$ kg Cu eq./kWh) as the main driver. Thus, both consumables ($CuSO_4$) and structural metals (platinum) are critical hotspots.

3.6.8. **Photochemical Oxidant Formation Potential ecosystem ($POFP_{ecosystem}$)**

The charging phase exhibits a high $POFP_{ecosystem}$ impact score of 49.01 kg NO_x eq./kWh, dominated almost entirely by municipal WWT (47.25 kg NO_x eq./kWh), as seen in Figure 69a. Secondary contributions arise from the electricity import from the grid mix (1.76 kg NO_x eq./kWh) and oil production ($1.31 \cdot 10^{-3}$ kg NO_x eq./kWh), while material and transport inputs are comparatively negligible (Figure 69b). This demonstrates that wastewater treatment-related emissions strongly outweigh all other processes in this phase. Overall, mitigation of wastewater treatment-related emissions could drastically improve the ozone formation profile in the charging stage.

a.

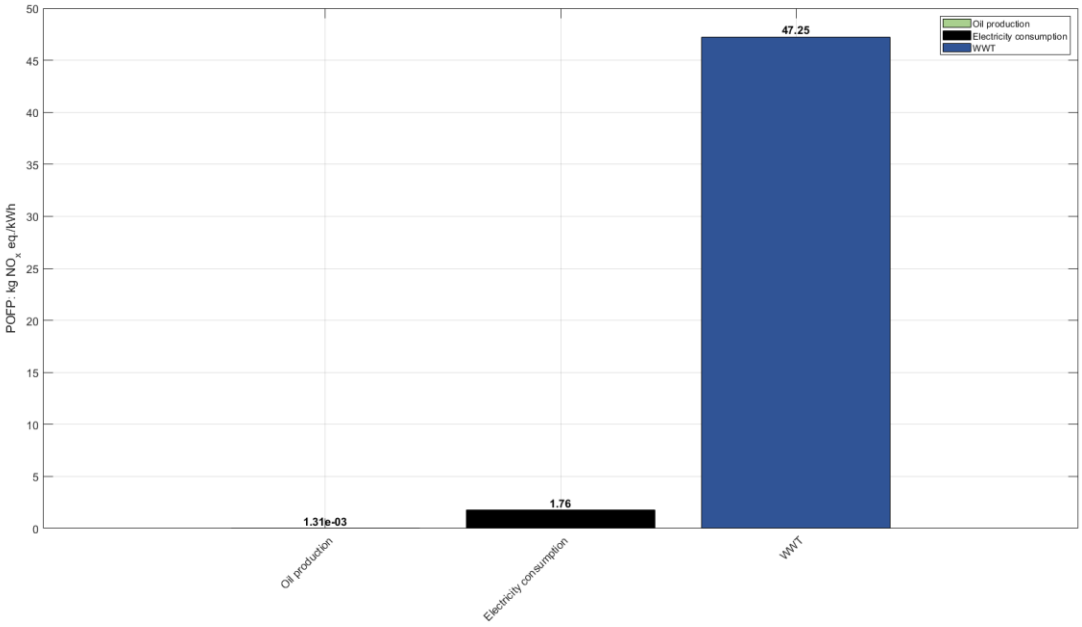

b.

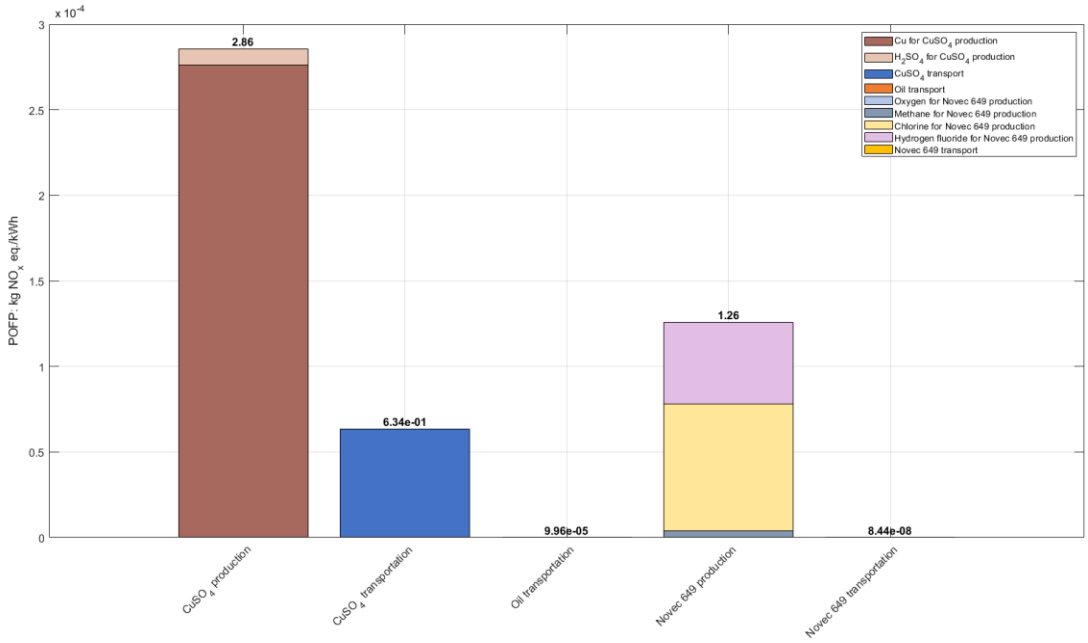

Figure 69. *$POFP_{ecosystem}$ of Use Case 6 – The charging phase: a) major contributors and b) minor contributors*

In contrast, the discharging step shows a negative $POFP_{ecosystem}$ impact (-1.76 kg NO_x eq./kWh), suggesting avoided environmental burdens. Herein, the electricity generated has a contribution of -1.76 kg NO_x eq./kWh, thus completely offsetting all positive impacts from $CuSO_4$ production and transportation ($5.21 \cdot 10^{-4}$ kg NO_x eq./kWh and $1.16 \cdot 10^{-4}$ kg NO_x eq./kWh, respectively), oil production ($3.28 \cdot 10^{-3}$ kg NO_x eq./kWh), and Novec 649 production ($3.16 \cdot 10^{-4}$ kg NO_x eq./kWh) (Figure 70a and Figure 70b). Transport processes add minor additional burdens. This phase thus provides a net environmental benefit in terms of photochemical smog reduction.

a.

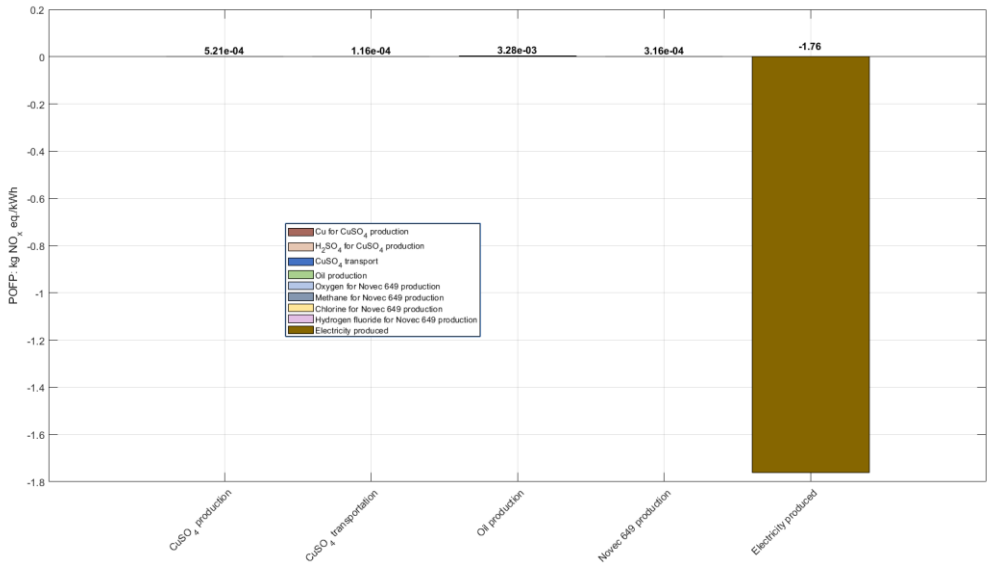

b.

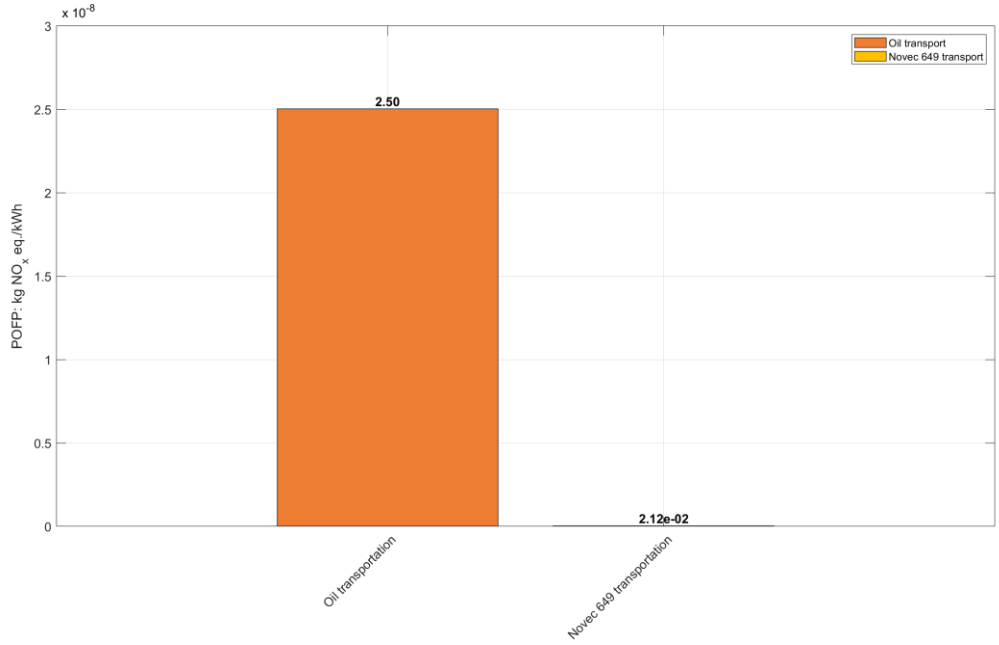

Figure 70. *$POFP_{ecosystem}$ of Use Case 6 – The discharging phase: a) major contributors and b) minor contributors*

For plant construction, $POFP_{ecosystem}$ is very small in absolute terms ($1.27 \cdot 10^{-3}$ kg NO_x eq./kWh) compared to the operational stages. The dominant contributor is platinum production ($1.14 \cdot 10^{-2}$ kg NO_x eq./kWh), while a lower impact arises from copper production ($1.30 \cdot 10^{-3}$ kg NO_x eq./kWh) and plastics ($2.21 \cdot 10^{-5}$ kg NO_x eq./kWh), as seen in Figure 71.

b.

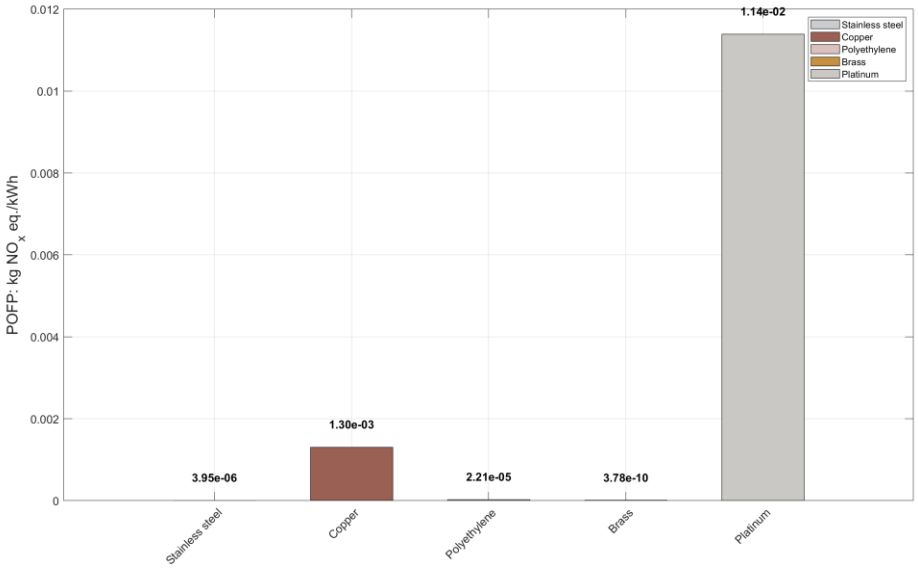

Figure 71. *$POFP_{ecosystem}$ of Use Case 6 – The plant construction*

Contributions from steel and brass are negligible. Although low in absolute magnitude, these results highlight the disproportionate influence of platinum on the photochemical ozone formation footprint. Given that plant construction impacts are cumulative over the system's lifetime, the use of platinum and copper could represent a hotspot if large-scale deployment is considered.

3.6.9. **Stratospheric Ozone Depletion Potential (ODP)**

The ODP in the charging phase amounts to $9.65 \cdot 10^{-7}$ kg CFC-11 eq./kWh. The largest single contribution comes from Novec 649 transportation ($8.29 \cdot 10^{-7}$ kg CFC-11 eq./kWh), which outweighs all other processes combined (Figure 72). $CuSO_4$ production ($4.09 \cdot 10^{-8}$ kg CFC-11 eq./kWh) and Novec 649 production ($1.54 \cdot 10^{-8}$ kg CFC-11 eq./kWh) rank second and third. The electricity imports and WWT contribute only marginally.

In the discharging phase, the ODP slightly increases to $2.14 \cdot 10^{-6}$ kg CFC-11 eq./kWh. The primary driver is the Novec 649 transport ($2.08 \cdot 10^{-6}$ kg CFC-11 eq./kWh). Material production ($CuSO_4$, Novec 649, and oil) adds smaller contributions, while the electricity generation provides a minor negative offset ($-6.15 \cdot 10^{-8}$ kg CFC-11 eq./kWh) (Figure 73). This demonstrates that the transport of Novec 649 is a major hotspot in terms of ODP during the discharging stage. Mitigation may require changes in logistics pathways or chemical supply chains.

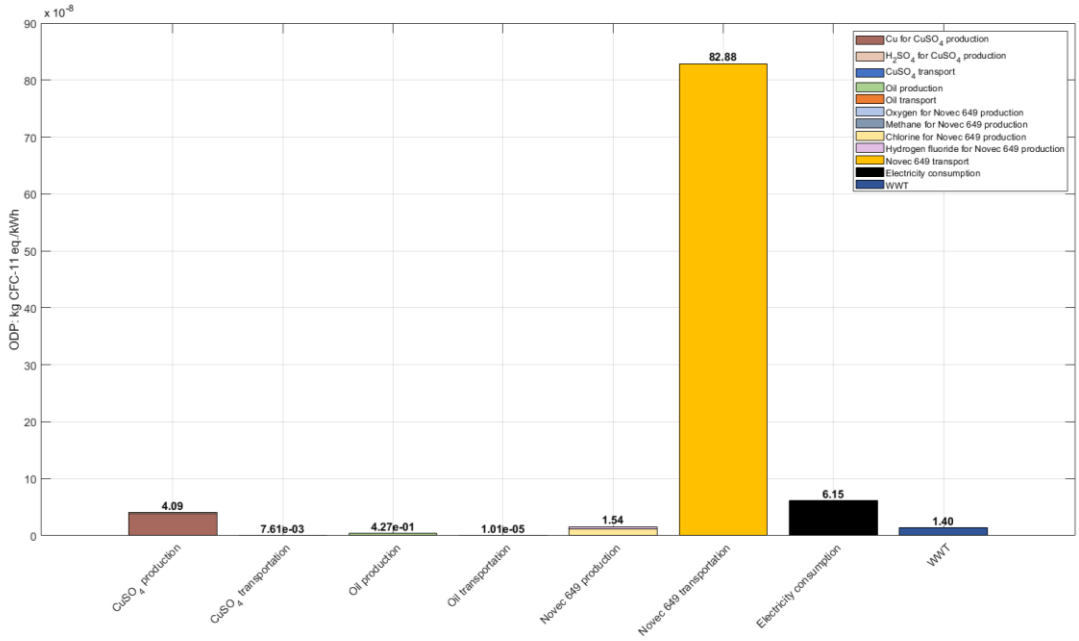

Figure 72. *ODP of Use Case 6 – The charging phase*

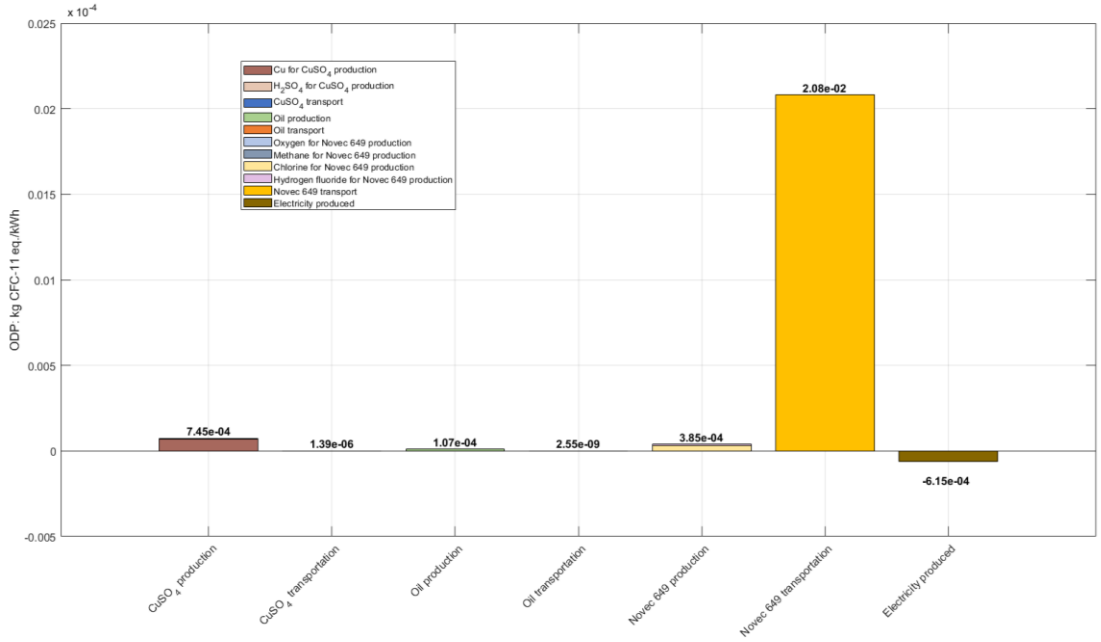

Figure 73. *ODP of Use Case 6 – The discharging phase*

The plant construction phase contributes $9.68 \cdot 10^{-8}$ kg CFC-11 eq./kWh, which is an order of magnitude lower than the operational stages. The largest contributions come from platinum and copper production ($6.96 \cdot 10^{-8}$ kg CFC-11 eq./kWh and $2.68 \cdot 10^{-8}$ kg CFC-11 eq./kWh, respectively).

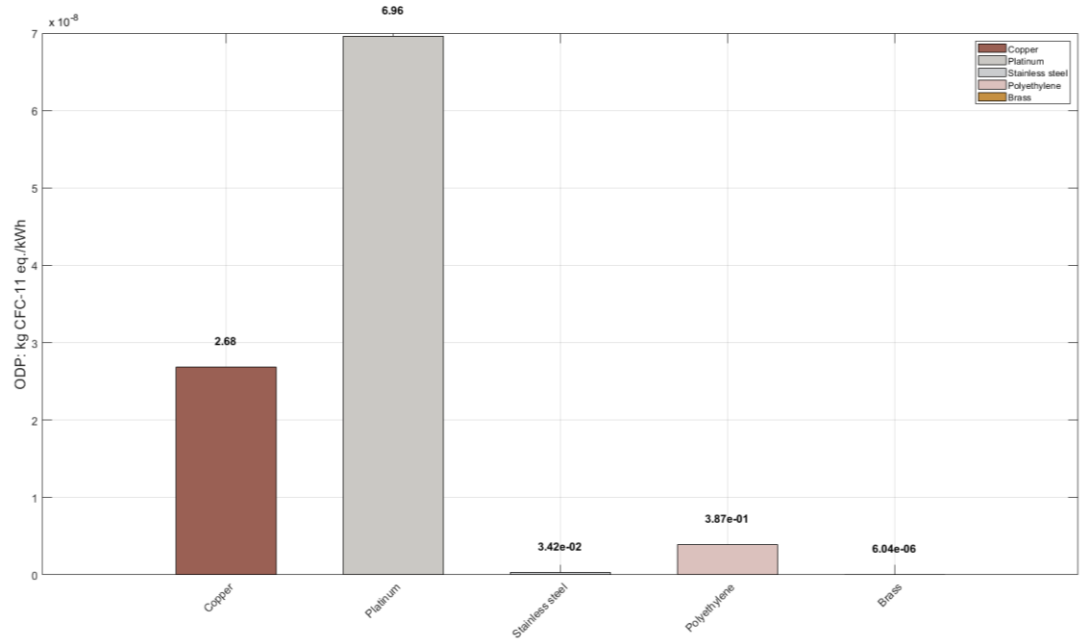

Figure 74. *ODP of Use Case 6 – The plant construction*

Contributions from plastics and steel are minimal, while brass is nearly irrelevant (Figure 74). Although relatively small in magnitude, construction-related ODP impacts are linked almost exclusively to material inputs, particularly platinum. These results reinforce the broader trend that construction emissions are strongly tied to high-value metal use.

3.6.10. **Terrestrial Acidification Potential (TAP)**

The charging phase reaches a total of $1.79 \cdot 10^{-3}$ kg SO_2 eq./kWh, with $CuSO_4$ ($0.70 \cdot 10^{-3}$ kg SO_2 eq./kWh) and WWT ($0.69 \cdot 10^{-3}$ kg SO_2 eq./kWh) ranking first and second in terms of contributions. Similar impact scores are registered during the discharging stage ($1.79 \cdot 10^{-3}$ kg SO_2 eq./kWh), with $CuSO_4$ production as the primary contributor once again ($1.27 \cdot 10^{-3}$ kg SO_2 eq./kWh). Plant construction adds $6.72 \cdot 10^{-3}$ kg SO_2 eq./kWh, mostly due to platinum production ($6.44 \cdot 10^{-3}$ kg SO_2 eq./kWh). Overall, material extraction and processing represent the largest burdens.

3.6.11. **Terrestrial Ecotoxicity Potential (TETP)**

The charging phase yields a total of $2.59 \cdot 10^{-1}$ kg 1.4-DB eq./kWh, dominated by $CuSO_4$ ($2.03 \cdot 10^{-1}$ kg 1.4-DB eq./kWh) and Novec 649 ($2.60 \cdot 10^{-2}$ kg 1.4-DB eq./kWh). During the discharge, the impact increases to $4.04 \cdot 10^{-1}$ kg 1.4-DB eq./kWh, primarily driven by $CuSO_4$ production (0.369 kg 1.4-DB eq./kWh). Plant construction, however, exceeds operational impacts with 1809.41 kg 1.4-DB eq./kWh, nearly entirely attributable to copper production (1807.22 kg 1.4-DB eq./kWh). This indicates extreme ecotoxicity potential from infrastructure.

3.6.12. **Use Case 6 – Main conclusions**

A summary of the key outcomes in Use Case 6 are reported bellow:

- GWP in the charging phase is primarily driven by grid electricity consumption and the production of chemical compounds (e.g., Novec 649 and $CuSO_4$). Although discharging reduced GWP through electricity credits, it does not result in a net negative outcome.
- FDP during charging reflects the combined contributions of chemical compound production (e.g., Novec 649 and $CuSO_4$) and electricity consumption. In the discharging phase, material-related fossil burdens persist, even though they are partially offset by electricity generation.
- $POFP_{ecosystem}$ impact score is considerably high in the charging phase, largely due to municipal WWT, while the discharging phase provides a net $POFP_{ecosystem}$ benefit through avoided grid emissions.
- Overall, Use Case 6 focuses on multiple environmental hotspots – particularly chemical compounds (e.g., Novec 649 and $CuSO_4$) and WWT – alongside the benefits of electricity credits.

4. General conclusions

This deliverable has presented the Life Cycle Assessment of the RESTORE solution (i.e., TCES systems integrated with HP and ORC) across six representative Use Cases. The analysis followed ISO 14040:2006 and ISO 14044:2006 principles and addressed a wide set of impact categories, enabling the identification of recurrent environmental hotspots and trade-offs between operational (charging and discharging) and construction phases, respectively.

In ***Use Case 1***, Brønderslev CHP hybrid plant, the charging phase records a high GWP impact, primarily attributable to electricity imports from the grid. However, this is counterbalanced by the discharging phase, which achieves a net negative GWP due to on-site electricity generation, thereby demonstrating the potential of the system to offset upstream impacts. A comparable trend is observed for FDP: while electricity demand – particularly that required for dehydrating the thermochemical compound – drives the charging impact, the discharging phase provides a valuable fossil-resource credit. Similarly, $POFP_{ecosystem}$ reaches elevated values in the charging phase, with grid electricity and municipal WWT as the main contributors, yet during discharging, avoided grid emissions result in a substantial reduction. Overall, electricity sourcing emerges as the decisive factor shaping the environmental performance of this Use Case, while the influence of materials and construction remains relatively limited. Importantly, compared with Use Cases 3 to 5, the RESTORE system integrated within the Brønderslev CHP hybrid plant benefits from not requiring a Heat Pump during charging. This design feature results in a notably lower overall electricity demand, thereby enhancing efficiency and reinforcing the system's environmental advantages.

In the second Use Case, ***Use Case 2*** (the Gmunden cement plant), the GWP of the charging phase is higher than that of both discharging and construction, reflecting the reliance on the Austrian grid mix. The discharging phase benefits from avoided burdens through electricity generation. FDP follows a similar trajectory: electricity imports dominate the charging impact, while fossil-resource credits are obtained during discharging. Unlike Use Case 1, TETP emerges as a hotspot in the construction phase, largely linked to copper production for plant components. This highlights that while operational performance yields significant environmental benefits, construction materials can introduce considerable ecotoxicity burden in industrial applications.

In the case of the Ružomberok paper mill, ***Use Case 3***, charging-phase GWP is again dominated by grid electricity consumption, while the discharging phase generates a climate credit. FDP exhibits the same pattern, with electricity driving the charging-phase impact and modest offsets observed during discharging. In contrast, MDP is strongly influenced by $CuSO_4$ production, with discharging impacts surpassing those of charging. This underscores the role of chemical consumables as a critical long-term sustainability concern. Nevertheless, an important advantage is that, at the end of the facility's lifetime, experimental evidence shows that the material can be recombined with water and made ready for reuse in other RESTORE systems. This regenerative characteristic not only extends the material's life cycle but also supports to a more circular and sustainable deployment of the technology.

For the ***Use Case 4***, Alfa Acciai steel plant, GWP impact during the charging phase is primarily driven by electricity consumption, while the discharging phase achieves a net negative balance

through electricity generation. FDP follows the same pattern, with electricity as the dominant contributor to charging burdens and avoided fossil use during discharging. Toxicity-related impacts are largely influenced by Therminol V66 production, with non-cancer human toxicity remaining substantial in both phases. Although avoided emissions from electricity generation do not fully compensate for these impacts, this highlights the importance of carefully selecting working fluids to further enhance environmental performance. Encouragingly, preliminary experimental activities have explored the use of mineral and vegetable oils, suggesting that the toxicity-related impacts associated with Therminol V66 could be significantly reduced. These results point toward promising alternatives that, with further development, may strengthen the overall sustainability profile of the system.

The Holzkirchen geothermal facility, ***Use Case 5***, exhibits similar trends, with charging-phase GWP dominated by grid electricity, while the discharging phase delivers a strong net negative outcome, underscoring the system's potential to offset upstream burdens. FDP is again influenced by electricity consumption during charging, yet discharging provides a valuable fossil-resource credit that strengthens the environmental balance. Non-cancer human toxicity is consistently dominated by Therminol V66 production, confirming upstream fluid manufacture as a critical operational hotspot. Nevertheless, this also highlights a clear opportunity: by optimizing working fluid selection and advancing toward lower-impact alternatives, the environmental performance of geothermal-based systems like Holzkirchen could be further enhanced. More broadly, the dominance of grid electricity in shaping GWP impacts emphasizes the importance integrating the RESTORE solution with renewable electricity sources, which would significantly reduce upstream burdens and unlock their full environmental potential.

Use Case 6, the POLIMI campus energy network, presents a different pattern compared to the other virtual Use Cases. Charging-phase GWP is influenced not only by electricity imports but also by chemical production, particularly Novec 649 and $CuSO_4$. While discharging reduces GWP through electricity credits, it does not result in a net negative balance. FDP reflects both chemical and electricity contributions, with discharging only partially offsetting fossil-related burdens. $POFP_{ecosystem}$ exhibits a considerably high impact score during the charging phase, primarily due to municipal WWT, whereas during discharging it provides a net reduction through avoided emissions. This case underscores how specific processes and chemical choices can dominate the overall performance of the system.

Taken together, the six virtual Use Cases highlight two consistent and encouraging patterns. First, electricity consumption during charging and the associated avoided burdens during discharging emerge as the principal drivers of GWP and FDP across all systems, highlighting the substantial leverage offered by optimized electricity sourcing. Second, other impact categories – such as ecotoxicity, metal depletion, or human health toxicity – are strongly shaped by specific chemicals (e.g., $CuSO_4$, Novec 649, or Therminol V66) and, in some cases, municipal WWT, indicating clear opportunities for targeted improvements. In contrast, construction-related impacts are generally less significant than operational impacts, further emphasizing the potential for environmental gains through operational optimization. Importantly, the demonstrated ability to regenerate the thermochemical material for reuse in future RESTORE systems highlights a promising pathway toward circularity, increasing the long-term sustainability and scalability of the concept. In addition, as previously stated,

preliminary experimental activities exploring the use of mineral and vegetal oils suggest that the toxicity-related impacts associated with Therminol V66 could be substantially reduced. Together, these findings point toward viable alternatives and strategies that, with continued development, may further enhance the overall environmental performance and resilience of RESTORE systems.

Overall, the LCA results demonstrate that TCES technologies can deliver meaningful environmental benefits by reducing reliance on fossil-based electricity generation. However, these advantages are partly offset by material-related burdens. To maximize sustainability, both system design and policy measures should prioritize: reducing dependence on impact-intensive materials such as $CuSO_4$, certain organic fluids, and platinum (in plant construction); promoting recycling and circularity of key components; improving WWT processes; and ensuring deployment within increasingly decarbonized energy systems. With these aspects addressed, TCES integrated with HP/ORC systems can contribute effectively to climate change mitigation and resource efficiency, while minimizing unintended environmental trade-offs.

Future research should focus on developing low-impact alternatives to critical materials, alongside strategies for grid decarbonization and optimized plant operation. Together, these efforts will be essential to fully realizing the climate and resource benefits of thermal energy storage.

5. References

[1] Jakučionytė-Skodienė M, Krikštolaitis R, Liobikienė G. The contribution of changes in climate-friendly behaviour, climate change concern and personal responsibility to household greenhouse gas emissions: Heating/cooling and transport activities in the European Union. Energy 2022;246:123387. https://doi.org/10.1016/j.energy.2022.123387.

[2] Okonkwo EC, AlNouss A, Shahbaz M, Al-Ansari T. Developing integrated direct air capture and bioenergy with carbon capture and storage systems: progress towards 2 °C and 1.5 °C climate goals. Energy Convers Manag 2023;296. https://doi.org/10.1016/j.enconman.2023.117687.

[3] Gustavsen M, Mikkelsen MS, Luft F, Riisgaard H, Elliot T. The role of excess heat in reducing the environmental impacts of district heating systems. J Environ Manage 2025;390. https://doi.org/10.1016/j.jenvman.2025.126234.

[4] Calvin K, Dasgupta D, Krinner G, Mukherji A, Thorne PW, Trisos C, et al. IPCC, 2023: Climate Change 2023: Synthesis Report. Contribution of Working Groups I, II and III to the Sixth Assessment Report of the Intergovernmental Panel on Climate Change [Core Writing Team, H. Lee and J. Romero (eds.)]. IPCC, Geneva, Switzerland. 2023. https://doi.org/10.59327/IPCC/AR6-9789291691647.

[5] IEA - International Energy Agency. Net Zero Roadmap: A Global Pathway to Keep the 1.5 °C Goal in Reach - 2023. 2023.

[6] Bang A, Moreno D, Lund H, Nielsen S. Regional CCUS strategies in the context of a fully decarbonized society. J Clean Prod 2024;477. https://doi.org/10.1016/j.jclepro.2024.143882.

[7] Schmieder L, Jezernik S, Gatt S, Steinacher N, Winter F. Influence of system pressure on gas–solid reactions for thermochemical energy storage in a suspension reactor. Energy Conversion and Management: X 2025;27:101179. https://doi.org/10.1016/j.ecmx.2025.101179.

[8] Galusnyak SC, Petrescu L, Chisalita DA, Cormos C-C. Life cycle assessment of methanol production and conversion into various chemical intermediates and products. Energy 2022;259:124784. https://doi.org/10.1016/j.energy.2022.124784.

[9] IEA - International Energy Agency. Tracking Clean Energy Progress 2023 – Analysis - IEA. https://www.iea.org/reports/tracking-clean-energy-progress-2023 (accessed June 20, 2025).

[10] Edenhofer Ottmar, Pichs-Madruga R, Sokona Y, Farahani E, Kadner S, Seyboth K, et al. IPCC, 2014: Climate Change 2014 : Mitigation of Climate Change : Contribution of Working Group III to the Fifth Assessment Report of the Intergovernmental Panel on Climate Change. Cambridge University Press; 2015.

[11] Lund H, Østergaard PA, Sorknæs P, Nielsen S, Skov IR, Yuan M, et al. District heating in clean energy systems. Nature Reviews Clean Technology 2025. https://doi.org/10.1038/s44359-025-00076-8.

[12] Schmieder L, Kuloglija S, Ilyina-Brunner K, Jezernik S, Winter F. Calcium chloride dihydrate as a promising system for seasonal heat storage in a suspension reactor. Appl Therm Eng 2025;258. https://doi.org/10.1016/j.applthermaleng.2024.124557.

[13] Luberti M, Gowans R, Finn P, Santori G. An estimate of the ultralow waste heat available in the European Union. Energy 2022;238:121967. https://doi.org/10.1016/j.energy.2021.121967.

[14] Moser S, Lassacher S. External use of industrial waste heat - An analysis of existing implementations in Austria. J Clean Prod 2020;264:121531. https://doi.org/10.1016/j.jclepro.2020.121531.

[15] Mathiesen B, Vad ;, Wild C;, Nielsen S. Aalborg Universitet Heat Matters: The Missing Link in REPowerEU 2030: District Heating Deployment for a long-term Fossil-free Future. 2023.

[16] Piron M, Wu J, Fedele A, Manzardo A. Industry 4.0 and life cycle assessment: Evaluation of the technology applications as an asset for the life cycle inventory. Science of the Total Environment 2024;916. https://doi.org/10.1016/j.scitotenv.2024.170263.

[17] Tessitore S, Testa F, Di Iorio V, Iraldo F. Life cycle assessment as an enabler of an environmental sustainability strategy evolution amid institutional pressures: A best practice from the furniture industry. Cleaner Environmental Systems 2025;16. https://doi.org/10.1016/j.cesys.2025.100255.

[18] Jolliet O, Saade-Sbeih M, Shaked S, Jolliet A, Crettaz P. Environmental Life Cycle Assessment 2015. https://doi.org/10.1201/B19138.

[19] Rihner MCS, Whittle JW, Gadelhaq MHA, Mohamad SN, Yuan R, Rothman R, et al. Life cycle assessment in energy-intensive industries: Cement, steel, glass, plastic. Renewable and Sustainable Energy Reviews 2025;211. https://doi.org/10.1016/j.rser.2024.115245.

[20] Klüppel H-J. The Revision of ISO Standards 14040-3 - ISO 14040: Environmental management - Life cycle assessment - Principles and framework - ISO 14044: Environmental management - Life cycle assessment; Requirements and guidelines. Int J Life Cycle Assess 2005;10:165–165. https://doi.org/10.1065/lca2005.03.001.

[21] ISO - ISO 14040:2006 - Environmental management — Life cycle assessment — Principles and framework. https://www.iso.org/standard/37456.html (accessed February 10, 2022).

[22] Curran AM. Goal and Scope Definition in Life Cycle Assessment. Dordrecht: Springer Netherlands; 2017. https://doi.org/10.1007/978-94-024-0855-3.

[23] Pillain B GESG. Identification of Key Sustainability Performance Indicators and related assessment methods for the carbon fiber recycling sector. Ecol Indic 2017;72:833–47.

[24] Huijbregts MAJ, Steinmann ZJN, Elshout PMF, Stam G, Verones F, Vieira M, et al. ReCiPe2016: a harmonised life cycle impact assessment method at midpoint and endpoint level. International Journal of Life Cycle Assessment 2017;22:138–47. https://doi.org/10.1007/s11367-016-1246-y.

[25] Sphera LCA for Experts Software (GaBi) 2024.

[26] Hauschild MZ, Huijbregts MAJ. Introducing Life Cycle Impact Assessment, 2015, p. 1–16. https://doi.org/10.1007/978-94-017-9744-3_1.

[27] ISO - ISO 14044:2006 - Environmental management — Life cycle assessment — Requirements and guidelines. https://www.iso.org/standard/38498.html (accessed February 10, 2022).

Abbreviations

EU	European Union
GHG	Greenhouse Gas
IPCC	Intergovernmental Panel on Climate Change
CCUS	Carbon Capture, Utilization, and Storage
RES	Renewable Energy Sources
IEA	International Energy Agency
NZE	Net-Zero Emissions
DHC	District Heating and Cooling
WWT	Wastewater Treatment
TCES	Thermochemical Energy Storage
ORC	Organic Rankine Cycle
HP	Heat Pump
CHP	Combined Heat and Power
CSP	Concentrated Solar Power
PTC	Parabolic Trough Collector
EAF	Electric Arc Furnace
PV	Photovoltaics
LCA	Life Cycle Assessment
EC	European Commission
EPD	Environmental Product Declaration
ISO	International Organization for Standardization
LCI	Life Cycle Inventory
LCIA	Life Cycle Impact Assessment
FU	Functional Unit
GWP	Global Warming Potential
TAP	Terrestrial Acidification Potential
FEP	Freshwater Eutrophication Potential
ODP	Stratospheric Ozone Depletion Potential
PRFV	Polyester Reinforced Fiber-glass
PMFP	Particulate Matter Formation Potential
FDP	Fossil Depletion Potential

MDP	Mineral Depletion Potential
$POFP_{ecosystem}$	Photochemical Oxidant Formation Potential ecosystem
$POFP_{human-health}$	Photochemical Oxidant Formation Potential human health
HTP_{cancer}	Human Toxicity Potential cancer
$HTP_{non-cancer}$	Human Toxicity Potential non-cancer
WDP	Water Depletion Potential
FETP	Freshwater Ecotoxicity Potential
METP	Marine Ecotoxicity Potential
TETP	Terrestrial Ecotoxicity Potential
TRL	Technology Readiness Level
LCE	Life Cycle Engineering
LCC	Life Cycle Costing
DfE	Design for Environment

Annex 1

The most significant datasets employed in the development of each specific Use Case are further presented. It is worth mentioning that all the corresponding values are reported to the chosen functional unit.

Table A1.1. Life cycle inventory for Use Case 1

Charging cycle		
Input	**Unit**	**Value**
Copper sulphate	[kg/h]	0.11
Oil	[kg/h]	0.05
Therminol V66	[kg/h]	12.87
Output	**Unit**	**Value**
Water	[kg/h]	1628.153
Discharging cycle		
Input	**Unit**	**Value**
Copper sulphate	[kg/h]	0.11
Oil	[kg/h]	0.07
Therminol V66	[kg/h]	0.75
Cyclopentane	[kg/h]	0.13
Water	[kg/h]	2341.61

Table A1.2. Life cycle inventory for plant construction in Use Case 1

Input	**Unit**	**Value**
Stainless steel	[kg/h]	$5.31 \cdot 10^{-4}$
Copper	[kg/h]	$8.53 \cdot 10^{-8}$
Polyethylene	[kg/h]	$1.77 \cdot 10^{-3}$
Fiberglass	[kg/h]	$2.25 \cdot 10^{-5}$

Table A1.3. Life cycle inventory for Use Case 2

Charging cycle		
Input	**Unit**	**Value**
Copper sulphate	[kg/h]	0.03
Oil	[kg/h]	0.08
Therminol V66	[kg/h]	0.26
Cyclopentane	[kg/h]	0.14
Output	**Unit**	**Value**
Water	[kg/h]	485.16
Discharging cycle		
Input	**Unit**	**Value**
Copper sulphate	[kg/h]	0.19
Oil	[kg/h]	0.44
Therminol V66	[kg/h]	1.69
Cyclopentane	[kg/h]	0.21
Water	[kg/h]	3923.12

Table A1.4. Life cycle inventory for plant construction in Use Case 2

Input	**Unit**	**Value**
Stainless steel	[kg/h]	$3.28 \cdot 10^{-4}$
Copper	[kg/h]	$5.73 \cdot 10^{-6}$
Polyethylene	[kg/h]	$3.10 \cdot 10^{-3}$
Fiberglass	[kg/h]	$2.24 \cdot 10^{-5}$

Table A1.5. Life cycle inventory for Use Case 3

Charging cycle		
Input	**Unit**	**Value**
Copper sulphate	[kg/h]	0.94
Oil	[kg/h]	0.40
Therminol V66	[kg/h]	12.68
Novec 649	[kg/h]	5.43
Output	**Unit**	**Value**
Water	[kg/h]	14210.00
Discharging cycle		
Input	**Unit**	**Value**
Copper sulphate	[kg/h]	5.80
Oil	[kg/h]	3.43
Therminol V66	[kg/h]	62.13
Novec 649	[kg/h]	0.78
Water	[kg/h]	245402.63
Output	**Unit**	**Value**
Water	[kg/h]	0.59

Table A1.6. Life cycle inventory for plant construction in Use Case 3

Input	**Unit**	**Value**
Stainless steel	[kg/h]	$1.62 \cdot 10^{-4}$
Copper	[kg/h]	$2.13 \cdot 10^{-7}$
Polyethylene	[kg/h]	$5.32 \cdot 10^{-8}$
Fiberglass	[kg/h]	$7.84 \cdot 10^{-7}$

Table A1.7. Life cycle inventory for Use Case 4

Charging cycle		
Input	**Unit**	**Value**
Copper sulphate	[kg/h]	0.87
Oil	[kg/h]	0.37
Therminol V66	[kg/h]	7.71
Cyclopentane	[kg/h]	7.49
Output	**Unit**	**Value**
Water	[kg/h]	13180.20
Discharging cycle		
Input	**Unit**	**Value**
Copper sulphate	[kg/h]	5.33
Oil	[kg/h]	3.15
Therminol V66	[kg/h]	37.33
Cyclopentane	[kg/h]	4.91
Water	[kg/h]	110875.23

Table A1.8. Life cycle inventory for plant construction in Use Case 4

Input	**Unit**	**Value**
Stainless steel	[kg/h]	$4.39 \cdot 10^{-5}$
Copper	[kg/h]	$1.07 \cdot 10^{-6}$
Polyethylene	[kg/h]	$2.69 \cdot 10^{-7}$
Fiberglass	[kg/h]	$8.71 \cdot 10^{-7}$

Table A1.9. Life cycle inventory for Use Case 5

Charging cycle		
Input	**Unit**	**Value**
Copper sulphate	[kg/h]	0.14
Oil	[kg/h]	0.06
Therminol V66	[kg/h]	1.25
Cyclopentane	[kg/h]	0.99
Output	**Unit**	**Value**
Water	[kg/h]	2169.45
Discharging cycle		
Input	**Unit**	**Value**
Copper sulphate	[kg/h]	0.87
Oil	[kg/h]	0.51
Therminol V66	[kg/h]	11.09
Water	[kg/h]	18183.51

Table A1.10. Life cycle inventory for plant construction in Use Case 5

Input	**Unit**	**Value**
Stainless steel	[kg/h]	$7.24 \cdot 10^{-5}$
Copper	[kg/h]	$4.40 \cdot 10^{-8}$
Polyethylene	[kg/h]	$1.10 \cdot 10^{-8}$
Fiberglass	[kg/h]	$5.31 \cdot 10^{-6}$

Table A1.11. Life cycle inventory for Use Case 6

Charging cycle		
Input	**Unit**	**Value**
Copper sulphate	[kg/h]	0.14
Oil	[kg/h]	0.06
Novec 649	[kg/h]	4.87
Output	**Unit**	**Value**
Water	[kg/h]	2020
Discharging cycle		
Input	**Unit**	**Value**
Copper sulphate	[kg/h]	0.09
Oil	[kg/h]	0.06
Novec 649	[kg/h]	4.87
Water	[kg/h]	11340

Table A1.12. Life cycle inventory for plant construction in Use Case 6

Input	**Unit**	**Value**
Stainless steel	[kg/h]	$6.84 \cdot 10^{-5}$
Copper	[kg/h]	0.01
Polyethylene	[kg/h]	$1.17 \cdot 10^{-3}$
Brass	[kg/h]	$1.83 \cdot 10^{-8}$
Platinum	[kg/h]	$8.84 \cdot 10^{-6}$

Annex 2

The process plans developed for specific Use Cases by means of the LCA for Experts software (formerly known as "GaBi software") are further illustrated. Each approach is supported by a number of assumptions and calculations presented in the previous chapters and subchapters.

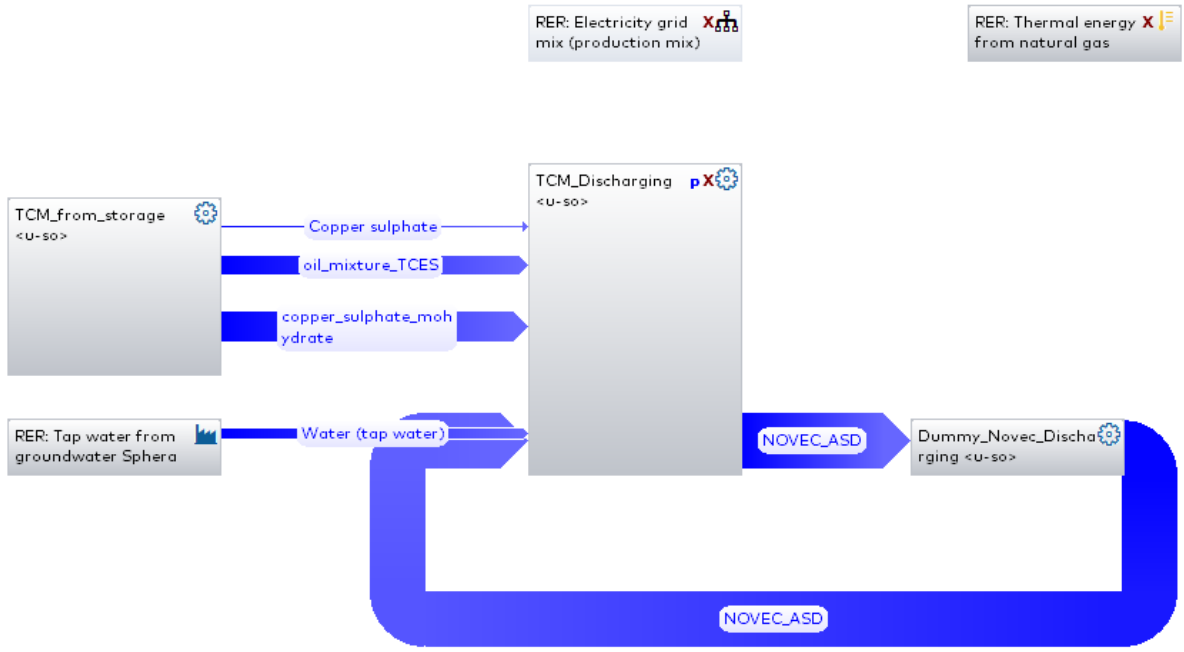

Figure A2.1. *LCA plan for the Discharging cycle for specific Use Cases*

Figure A2.2. *LCA plan for the oil transportation*

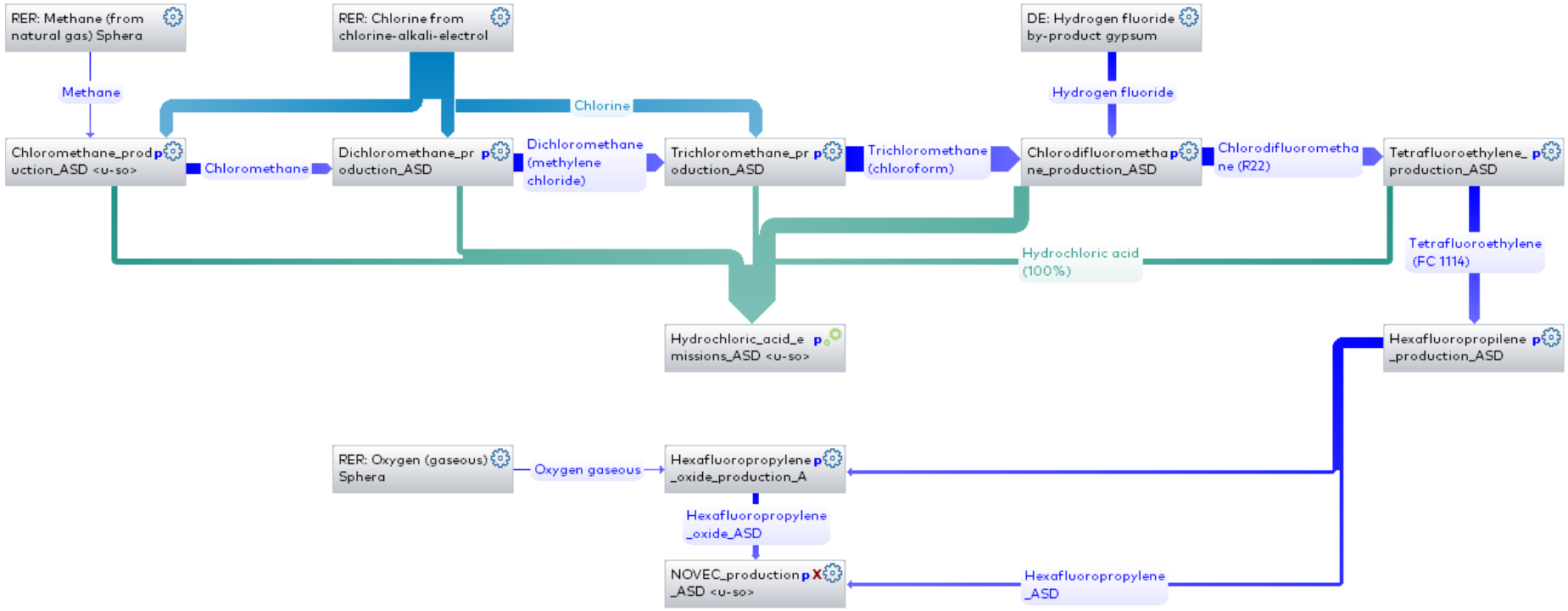

Figure A2.3. *LCA plan for Novec 649 production*

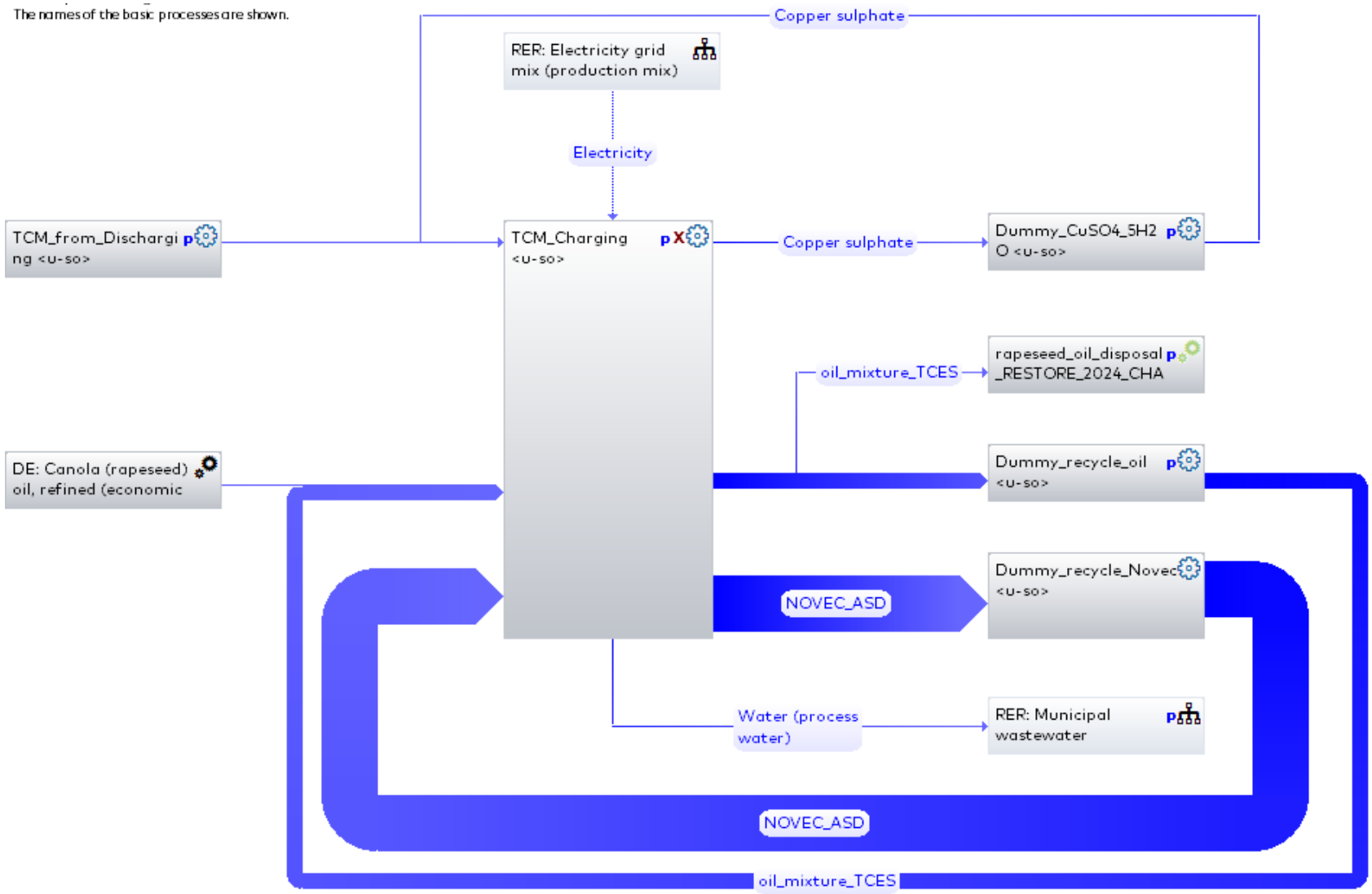

Figure A2.4. *LCA plan for the Charging cycle for specific Use Cases*

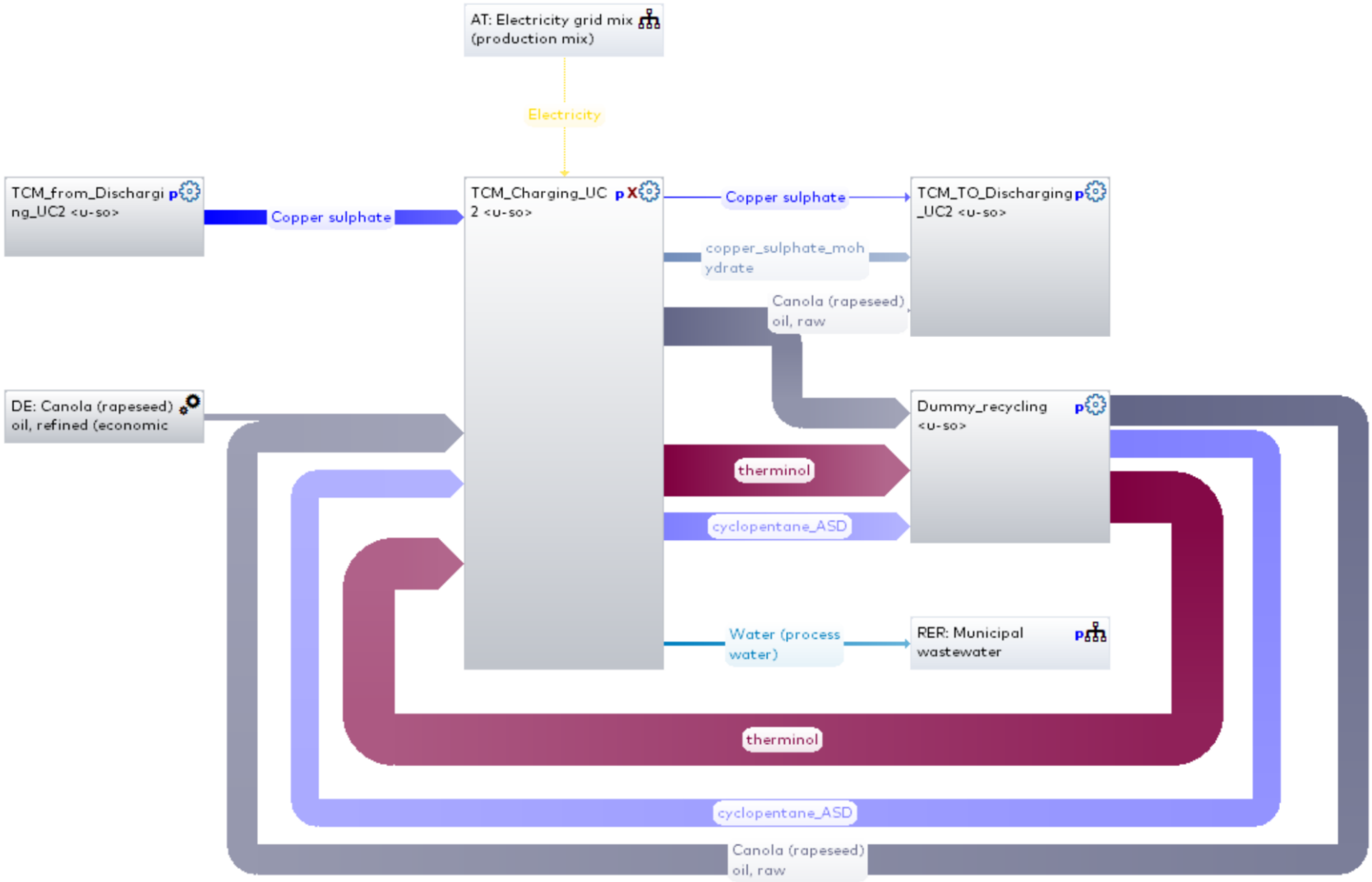

Figure A2.5. *LCA plan for the Charging cycle for specific Use Cases*

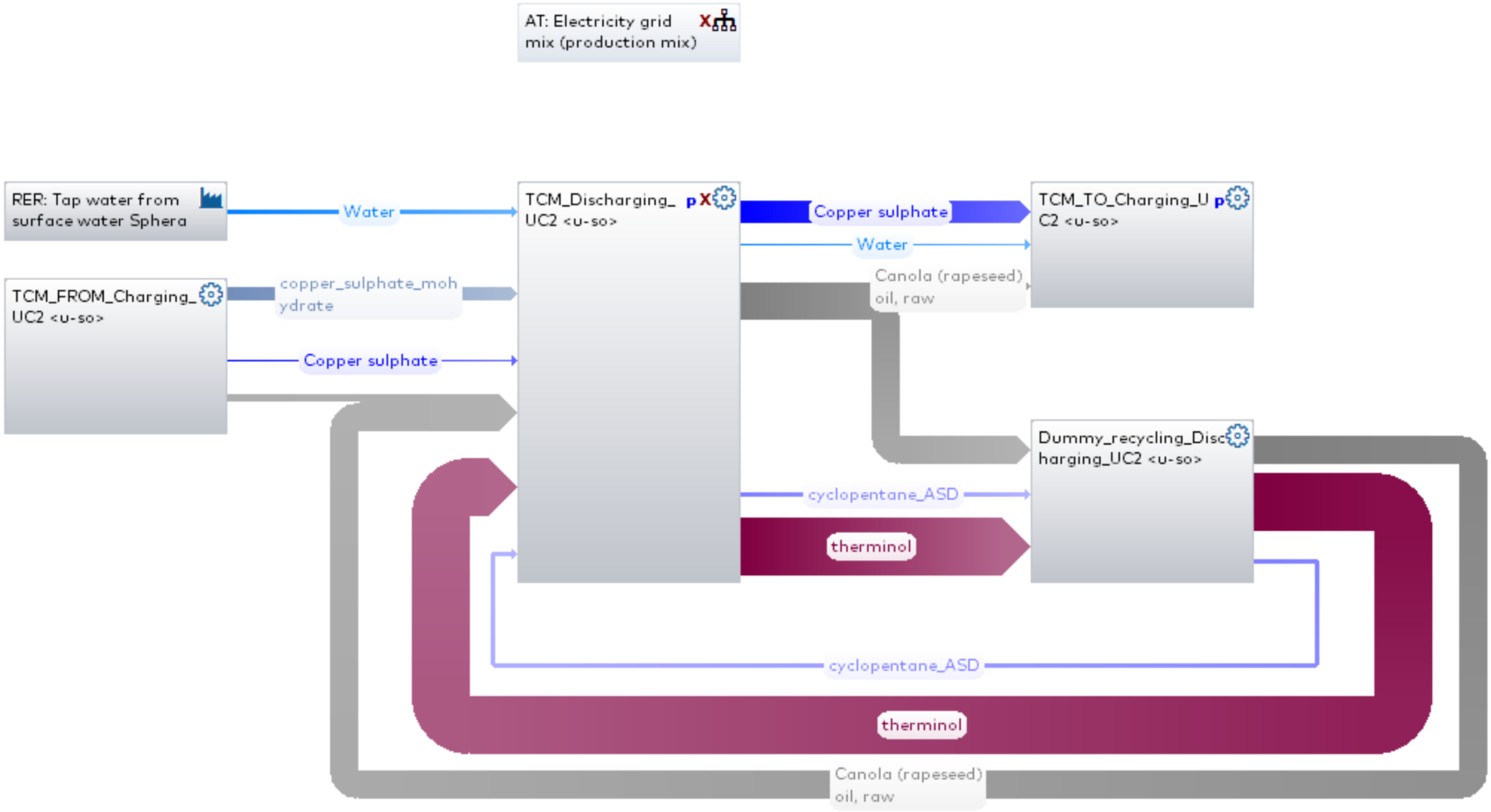

Figure A2.6. *LCA plan for the Discharging cycle for specific Use Cases*

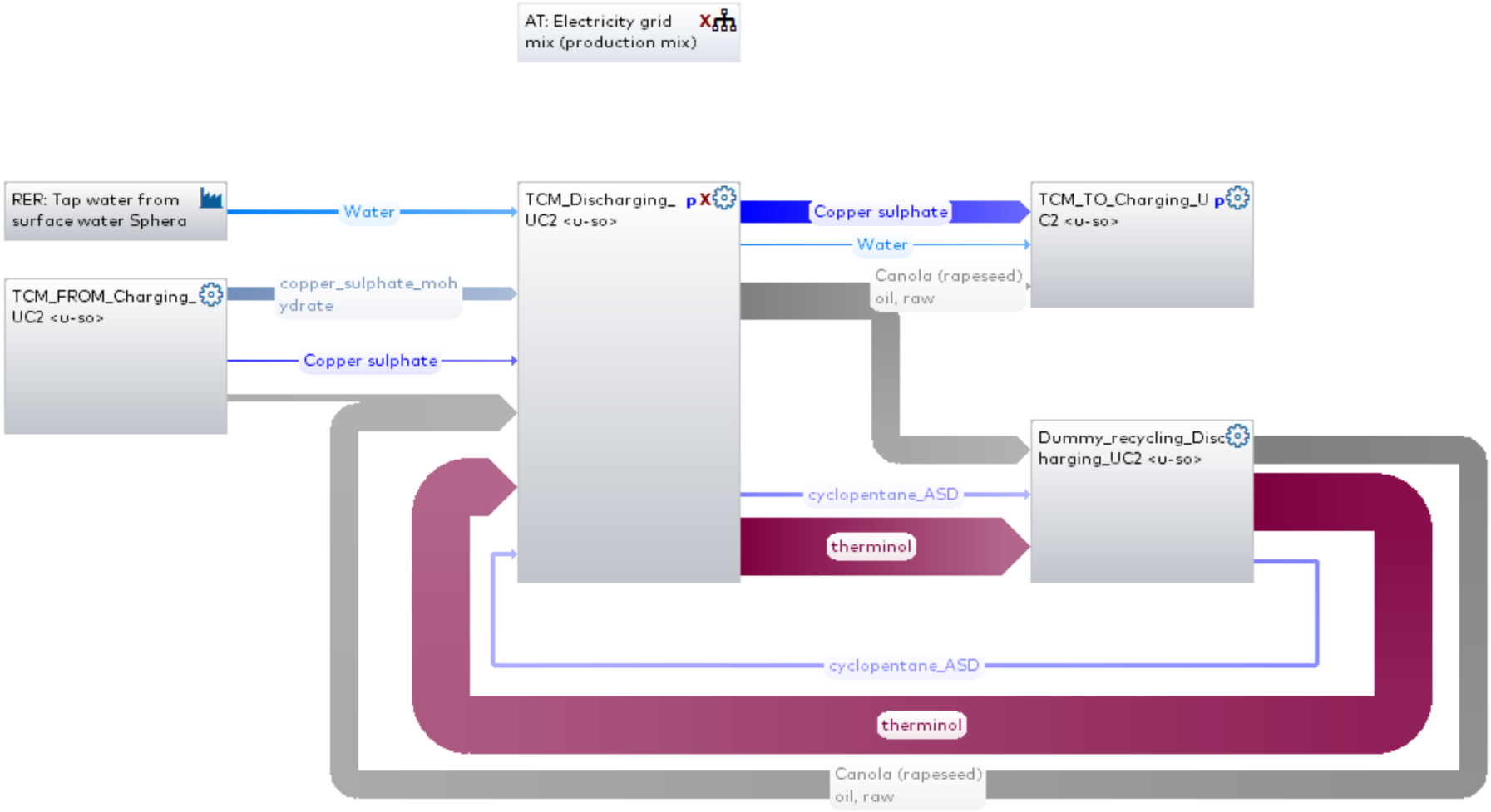

Figure A2.7. *LCA plan for the Discharging cycle for specific Use Cases*

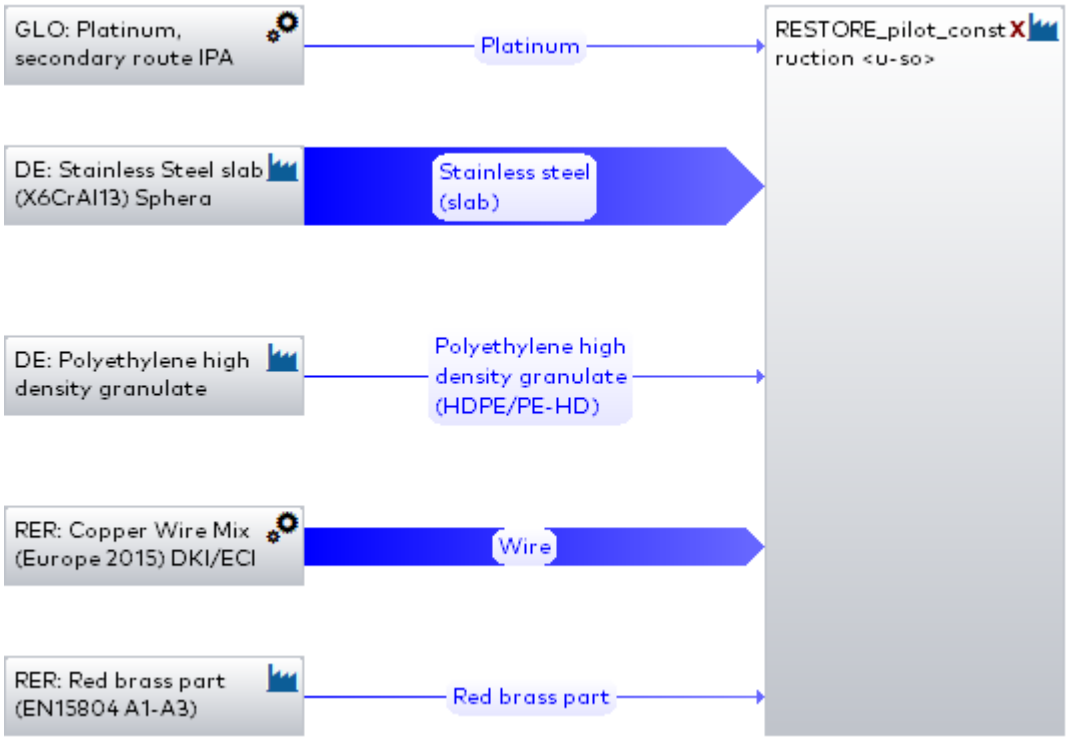

Figure A2.8. *LCA plan for the RESTORE plant construction for specific Use Cases*

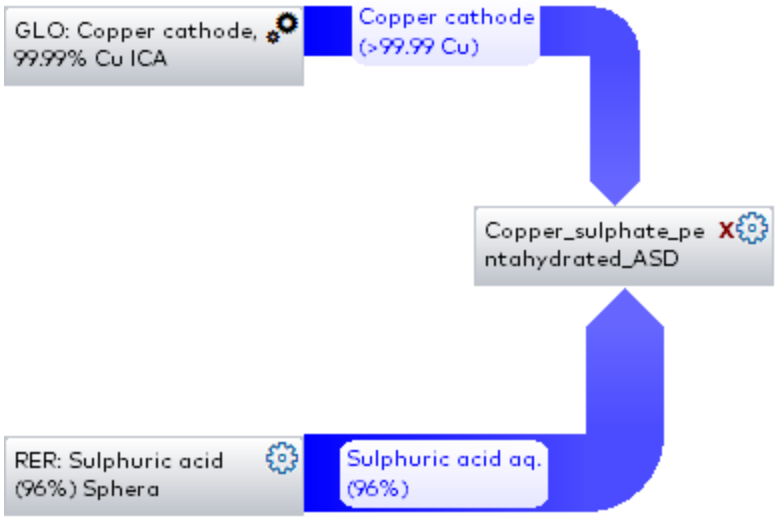

Figure A2.9. *LCA plan for the Copper sulphate production*

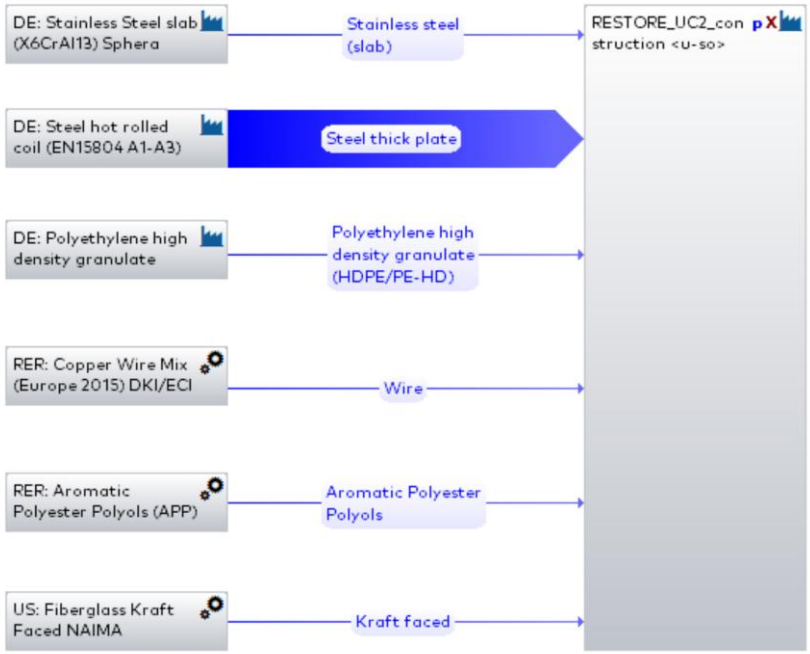

Figure A2.10. *LCA plan for the RESTORE plant construction for specific Use Cases*

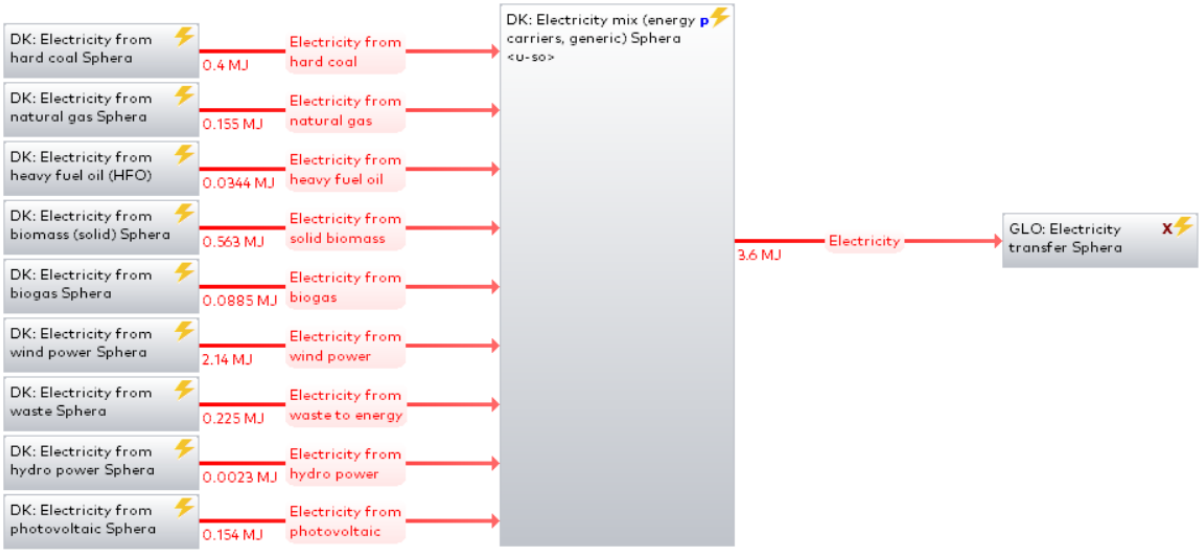

Figure A2.11. *LCA plan for Denmark' electricity grid mix*

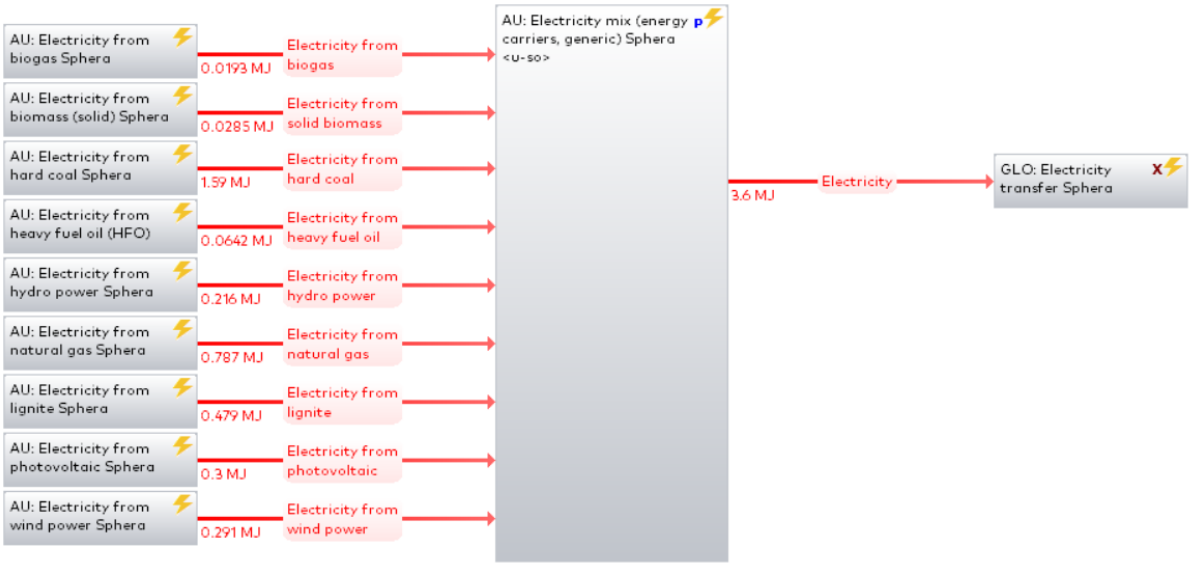

Figure A2.12. *LCA plan for Austria' electricity grid mix*

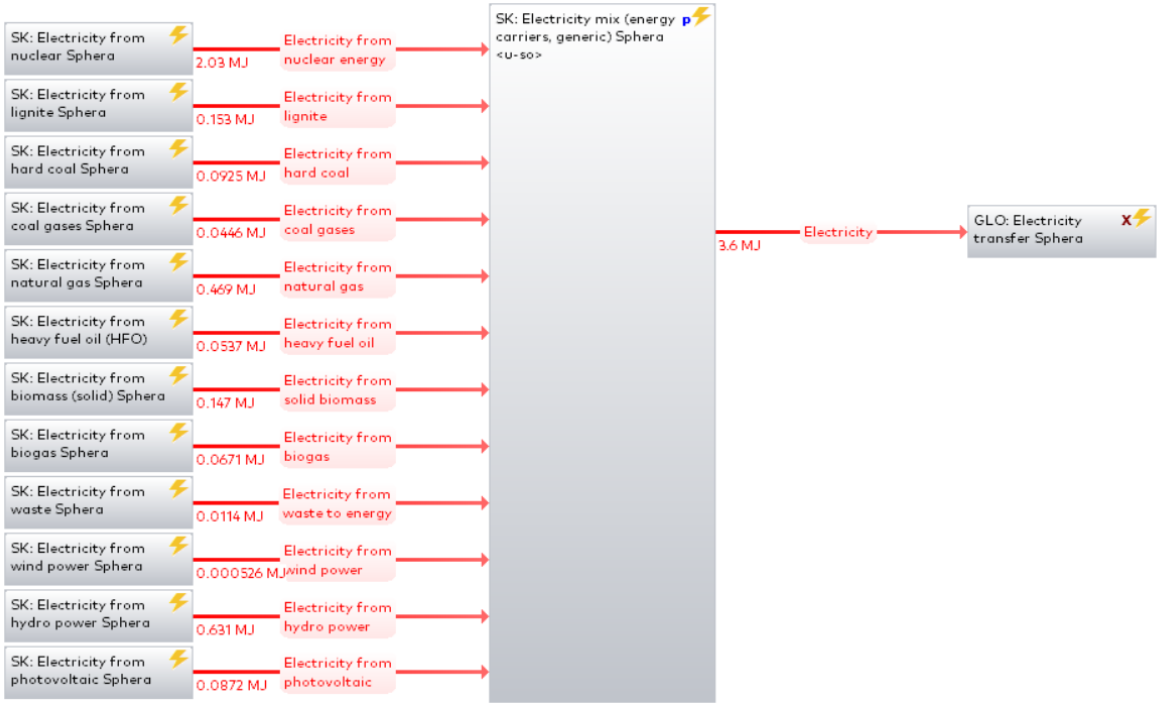

Figure A2.13. *LCA plan for Slovakia' electricity grid mix*

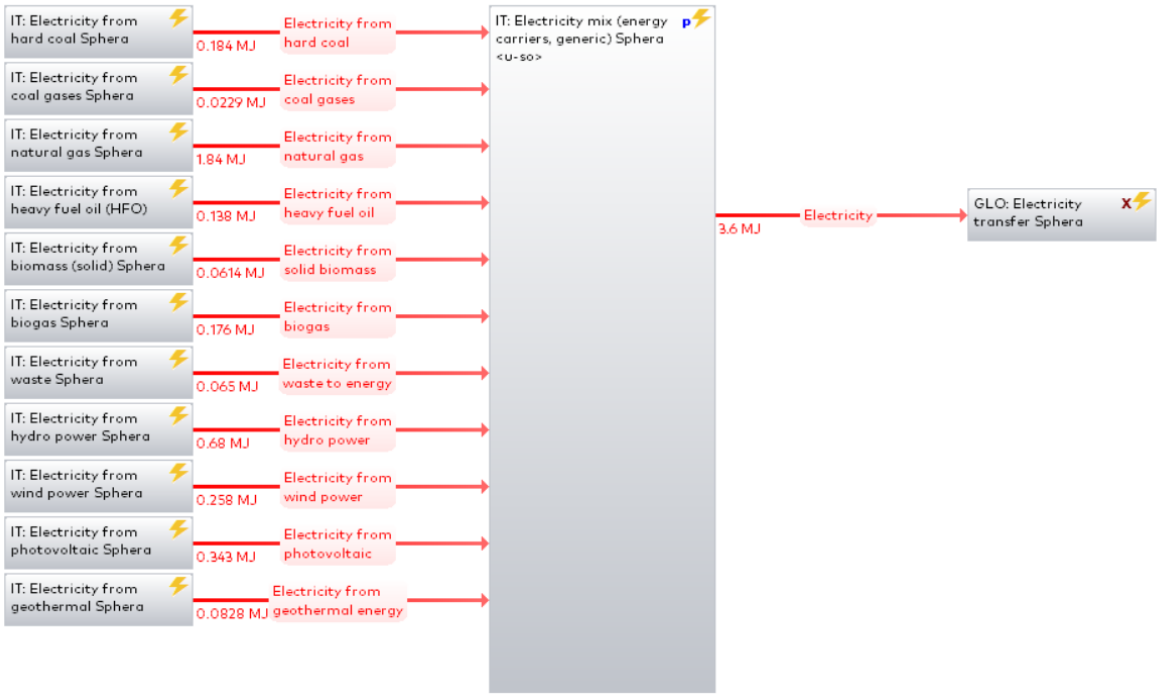

Figure A2.14. *LCA plan for Italy' electricity grid mix*

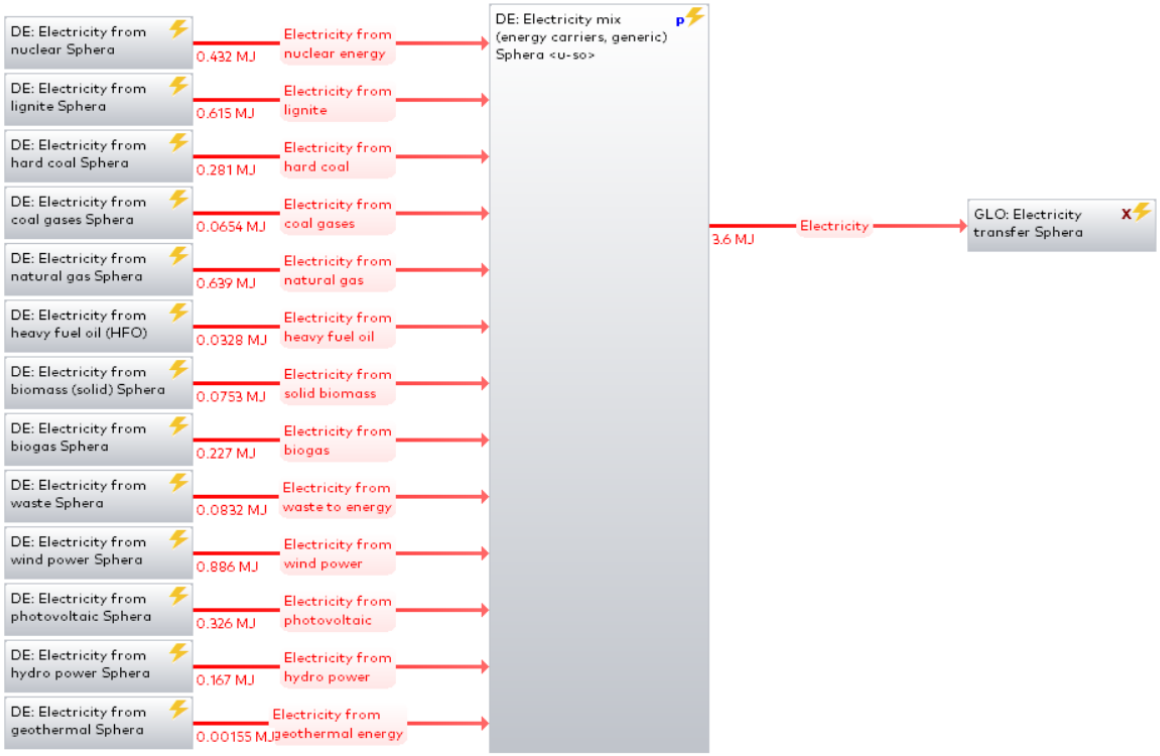

Figure A2.15. *LCA plan for Germany' electricity grid mix*